

POLITECNICO DI MILANO

*School of Industrial and Information Engineering*

*Department of Chemistry, Materials and Chemical Engineering “Giulio Natta”*

*Master of Science in Materials Engineering and Nanotechnology*



**POLITECNICO  
MILANO 1863**

**THERMO-REVERSIBLE POLYMERIC MATERIALS  
BASED ON THE DIELS-ALDER REACTION**

*Supervisor: Gianmarco Griffini*

*Co-Supervisor: Benedetta Rigatelli*

*Giulia Siffredi*

898217

Academic Year 2019- 2020



# Contents

Contents .....	I
List of figures .....	IV
List of tables .....	VIII
Abstract .....	IX
Estratto in lingua italiana .....	XI
Thesis outline and goal .....	XIV
<b>1. Introduction.....</b>	<b>1</b>
1.1 Composite Materials .....	2
1.1.2 Polymer-based composites .....	4
1.1.2.1 Manufacturing techniques.....	4
1.1.2.2 Types of fibers.....	6
1.1.2.3 Types of Matrix .....	9
1.1.3 Recycling of composite materials.....	10
1.1.3.1 Mechanical recycling.....	11
1.1.3.2 Thermal recycling.....	12
1.1.3.3 Chemical recycling .....	13
1.2 Covalent Adaptable Networks .....	15
1.2.1 Vitrimers .....	18
1.3 Diels-Alder Reaction.....	21
1.3.1 Diels-Alder in Furan/Maleimide system .....	24
1.3.1.1 Bismaleimides.....	37
1.3.2 Diels-Alder in composite materials.....	40
<b>2. Materials.....</b>	<b>45</b>
2.1 Furfurylamine .....	46
2.2 Epoxy resins .....	47

2.3 Maleimido hexanoic acid.....	50
2.4 Aromatic Bismaleimide .....	51
2.5 Pyridine .....	52
2.6 Solvents .....	53
2.7 Carbon fibers.....	54
2.8 Glass fibers.....	54
3. Methods.....	55
3.1 Synthesis.....	56
3.1.1 Bismaleimide synthesis (BM).....	56
3.1.2 Furan Compounds Synthesis .....	57
3.1.2.1 Aromatic Bifunctional Furan (Aromatic 2F).....	58
3.1.2.2 Aromatic Trifunctional Furan (Aromatic 3F).....	59
3.1.2.3 Aliphatic bifunctional furan (aliphatic 2F).....	60
3.1.2.4 Aliphatic Trifunctional Furan (aliphatic 3F).....	61
3.1.3 Dies-Alder Polymers .....	62
3.2 <sup>1</sup> H NMR Spectroscopy .....	68
3.3 Differential scanning calorimetry (DSC).....	70
3.4 Thermogravimetric analysis (TGA).....	72
3.5 Fourier Transformed Infra-Red Spectroscopy (FT-IR).....	73
3.6 Solubility test.....	76
3.7 Gel content measurement .....	77
4. Results and Discussion .....	78
4.1 Aliphatic bismaleimide synthesis and characterization .....	79
4.1.1 FT-IR .....	83
4.1.2 <sup>1</sup> H NMR.....	86
4.1.3 DSC.....	92
4.2 Synthesis and characterization of furan compounds.....	95

4.2.1 FT-IR.....	96
4.2.2 <sup>1</sup> H NMR .....	99
4.2.3 DSC .....	106
4.3 DA polymers synthesis and characterization.....	107
4.3.1 Solubility tests.....	109
4.3.2 DSC .....	111
4.3.3 FT-IR .....	115
4.3.4 Gel content .....	118
4.3.5 TGA.....	119
Conclusion .....	121
Further development.....	123
References.....	125

## List of figures

Figure 1. 1 Classification of composite materials <sup>4</sup> .....	3
Figure 1. 2 Composite manufacturing techniques <sup>4</sup> .....	5
Figure 1. 3 Graphitic structure of carbon fibres <sup>10</sup> .....	7
Figure 1. 4 Life-cycle of composite materials <sup>15</sup> .....	10
Figure 1. 5 Examples of polymer engineering <sup>14</sup> .....	16
Figure 1. 6 Examples of CANs polymers reactions <sup>22</sup> .....	17
Figure 1. 7 CANs mechanism <sup>22</sup> .....	18
Figure 1. 8 V-T vitrimers characteristic <sup>23</sup> .....	19
Figure 1. 9 Temperature dependence of viscosity for $T_v > T_g$ <sup>23</sup> .....	20
Figure 1. 10 Temperature dependence of viscosity for $T_v < T_g$ <sup>22</sup> .....	20
Figure 1. 11 Diels-Alder reaction between cyclopentadiene and quinone <sup>24</sup> .....	21
Figure 1. 12 Endo and Exo adduct of Diels-Alder reaction <sup>26</sup> .....	22
Figure 1. 13 Examples of Diels-Alder reaction: a classical DA reaction A, an intramolecular DA reaction B, a hetero-DA reaction C and a reverse electron demand DA reaction D <sup>25</sup> .....	23
Figure 1. 14 DA reaction between Furan and Maleimide groups <sup>29</sup> .....	24
Figure 1. 15 Polymerization between a difuran and a bismaleimide <sup>31</sup> .....	25
Figure 1. 16 2-furfurylmaleimide <sup>29</sup> .....	26
Figure 1. 17 DA reaction between an AA and BB monomer <sup>29</sup> .....	26
Figure 1. 18 UV spectra during polymerization (left) and depolymerization (right) <sup>33</sup> .....	27
Figure 1. 19 Polymerization of a furan/maleimide A-B monomer <sup>29</sup> .....	27
Figure 1. 20 Synthesis of a DA polymer from two poly(oxazoline)s <sup>37</sup> .....	29
Figure 1. 21 DSC analysis of 2M-2F3F polymer <sup>42</sup> .....	31
Figure 1. 22 DMA analysis of 2M-2F3F polymer <sup>42</sup> .....	31
Figure 1. 23 GPC analyses of polymer 1 and polymer 2 compared with monomers <sup>45</sup> .....	34
Figure 1. 24 Synthesis of a thermoreversible crosslinked commercial polyethylene <sup>46</sup> .....	35
Figure 1. 25 Trend of the intensity of the peaks associated to furan and maleimide groups during rDA <sup>46</sup> .....	35
Figure 1. 26 DSC analyses of transparent DA-based acrylate polymers <sup>47</sup> .....	36
Figure 1. 27 Examples of Bismaleimides available on the market .....	38
Figure 1. 28 Synthesis of aliphatic bismaleimide by Kossmehl <sup>49</sup> .....	39
Figure 1. 29 Decane Diol Diester Bismaleimide <sup>50</sup> .....	39

Figure 1. 30 dimer diester bismaleimide <sup>50</sup> .....	39
Figure 1. 31 Schematic diagram of the shape memory, healing and reprocessing mechanism by triggering glass transition and rDA reaction in thermally reversible DA-crosslinked PAN-DA/GR nanocomposites via multiple approaches including heat, microwave and IR light <sup>53</sup> .....	41
Figure 1. 32 Mechanical properties of the different composite materials compared with the one of a composite based on a commercial epoxy resin <sup>21</sup> .....	44
Figure 2. 1 Chemical structure of Furfurylamine .....	46
Figure 2. 2 Chemical structure of DGEBA.....	48
Figure 2. 3 Chemical structure of DGGO .....	48
Figure 2. 4 Chemical structure of 1,4BDE.....	49
Figure 2. 5 Chemical structure of TMPTE.....	49
Figure 2. 6 Chemical structure of maleimido hexanoic acid .....	50
Figure 2. 7 Chemical structure of 1,1'-(Methylenedi-4,1-phenylene) bismaleimide.....	51
Figure 2. 8 Chemical structure of Pyridine .....	52
Figure 2. 9 Chemical structure of toluene .....	53
Figure 2. 10 Chemical structure of DMF.....	53
Figure 3. 1 reaction scheme of the synthesis of bismaleimide .....	56
Figure 3. 2 2F Aromatic synthesis .....	58
Figure 3. 3 3F Aromatic synthesis.....	59
Figure 3. 4 Reaction scheme of the functionalization of 1,4BDE to obtain aliphatic 2F .....	60
Figure 3. 5 reaction scheme of the functionalization of TMPTE to obtain aliphatic 3F .....	61
Figure 3. 6 Reaction scheme of the synthesis of DA polymer 1 .....	66
Figure 3. 7 Reaction scheme of the synthesis of DA polymer 2.....	67
Figure 3. 8 Reaction scheme of the synthesis of DA polymer 3.....	67
Figure 3. 9 orientations of the magnetic field of the hydrogen atom due to the application of an external magnetic field .....	68
Figure 3. 10 Orientation of $\beta$ with respect to $B_{eff}$ .....	70
Figure 3. 11 Signal given by the methyl group above .....	70
Figure 3. 12 Stretching and bending mode of vibrations .....	74
Figure 3. 13 Nicolet 760-FTIR nexus spectrometer .....	75
Figure 4. 1 Schematic picture of the synthesis of the aliphatic bismaleimide .....	80
Figure 4. 2 IR spectra of the reaction carried out without catalyst .....	83
Figure 4. 3 IR spectra of the reaction carried out with Pyridine but with no thermal treatment...	84

Figure 4. 4 IR spectra Bismaleimide reaction with pyridine and thermal treatment .....	85
Figure 4. 5 IR spectra of Bismaleimides BMA, BMB, BMC and BMD.....	85
Figure 4. 6 <sup>1</sup> H NMR spectra of MHA .....	86
Figure 4. 7 <sup>1</sup> H NMR spectra of 1,4BDE.....	87
Figure 4. 8 <sup>1</sup> H NMR spectra of the product of the reaction carried out with catalyst and no thermal treatment.....	88
Figure 4. 9 <sup>1</sup> H NMR of Bismaleimide (BM).....	89
Figure 4. 10 <sup>1</sup> H NMR spectrum of BMA and BMB .....	90
Figure 4. 11 DSC of Bismaleimide .....	92
Figure 4. 12 DSC of BMO .....	93
Figure 4. 13 DCS of MHA and 1,4BDE .....	93
Figure 4. 14 DSC of BMA, BMB, BMC and BMD.....	94
Figure 4. 15 Schematic representation of furan functionalization.....	95
Figure 4. 16 IR spectra of 1,4BDE and aliphatic 2F.....	96
Figure 4. 17 IR spectra of TMPTE and aliphatic 3F .....	97
Figure 4. 18 IR spectra of DGEBA and aromatic 2F.....	97
Figure 4. 19 IR spectra of DGGO and aromatic 3F .....	98
Figure 4. 20 <sup>1</sup> H NMR spectrum of 1,4BDE.....	99
Figure 4. 21 <sup>1</sup> H NMR spectrum of aliphatic 2F.....	99
Figure 4. 22 <sup>1</sup> H NMR spectrum of TMPTE.....	101
Figure 4. 23 <sup>1</sup> H NMR spectrum of aliphatic 3F.....	101
Figure 4. 24 <sup>1</sup> H NMR of DGEBA .....	103
Figure 4. 25 <sup>1</sup> H NMR of aromatic 2F.....	103
Figure 4. 26 <sup>1</sup> H NMR of DGGO.....	104
Figure 4. 27 <sup>1</sup> H NMR of aromatic 3F.....	104
Figure 4. 28 DSC of Furan compounds.....	106
Figure 4. 29 Solubility test at low temperature.....	109
Figure 4. 30 Solubility test at high temperature.....	109
Figure 4. 31 Gelification .....	110
Figure 4. 32 DSC of DA polymers 1.....	112
Figure 4. 33 DSC of DA polymers 2.....	112
Figure 4. 34 DSC of DA polymers 3.....	113
Figure 4. 35 IR of So with $f_{av}=2,2$ .....	116



Figure 4. 36 FT-IR of DA polymers 2 with $f_{av}$ 2,2 and bismaleimide .....	116
Figure 4. 37 FT-IR of DA polymers 3 with $f_{av}$ 2,5 and bismaleimide .....	117
Figure 4. 38 TGA of S2 2,2 .....	119
Figure 4. 39 TGA of S3 2,5 .....	120
Figure 4. 40 Examples of Composites: A with glass fibers, B with non-woven carbon fibers, C with woven carbon fibers .....	124

## List of tables

Table 2. 1 chemical properties of Furfurylamine .....	46
Table 2. 2 Chemical properties of DGEBA .....	48
Table 2. 3 Chemical properties of DGGO.....	48
Table 2. 4 Chemical properties of 1,4BDE .....	49
Table 2. 5 Chemical properties of TMPTE .....	49
Table 2. 6 Chemical properties of maleimido hexanoic acid .....	50
Table 2. 7 Chemical properties of 1,1'-(Methylenedi-4,1-phenylene) bismaleimide .....	51
Table 2. 8 Chemical properties of Pyridine.....	52
Table 3. 1 bismaleimide synthesis.....	57
Table 3. 2 2F aromatic synthesis.....	58
Table 3. 3 3F aromatic synthesis.....	59
Table 3. 4 functionalization of 1,4BDE to obtain aliphatic .....	60
Table 3. 5 functionalization of TMPTE to obtain aliphatic 3F.....	61
Table 3. 6 DA polymers.....	62
Table 3. 7 DA polymer S0 synthesis.....	64
Table 3. 8 DA polymer S1 synthesis .....	64
Table 3. 9 DA polymer S2 synthesis .....	65
Table 3. 10 DA polymer S3 synthesis.....	65
Table 3. 11 DSC parameters.....	71
Table 4. 1 Attempts to defined bismaleimide reaction procedure: Mixing: in toluene at 110°C, Catalyst: pyridine, Thermal treatment: mixing after solvent evaporation at 130°C.....	80
Table 4. 2 Bismaleimides reactions.....	81
Table 4. 3 Scaling up of the bismaleimide reaction.....	82
Table 4. 4 quantification of reacted epoxies.....	90
Table 4. 5 predicted and effective functionalities.....	105
Table 4. 6 % reacted furan groups .....	105
Table 4. 7 DA polymers obtained without the usage of solvents .....	108
Table 4. 8 T <sub>g</sub> of DA polymers.....	114
Table 4. 9 DA %.....	117
Table 4. 10 Gel content measurements .....	118
Table 4. 11 TGA data.....	120

## Abstract

Nowadays, composite materials are exploited in a lot of applications thanks to their excellent mechanical and structural properties. One of the biggest challenges for researchers is the recycling of both the fibers and the matrix at their end of life.

Matrices of composite materials are typically thermosets polymers which showed an excellent chemical and thermal resistant and outstanding mechanical properties. The drawback of this kind of polymers is related to their chemical structure, which is formed by a crosslinked network which do not permit their recycle. Fibers can be recovered but with not environmentally friendly technique, which can lead to a decrease of the mechanical properties of the recycled fibers.

To overcome this issue, covalent adaptable networks (CAN) polymers such as Diels-Alder (DA) polymeric matrices can be exploited. This kind of thermoset polymers, due to their thermoreversibility, could allow the repairing of a composite and the recovery of both the matrix and the fibers. Polymers based on DA reaction are usually obtained thorough the crosslinking between multifunctional furan compound and commercially available aromatic bismaleimide. These systems showed self-healing behaviour and good thermal properties, but they are characterized also by incomplete fibers impregnation within the matrix likely due to the rigidity of aromatic compounds.

Moreover, they are prepared through solvent-based mixing which would not allow for many processing techniques commonly employed in this kind of applications.

In this experimental work, new Diels-Alder polymeric matrices were prepared through solvent-free processes: the use of aliphatic monomers, synthesized in this thesis through new simple reaction procedures, allowed to obtain a thermoset matrix in the absence of solvents.

Three aliphatic compounds were prepared: aliphatic bifunctional furan monomer, aliphatic trifunctional furan monomer and an aliphatic bismaleimide, synthesized from 1,4-butanediol diglycidyl ether and maleimido hexanoic acid catalysed with Pyridine.

Differently from other aliphatic bismaleimide syntheses which are long, have a low yield and are followed by many purification steps, the reaction procedure developed in this

work consists in three quick steps, it has a higher yield (around 67%) and does not require additional steps for the purification of the product.

Since a polymer completely based on aliphatic precursors would have had a low glass transition temperature ( $T_g$ ) due to the high molecular mobility, two aromatic furan components were synthesized too.

All the reactions were monitored with Fourier Transform Infrared Spectroscopy and the products were analysed with  $^1\text{H}$  NMR spectroscopy and Differential Scanning Calorimetry (DSC).

Since it was demonstrated that making use of commercially available aromatic bismaleimide would require the usage of a solvent for the mixing procedure utilized to obtain the polymer, different combinations of aromatic and aliphatic furan molecules were mixed with aliphatic bismaleimide with different average functionalities.

The thermoreversibility of all the obtained polymers was verified with solubility tests, which demonstrated as the final product appeared insoluble at room temperature but completely dissolved at high temperature. DSC analyses were performed to find out the glass transition temperatures and the retro DA peaks in order to define application temperature range. DA polymers with the highest  $T_g$  were selected for further analyses: the degree of crosslinking was demonstrated by means of FTIR technique and the thermal stability was determined through thermal gravimetric analyses.

Some efforts were made in order to obtain composite material with glass and carbon fibers. The impregnation seemed good but other studies are needed.

This study can be considered as a proof of the production of solvent-free DA-based polymers which can be employed as a thermo-reversible matrix for composite materials.

## Estratto in lingua italiana

I materiali compositi a matrice polimerica sono attualmente impiegati in svariate applicazioni grazie alle loro eccellenti proprietà meccaniche e strutturali. Comunemente, i polimeri termoindurenti vengono impiegati come matrici in virtù di peculiari proprietà, quali ottima resistenza agli agenti chimici, elevata resistenza termica ed eccellenti prestazioni meccaniche. Tuttavia, uno dei principali svantaggi dell'uso di questa classe di polimeri è legato all'impossibilità di riprocessare e riciclare il componente dopo l'utilizzo: la stabilità chimica nelle catene covalentemente reticolate non ne permette alcun efficiente processo di riciclo. Una delle più importanti sfide, a livello scientifico -ambientale, è dunque la possibilità di riparare e riciclare il componente e permettere il recupero sia della matrice che delle fibre dei compositi a fine vita.

Le fibre dei materiali compositi possono essere recuperate tramite un processo meccanico, termico o con l'uso di solventi. Tali metodi presentano degli svantaggi non trascurabili. Il processo meccanico consiste in una macinazione del componente, che dà luogo ad accorciamento delle fibre con conseguente riduzione delle proprietà meccaniche; quello termico avviene a temperature molto alte che portano a una degradazione delle fibre riciclate; il processo con solventi avviene a temperature più basse ma si basa sull'uso di acidi, dannosi per l'ambiente. Quindi con nessuno dei processi sopra descritti è possibile riutilizzare la matrice o recuperare fibre con proprietà meccaniche simili a quelle delle fibre iniziali.

Per risolvere questo problema, polimeri reticolati attraverso legami covalenti in grado di modificare la loro natura in presenza di uno stimolo possono essere utilizzati come matrici (Covalent Adaptable Network or CAN polymers). In questo modo polimeri termoindurenti possono essere riprocessati e riciclati. Tra questi polimeri, quelli basati sulla reazione di Diels-Alder (DA) sono tra i più diffusi. La reazione di Diels-Alder è una cicloaddizione [4+2] tra un diene e un alchene, chiamato anche dienofilo. Il prodotto di questa reazione è un cicloesano sostituito: in seguito al riarrangiamento di sei elettroni  $\pi$  avviene la formazione di due legami  $\sigma$  e un legame  $\pi$ . Questa reazione è termo-reversibile: al di sotto della temperatura di retro-Diels-Alder prevale la formazione del prodotto, mentre al di sopra di questa si riformano i monomeri. Grazie a questa

caratteristica, nei compositi basati su matrici Diels-Alder, le fibre possono essere separate dalla matrice e quindi entrambi i componenti possono essere riciclati. Inoltre, se avviene la formazione di una crepa in una matrice DA, questa può essere riparata tramite un trattamento termico: il materiale viene portato alla temperatura di retro-DA in modo da riformare i monomeri e poi viene raffreddato per permettere la riformazione dei legami reticolati covalenti.

I dieni più utilizzati in questa reazione sono molecole a funzionalità furano, mentre le maleimmidi sono i dienofili più diffusi (più economiche di quelle alifatiche). Sistemi basati su questa coppia di reagenti sono caratterizzati da buone proprietà termiche e meccaniche, ma a causa della rigidità delle molecole aromatiche, in particolare delle bismaleimmidi commerciali, l'impregnazione delle fibre nella matrice non è ottima e porta alla formazione di vuoti tra il rinforzo e la matrice. Inoltre, questi polimeri vengono preparati miscelando i monomeri in un solvente e quindi è sempre necessario uno step di purificazione per rimuovere il solvente e molte tecniche di processo, comunemente utilizzate per i materiali compositi, non possono essere prese in considerazione.

In questa tesi sperimentale nuove matrici polimeriche basate sulla reazione di Diels-Alder sono state sintetizzate attraverso un processo senza solventi. L'utilizzo di monomeri alifatici, ottenuti tramite nuove e semplici procedure, ha permesso di ottenere polimeri termoindurenti riprocessabili in assenza di solvente. Sono stati sintetizzati tre nuovi composti alifatici: un furano alifatico bifunzionale, un furano alifatico trifunzionale e una bismaleimide alifatica. Diversamente da altre sintesi di bismaleimmidi alifatiche che sono lunghe, complesse, hanno una resa bassa e sono seguite da lunghi step di purificazione, la reazione sviluppata in questa tesi è semplice, ha una resa di circa l'85% e non richiede step lunghi. Sono stati studiati diversi rapporti tra le moli di acido e quelle di epossido in modo da trovare il rapporto ottimale per non avere epossidi residui non reagiti nel prodotto finale.

Dato che un polimero termoindurente ottenuto solo da monomeri alifatici avrebbe avuto una temperatura di transizione vetrosa ( $T_g$ ) troppo bassa e quindi proprietà meccaniche non soddisfacenti, due furani aromatici sono stati sintetizzati e fatti reagire con la bismaleimide alifatica.

Per quanto riguarda la sintesi dei furani sia alifatici che aromatici, è stata fatta un'analisi quantitativa dei prodotti di reazione tramite gli spettri  $^1\text{H}$  NMR, in modo da trovare le reali funzionalità di ognuno.

Tutte queste reazioni sono state monitorate con la spettroscopia IR in trasformata di Fourier e i prodotti sono stati analizzati con spettroscopia  $^1\text{H}$  NMR e con calorimetria differenziale a scansione (DSC).

Dopo aver dimostrato che l'uso di bismaleimmidi aromatiche richiede l'uso di un solvente per miscelare i vari monomeri, solo la bismaleimide alifatica è stata presa in considerazione per la sintesi di matrici DA.

I polimeri DA sono stati preparati miscelando un furano bifunzionale, uno trifunzionale e la bismaleimide alifatica, valutando diversi valori di funzionalità medie. La termoreversibilità di tutti i polimeri è stata verificata tramite test di solubilità: tutti i polimeri erano insolubili a temperatura ambiente e solubili ad alta temperatura. Analisi DSC sono state eseguite per determinare la  $T_g$  e il picco di retro DA in modo da definire l'intervallo di temperatura di applicazione. I polimeri con la  $T_g$  più alta sono stati selezionati per ulteriori analisi: il grado di crosslinking è stato valutato confrontando gli spettri IR dei prodotti con quello della bismaleimide, mentre la stabilità termica è stata studiata attraverso analisi termo gravimetriche.

Infine, alcuni tentativi sono stati intrapresi per cercare di ottenere un materiale composito, sia con fibre di vetro che con fibre di carbonio.

In conclusione, in questa tesi una nuova reazione per ottenere una bismaleimide alifatica è stata realizzata con successo. Matrici DA sono state in seguito ottenute tramite un processo senza solventi grazie a questa bismaleimide. Quindi, questa tesi può essere considerata come una prova della produzione di polimeri DA senza solventi che possono essere impiegati come matrici termo-reversibili per compositi.

## Thesis outline and goal

Fiber reinforced thermoset and thermoplastic polymers are increasingly used to replace metals in several applications. One of the principal challenges for researchers regarding the use of these materials is their recycling. Different recycling technologies were studied and proposed in the last years: mechanical recycling, thermal recycling and recycling by using solvolysis processes. Anyway, fibers recovered with these techniques are degraded with a low possibility of reusing. Furthermore, none of these methods allows a good separation of the fibres from the matrix and so a reuse of the matrix is in neither case possible. To solve this issue covalent adaptable networks polymers can be exploited (such as Diels-Alder polymers). The presence of these bonds allows thermosets to become malleable, in fact this kind of bonds can be broken and reformed under a certain stimulus making possible the reprocessability and the recyclability. The Diels-Alder reaction, thanks to its reversibility, allows to create thermoset polymers with reversible crosslinks. In fact, below a specific temperature range, DA polymers behave like thermosets while above a specific temperature range they behave like thermoplastics. Diels-Alder (DA) polymers which are usually obtained through a crosslinking between furan functionalized monomers and aromatic commercial maleimides, present good mechanical and thermal properties but do not permit a well impregnation of the fibers in the matrix.

The aim of this thesis consists in the development of a solvent free process to obtain Diels-Alder polymers which can be potentially employed as matrices in composite materials ensuring a good impregnation of the fibers. To accomplish this goal a new aliphatic bismaleimide was synthesized through a simple procedure. In addition, two aliphatic epoxy resins and two aromatic epoxy resins were functionalized with furfurylamine in order to obtain multifunctional furan monomers. After a characterization of these products, Diels-Alder polymers were prepared by mixing the aliphatic bismaleimide with different combinations of furan monomers. Chemical resistance and thermal properties of these new matrices were analysed. Finally, it was demonstrated that it was possible to obtain composite materials with these new matrices. On the base of successful results obtained and with further studies on the



composite materials based on the new matrices, these new DA polymers could open new ways towards next-generation recyclable composite materials.

The thesis is organized as follow:

- *Introduction:* an overview on composite materials is treated, in particular about polymer composites: manufacturing techniques, the kind of fibers and of matrix are explained. Then, the technique to recycle these materials are described. Successively, after a description of covalent adaptable networks polymers, the topic of Diels-Alder reaction is introduced: first the chemistry of the reaction is explained, then an overview on the Diels-Alder in furan/maleimide system is presented with a further insight on bismaleimides; finally examples of Diels-Alder based matrices in composite materials are reported;
- *Materials:* materials used in this thesis are described;
- *Methods:* the synthesis of the aliphatic bismaleimide, of the furan compounds and of the Diels-Alder polymers are presented. Then, the characterization techniques employed are explained;
- *Results and discussion:* the first section presents the characterization of the bismaleimide, the second one the characterization of aliphatic and aromatic furan compounds, while in the third section the Diels-Alder polymers were analysed. At the end, an attempt to obtain a composite material was explained;
- *Conclusion and Further Development:* the conclusions of the work are drawn and further possible studies are described.

# ***1. Introduction***

## 1.1 Composite Materials

Emerged in the middle of 20th century, composite materials are nowadays extremely widespread for many applications such aerospace, automotive, construction, sports, bio-medical and others thanks to their promising characteristics. In fact, these materials are characterized by remarkable structural and mechanical properties, such as high strength to weight ratio, and resistance to chemicals, fire, corrosion and wear.

A composite material is a composition of two or more constituent materials, which have different physical and chemical properties. The different components, when combined together, produce a material with unique characteristics different from the constituent elements.<sup>1</sup>

Composite materials are composed by a base material and a filler material. The base material, usually characterized by good ductility, formability and thermal conductivity, surrounds and binds the reinforcing material, protecting it from hard environmental conditions such as high temperatures or humidity. This is called matrix or binder material and it represents the relatively soft phase.<sup>2</sup>

Fillers are materials with high strength and stiffness, in fact they withstand the applied load. They possess also a low thermal expansion since they are embedded in the matrix. Reinforcements can have different forms: fragments, particles, fibres or whiskers of natural or synthetic material.

Binder and filler materials, when combined, do not dissolve and do not lose their identities, unlike solid solution. They synergistically contribute their properties making the final structure superior compared to starting materials. Examining with a microscope the finished materials it is possible to identify the characteristics of distinct components.<sup>3</sup>

Examples of composite materials can be found also in nature as wood and bones. Wood is made of fibrous chains of cellulose molecules in a matrix of organic polymer lignin and bones are composed by inorganic crystals called hydroxyapatite in a matrix of an organic material called collagen.

Composite materials can be classified according to the kind of constituents as illustrated in Figure 1. 1.

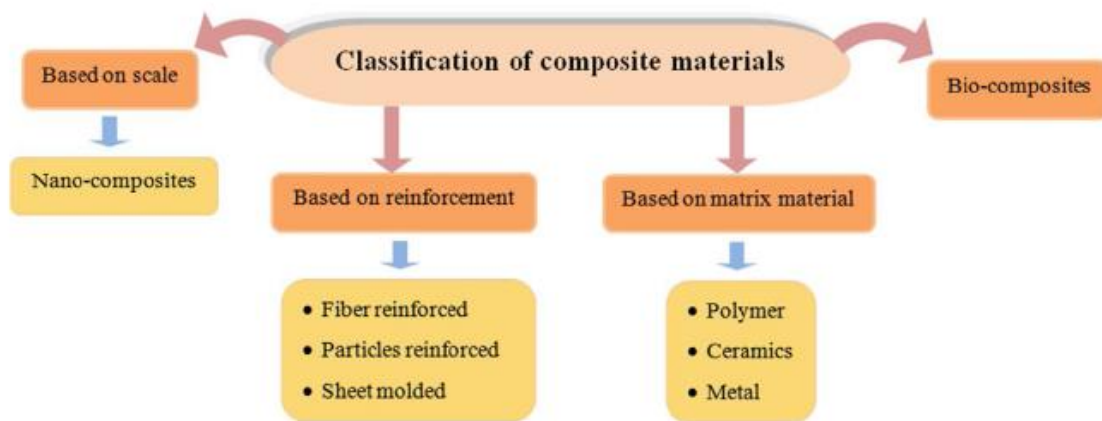


Figure 1. 1 Classification of composite materials<sup>4</sup>

Considering a classification based on the matrix material, composite materials can be distinguished in polymer, ceramic or metal based materials.

Most of polymer composites are made of a thermoplastic or thermosetting matrix reinforced with carbon, glass or Kevlar fibres. They are low cost composite thanks to the simple fabrication methods; in particular the laminar structure is the most used one and it is obtained by stacking and bonding thin layers of fibers and polymers.<sup>5</sup>

Ceramics can be reinforced with silicon carbide, aluminium oxide or silicon nitride to improve their toughness. They are obtained with gas or liquid phase route, a process in which the matrix is formed around the filler from a gas or a liquid precursor.

In metal composites, metal such as Al, Mg, Cu and Ti are often used as matrix materials which can be reinforced with ceramics, as carbides or oxides, or with metal as lead or tungsten. Al based composites are very common. They are reinforced by adding SiC or Al<sub>2</sub>O<sub>3</sub> in molten Al improving stiffness and wear resistance with respect to pure Al.

Composite materials can be also classified according to the form of the fillers which give different properties to final structure. Fibers made by carbon, glass or basalt provide a high strength and stiffness while particles are used when a high wear resistance is required. Sheet composites consist of a thermoset reinforced with glass which is prepared by compression molding, obtaining a high strength composite which is used for large structural components.

Moreover, exceptional optical properties can be achieved by embedding materials at the nanoscale in a transparent matrix obtaining a nano-composite.

Because of the increasing attention to environmentally friendly material researchers are looking for new bio-composites. For example, a bio composite can be prepared exploiting sugar palm fibers that are embedded in a starch matrix.<sup>4</sup>

Polymer composites have been taken into account in this thesis because of their large diffusion in many sectors (such as automotive, aerospace and electrical).

### **1.1.2 Polymer-based composites**

Composite polymers are heterogeneous and anisotropic materials which do not exhibit plastic deformation, consisting of a polymeric matrix reinforced with different reinforcement phase such as carbon, glass or Kevlar fibres. These materials, thanks to their properties and their low cost, are used in large quantities and in a lot of applications such as in space, automotive and in manufacturing of sports equipment. In particular, carbon fiber reinforced polymer (CFRP) and glass fiber reinforced polymer (GFRP), due to their excellent strength and low specific weight, are replacing conventional materials.<sup>6</sup>

#### **1.1.2.1 Manufacturing techniques**

Composites can be obtained with different techniques according to the type of matrix and of fiber materials. These techniques are classified in four classes: open molding, closed molding, cast polymer molding and additive manufacturing (Figure 1. 2).<sup>7</sup>

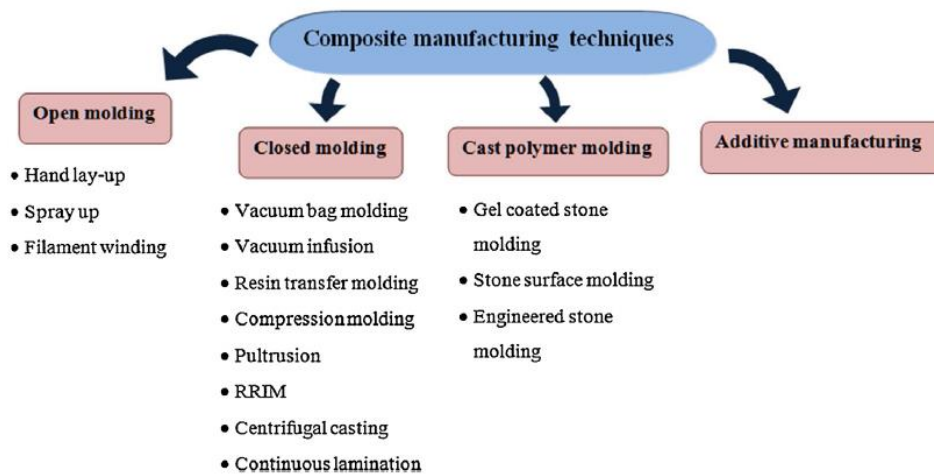


Figure 1. 2 Composite manufacturing techniques<sup>4</sup>

Open molding process can be realized in three different ways. In the hand lay-up process a gel coat is applied to an open mold and then layers of resin and woven or knitted fibers are manually applied. In the spray-up technique chopped fibers and the resin are simultaneously sprayed into the mold. In both these techniques a roller is used to remove bubbles and to fuse resin with the reinforcement. The third kind of open molding technique is the filament winding process that exploits a rotating mandrel as mold and allows to obtain hollow cylindrical shapes. The composite material obtained with open molding processes is exposed to air to cure and to get harder.

Closed mold techniques are used for large volume of production. In these processes the curing of the composites takes place inside the mold. Closed molding process can be performed for instance by using vacuum. Vacuum can be applied after the introduction of the material in the mold as in the case of vacuum bag molding process or before as in vacuum infusion process. The composites are consolidated by removing entrapped air with the application of vacuum.

In resin transfer molding method fibers are placed in the mold cavity where the resin is injected with injection equipment, while in compression molding process the resin with the reinforcing materials is put in a metal mold which is mounted on a hydraulic press and successively heat and pressure are concurrently applied.

Another closed mold technique is pultrusion, which is a continuous process, exploited to produce composites with simple and complex constant cross-sectional shape.

In reinforced reaction injection molding process two or more resin are mixed in a chamber mixing, then the fibers are added and successively, with the help of a pump, the mixture is sent to a mold cavity where the polymerization occurs.

A cylindrical rotating mold is employed in centrifugal casting method where resin and fibers are deposited. Then centrifugal forces are applied, which keep the materials against the wall of the cylindrical mold until curing occurs.

In continuous lamination process a panel made of resin and reinforcement material, after the removal of trapped air and a curing step in oven, is rolled on a huge roller to form a laminate sheet. This process is used for products with an opaque or translucent flat structure.

Cast polymers have not reinforcement in it and are designed to meet specific requirements with three molding processes: in gel coated cultures stone molding process the material is spread on a surface and then it can be blended with different fillers; in engineered stone molding process resin is combined with stone particles to achieve low porosity; and solid surface molding process is used to make material surface alluring.

Additive manufacturing techniques include: material extrusion, vat photo polymerization which exploit UV light to cure photopolymer, sheet lamination and powder bed fusion which uses thermal energy to fuse different layers.<sup>4</sup>

### **1.1.2.2 Types of fibers**

Glass fibers have a high resistance and when embedded in a polymeric matrix form a composite with an excellent resistance. They show also high values of hardness, resistance to chemical attack and good stability.<sup>8</sup> Moreover, glass is inert when coupled with polymers making possible the use of these composites in corrosive environment. Because of the low interaction between polymer and glass a coupling agent can be applied on the glass surface that form a chemical bond between the fibers and the matrix. The use of GFRP has some limitations such as the low operating temperatures and the low stiffness.<sup>6</sup> The formation of glass fibers involves a combination of extrusion and attenuation of molten glass. The molten glass flows from a melting furnace to an

array of bushings containing a great number of orifices, through which the glass drop forming fine fibers. These bushing plates are heated to control the glass viscosity. A sizing applicator is placed one or two meters below the bushing plates. At the end the sized fibers are brought together to form a multifilament strand at a gathering shoe.<sup>9</sup> Size and binders are applied before the gathering of the fibers to avoid degradation of the filaments strength that can be caused by abrasion among different filament and to provide protection or coupling. Glass fibers are classified in two classes: low-cost general-purpose fibers and special-purpose fibers. The first type is designed as E-glass and includes fibers characterized by a low electrical conductivity, while the second category includes fibers with high strength, high corrosion resistance, low dielectric constant and pure silica and quartz fibers which can be used at very high temperatures.<sup>8</sup> Carbon fibers are fibers which contain at least 92 wt% carbon differently from graphite fibers which contain 99 wt% carbon.<sup>10</sup>

The atomic structure of carbon fibers consists in graphene sheets and so in carbon atom layers arranged in a regular hexagonal structure where atoms within a plane are bonded with sp<sup>2</sup> bonded and the different planes interact through Van der Waals forces. The layers can have a turbostratic, graphitic or hybrid structure according to the precursors and to the manufacturing process. In graphitic structures (Figure 1. 3) the parallel layers are stacked regularly differently from turbostratic structures, where the parallel layers are stacked in an irregular way, in fact the different layers can be folded, tilted or splitted one respect to another.<sup>10</sup>

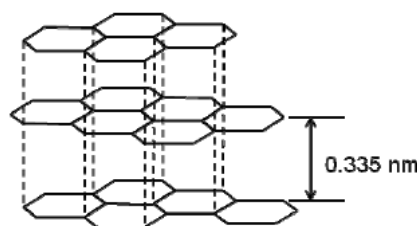


Figure 1. 3 Graphitic structure of carbon fibres<sup>10</sup>

They are often used as reinforcing materials in polymers in fact they have the highest value of modulus and of resistance with respect to all fibers. Then these fibers are not affected by humidity and solvents and show a good tensile modulus, a high strength at break even at high temperatures, low densities, high thermal and chemical stability,



good thermal and electrical conductivity and a high creep resistance.<sup>6</sup> Carbon fibers can be used in the form of woven textiles, continuous fibers or chopped fibers and are obtained from pyrolysis of stabilized precursor fibers consisting in a first oxidation at 200-400°C followed by a carbonization process, a heat treatment around 1000°C, to remove hydrogen, oxygen, nitrogen and other non-carbon elements.<sup>10</sup>

The range of application of carbon fibers depends on the type of precursors which must have some characteristics, such as easy conversion to carbon fibers, high carbon yield and cost-effective processing. Considering these features, four precursors are widely used: acrylic precursors, which contains >85% of acrylonitrile monomer (in particular polyacrylonitrile is the most utilized); Cellulosic precursors, characterized by a content of carbon of 44,4% and a low yield; pitch-based precursors, which have a higher yield and lead to the production of fibers with a high modulus but lower compression and transverse properties compared with PAN fibers; other forms of precursors such as vinylidene chloride or phenolic resins.

Carbon fibers can be classified according to mechanical properties in ultra high modulus (>500 GPa), high modulus (>200 GPa), intermediate modulus (>200 GPa), low modulus (100 GPa), and high strength (>4 GPa) carbon fibers. Carbon fibers can be also classified in terms of heat treatment in type I (2,000 °C heat treatment), type II (1,500 °C heat treatment), and type III (1,000 °C heat treatment). Type I carbon fibers are high modulus while high strength belongs to type II.<sup>11</sup>

Kevlar fibers belong to aramid fibers characterized by a high temperature resistance, high longitudinal tensile strength and a high modulus thanks to their chemical structure. Their structure consists in rigid long chain aligned in the fibers direction held together through strong covalent bonds, which provide a high longitudinal tensile strength, while in the transverse direction the fibers are bonded with weak hydrogen bonds resulting in low transverse strength. They provide the highest value of strength to weight compared with all other reinforcing fibers. They are employed for their good values of toughness and for their high resistance to creep and to fatigue break. Although they are thermoplastic, aramid fibers can resist to combustion and are stable at relatively high

temperatures. They can be degraded by strong acids or bases but are inert with respect to a lot of chemical substances.<sup>6</sup>

The most common aramid fibers are three kinds of Kevlar fibers: Kevlar 29 (low modulus), Kevlar 49 (intermediate modulus) and Kevlar 149 (high modulus). Kevlar fibers are obtained from a condensation reaction between paraphenylene diamine and terephthaloyl chloride in an organic solvent to form polyparaphenylene terephthalamide. The reaction is followed by extrusion, stretching and drawing. Successively the polymer is washed and dissolved in sulfuric acid to form a polymer solution where the polymer is a partially oriented liquid crystal. This solution is extruded, then the fibers pass through the spinneret and finally the fibers are washed, dried and wound up.<sup>12</sup>

### **1.1.2.3 Types of Matrix**

Thermosetting matrix, such as epoxy or polyester resins, are the most used in composite polymers thanks to their better properties with respect to thermoplastic polymers. Sometimes also some kinds of thermoplastic resins, such as poly phenylene sulfide (PPS) or polyether ether ketone (PEEK), which are resistant to high temperatures can be exploited too in composite polymers.

Thermosets are highly crosslinked polymers which are formed from an irreversible curing reaction that can be induced by heat, radiation or both. These polymers are characterized by outstanding thermal and mechanical properties, a high chemical resistance and an excellent dimensional stability; indeed they find a lot of application for example as coatings, composites, electronic packaging and adhesive and are irreplaceable in high performance coatings and adhesive, light emitting diodes and rubbers. Because of the crosslinked network, thermosets are not recyclable or re-processable and cannot be reshaped, contrarily to thermoplastic polymers. This second class of polymers consists of linear chains without crosslinking points, in fact they can be recycled, reprocessed and can be reshaped by heating without changing the physical properties of the materials. However, thermoplastic polymers show a lower environmental resistance with respect to thermosets.<sup>13</sup> The two kinds of polymers are

also differently processed depending on the flow behaviour of the material. Thermoplastics are processed with extrusion, injection or blow molding. Instead, for what concern thermosets, which cannot be softened by heating, the techniques used are compression molding, resin transfer molding or liquid casting.<sup>14</sup>

### 1.1.3 Recycling of composite materials

Composite materials are used in many industrial fields and nowadays researchers are focused on improving composites properties, finding new materials and developing efficient ways to recycle these materials, since the large use of composite materials results in an increase of waste.<sup>15</sup> For example, the demand of carbon fibres is increased from 16,000-55,000 tonnes per years and is expected to reach 140,000 tonnes by 2020 that leads to larger volumes of CFRP waste that should be managed with minimum impact on the environment.<sup>16</sup> However, composite waste is relatively inert in the environment, so can be disposed in landfills or incinerated, but new solution should be taken into account, indeed these techniques are not sustainable in the long term. So, to facilitate the continued use of the composite it is important to transform composite into a valuable resource and to close the loop in the composite lifecycle represented in the Figure 1. 4.

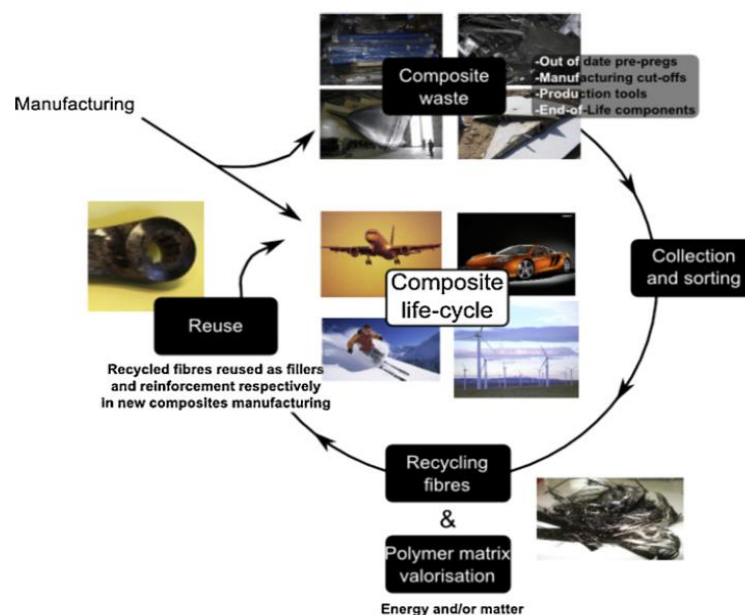


Figure 1. 4 Life-cycle of composite materials<sup>15</sup>

There are three categories of recycling technologies for CFRPs: primary, secondary and tertiary. Primary approach is based on the mixing of some waste material with virgin raw material to form a new material with properties equal to the starting material. Secondary approach involves the same mixing, but the obtained material has inferior properties compared to the original one. Tertiary recycling refers to the chemical decomposition of the polymer into useful chemical substances and/or fuel. The first two recycling technologies are also known as material mechanical recycling, while pyrolysis and solvolysis process belong to tertiary approach.<sup>15</sup>

### **1.1.3.1 Mechanical recycling**

Mechanical grinding is utilized for glass and carbon reinforced composites. It involves two reduction size steps: the initial reducing step and the main size reduction stage. First, the large waste composite is cut into small pieces of the order of 50-100 mm in size with the use of a small speed cutting or a crushing mill; then the material is ground in finer product ranging from 10 mm to 50 $\mu$ m with a hammer mill or a high speed mill. Lower is the size of the final material higher is the energy consumption of the process. Successively the resulting recycled is separated by size by using cyclones and sieves into two fractions: the coarse and the fine fractions. In the mechanical recycling the resulting recycled is a mixture of all the constituents of the original material and so it is a mix of polymer, fibres and fillers. The coarse particles have a fibrous nature and contain a higher portion of reinforcement compared to fine fractions, also called fine powders fractions, which are composed of polymeric matrix.<sup>17</sup> The advantage of this method is the recovery of both the matrix and the fibers without the use or the production of dangerous materials, but it presents also some disadvantages since the recovered fibers are degraded and so the possibilities of re-use are limited.<sup>15</sup> For example, powders particles can be used in sheet molding compound (SMC) or bulk molding compound (BMC) as fillers instead of calcium carbonate with a reduction of 10% of mechanical properties, but the excessive increase of the content of recycled fillers leads to processing problem, such as an increase of viscosity and to a further reduction of the mechanical properties. The use of the coarse fraction is more difficult because, even

with a small amount of these recycled particles used as fillers, it leads to a reduction of strength and toughness. Furthermore, mechanical recycling produces a lower global warming impact with respect to the other methods, but presents high cost and a low rate of carbon fibers recovery.<sup>18</sup>

### **1.1.3.2 Thermal recycling**

There are three kinds of thermal recycling: pyrolysis, fluidised-bed pyrolysis and pyrolysis assisted with microwaves, which operate in a temperature range between 450°C and 700°C according to the resin. These processes lead to the recovery of fibers, fillers and inserts but not of the matrix, which is volatilized into lower weight molecules with the production of gases and of char that can be deposited on fibers.<sup>19</sup>

Pyrolysis consists in the thermal degradation of the organic part of the composite material carried out in the absence or in the presence of oxygen, and more recently also in the presence of steam.<sup>15</sup> The product of the process is constituted by gaseous, oily and solid fractions. The gases produced are methane, hydrogen and other hydrocarbons which can be reused to produce the energy needed for the process. The oily and solid fractions consist by lower molecular weight substances, by recovered glass or carbon fibres and by char which is deposited on the fibres. For this reason, recovered fibres undergo a post-treatment in furnace at 450°C to burn the char.<sup>19</sup> Glass fibres are more sensitive than carbon fibres to high temperatures, indeed their mechanical properties decrease of 50% even at 450°C. The mechanical properties of recycled carbon fibres are comparable with the ones of virgin material, but they can be contaminated by char which can reduce the adhesion with the new matrix. Recovered glass fibres can be reutilized as reinforcement in the same way as the fibrous fractions obtained from mechanical drilling. Recycled carbon fibres can be re-used considering that the properties of the final product depend on the processing parameters.

Pyrolysis have two advantages: no solvents are involved in the process and all products are recovered and can be reused.<sup>15</sup>

Fluidised-bed pyrolysis process exploits a bed of silica sand which is fluidized by a stream hot air at temperatures ranging from 450°C to 550 °C. Composites are first reduced to 25

mm in size and then are fed into this bed. Fibers are released from the matrix which is vaporized in the fluidised-bed, then are brought out from the chamber with the gas stream and successively are separated by gases with a cyclone. At this point, fibers are not completely separated from the matrix, so a secondary combustion at higher temperature (1000°C) is needed. With this process contaminated materials as vehicle components can be treated and the obtained gas is used to recover energy as in the first case. Clean carbon fibres are recovered with fluidised-bed pyrolysis but with an unstructured architecture because their length and strength are damaged during the process.<sup>15</sup>

Carbon and glass fibres can be recovered also through micro-wave assisted pyrolysis process which is carried out in an inert atmosphere. In this process the thermal transfer is very fast since the composite material is heated in its core leading to energy saving.<sup>19</sup>

### **1.1.3.3 Chemical recycling**

Solvolysis is a chemical treatment which uses a solvent to degrade the resin. After its first application to unsaturated polyesters (UPs)<sup>20</sup>, a large number of different conditions were tested in order to recycle thermoplastics, thermosets and their fibre reinforced composites. Solvolysis offers many possibilities thanks to a broad range of solvents, temperature, pressure and catalysts. The temperature necessary to degrade polymers, such as UP and epoxides, are lower compared to pyrolysis, and this represents an advantage. To degrade the resin more or less high temperature and pressure are necessary. For example, polyester resins are easier to be recycled by solvolysis and require lower temperature than epoxy resins to be degraded. Water is the most used solvent, due to its temperature and pressure dependent properties and it is often used with alkaline catalysts (NaOH or KOH). To degrade polyether ether ketone (PEEK), more resistant resin, or epoxy resins at low temperature, water with acidic catalysts were used. Other solvents used are alcohols, acetone, glycols with or without catalysts. Solvolysis can be carried out at high temperature (>200°C) and pressure (HTP) or at low temperature (<200°C) and pressure (LTP). HTP often uses supercritical water in alkaline conditions, whereas for low temperature additives and catalysts in acid

medium are necessary to degrade resins. The advantage of LTP is the possibility of a better control of the reactions, however it uses solutions that are difficult to dispose or to recycle. With the aim to reclaim fibres, solvolysis, together with pyrolysis, is the most preferred technique to recycle composites: it enables the recovery of carbon fibres, maintaining their reinforcement capability. Solvolysis is also able to avoid the formation of char that contaminates the fibres. In oxidant, very acidic or alkaline conditions, solvolysis allows the recovery of cleaner fibres with respect to pyrolysis.<sup>19</sup>

In all the recycling methods explained above the reuse of the matrix in a new composite is not considered. This is due to the fact that the matrix of a lot of composite materials is a thermosetting material which is not soluble or reworkable. The problem can be overcome with the use of a polymer containing covalent adaptable network (CANs).<sup>21</sup>

## 1.2 Covalent Adaptable Networks

The increasing concern on sustainability and environmental responsibility as well as the rapid technological advancement, that have led to a decrease of the lifetime of products, make the reuse of thermosets after service life a very important topic and provide the motivation for the development of recyclable thermosets.<sup>13</sup>

This can be realized through covalent adaptable networks polymers or CANs, polymers that incorporate dynamic covalent bonds. With the presence of these bonds, by means of exchange reaction, thermosets become malleable, because they can be broken and reformed under a certain stimulus allowing the restructure of the network connections and making possible the reprocessability, the remendability and the recyclability.<sup>22</sup> Furthermore, self-healing, structural modification, processing of difficult-processing thermosetting polymers in solid phase can be achieved with reversible covalent bonds. These processes are energy saving and environmentally friendly. In addition, they are reversibly correlated with each other, so that life circle of synthetic polymers can be greatly extended.<sup>14</sup>

CAN combines the excellent mechanical properties of thermosets with the reprocessability of thermoplastics and so in this context the boundary between the two classes of polymers does not exist to a great extent. (Figure 1. 5)<sup>22</sup> These polymers are called covalent adaptable networks because they are adaptable to an external stimulus.



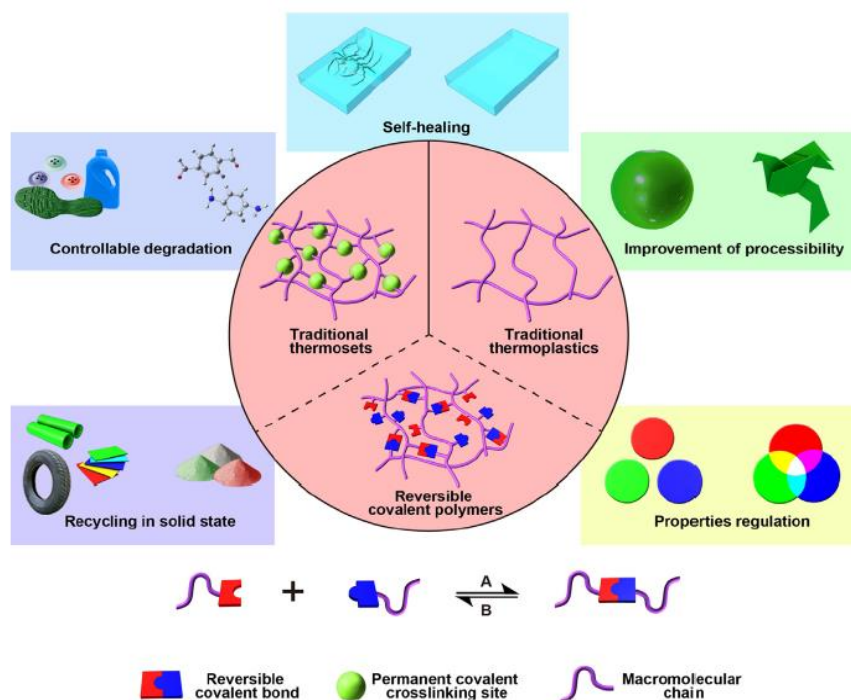
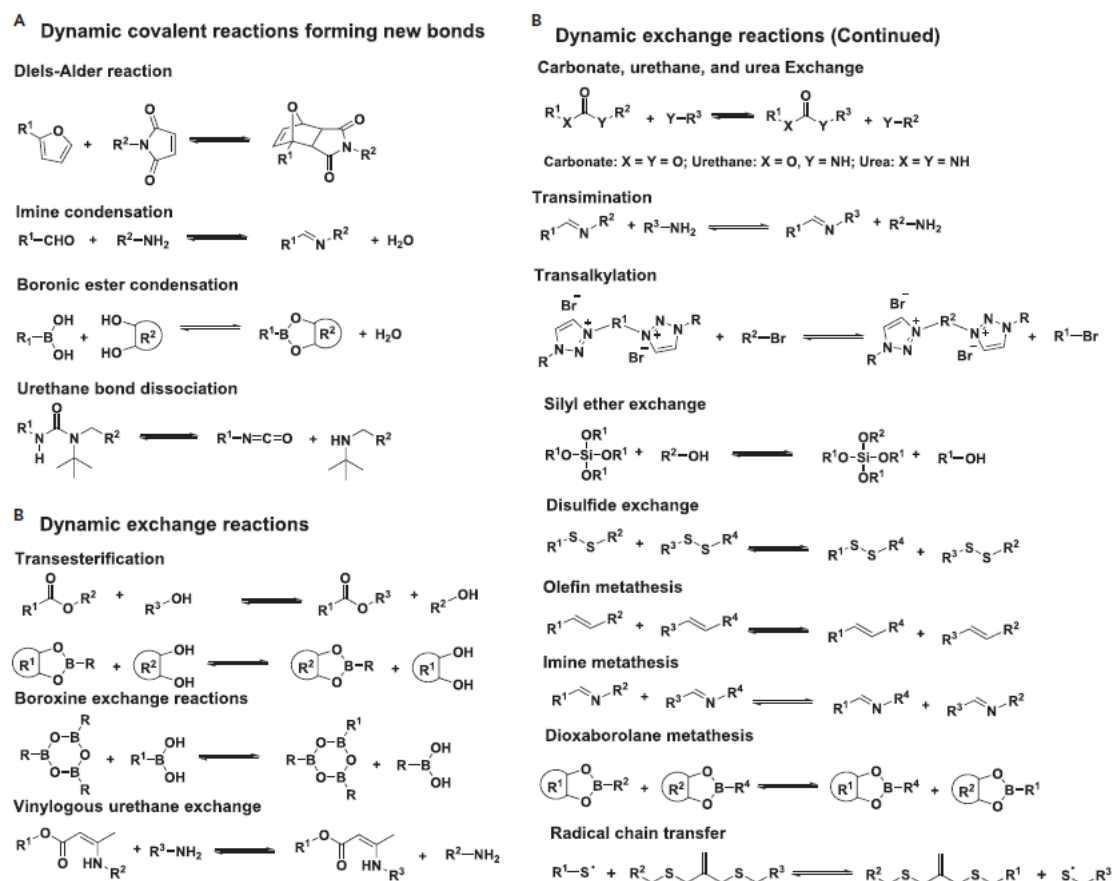


Figure 1. 5 Examples of polymer engineering<sup>14</sup>

There are a lot of dynamic covalent reactions that can be exploited in CANs and they are classified in two groups: 1) Exchange reaction, where the products and the reactants have the same type of bonds, as for example transesterification reaction or olefin metathesis; 2) reactions that involve the formation of new dynamic covalent bonds as addition or condensation reactions. Diels-Alder cycloaddition and imine condensation are two examples of reactions of the second group. These and other examples are reported in Figure 1. 6.

Figure 1. 6 Examples of CANs polymers reactions<sup>22</sup>

CANs reactions can follow two possible mechanisms. The first one is the one step mechanism. In this case the crosslinking density can be considered constant because the formation and the breakage of bonds occur almost at the same rate through the associative formation of a short-lived intermediate. In fact, this mechanism is also named associative pathway. The second one is called two step mechanism because two chemical steps are needed to accomplish the rearrangement of polymer chain connectivity. This is characteristic for example of Diels-Alder reactions where the retro-DA takes place to break the connected polymer chains and then the reconnection occurs through DA reaction by changing reaction temperature. In this case the crosslinking density depends on the kinetic of these two steps. This mechanism involves the breaking of crosslink and so it is also called as dissociative pathway.

These two mechanisms are explained in Figure 1. 7.

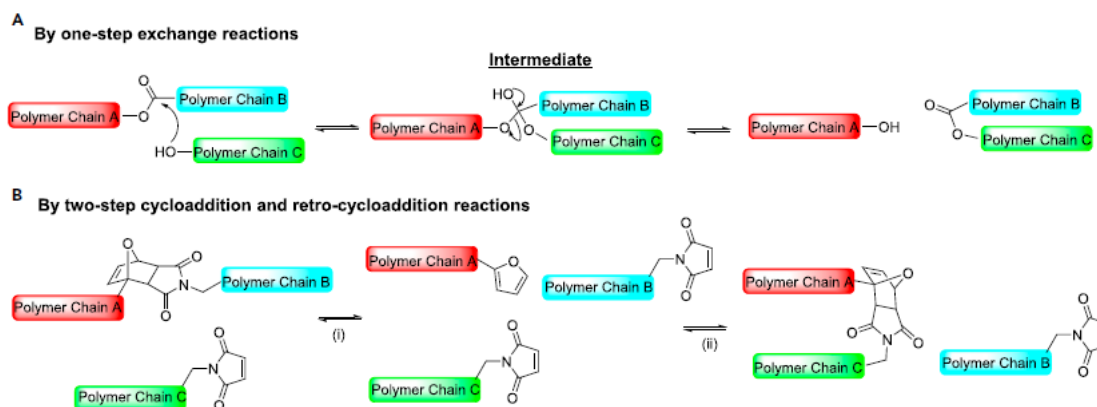


Figure 1. 7 CANs mechanism<sup>22</sup>

Sometimes more than one exchange mechanism can be present in the same system as it happens for polyhydroxyurethane CANs, where both an exchange reaction (the transcarbamoylation) and the breaking and the reforming of crosslinks (through reversible cyclic carbonate aminolysis) occur.

How the reversibility can be tuned on and off is one important criterion that has to be considered when choosing a dynamic covalent bond for malleable thermosets. Reversibility can be induced by an external physical factor such as light and temperature or by a catalyst. The activation energy associated to the reversible bond can be tuned by the choice of catalyst, monomer stoichiometry or substituent effects.<sup>22</sup>

### 1.2.1 Vitrimers

Usually in CANs polymers the reformation of crosslinks occurs at a temperature higher than the glass transition temperature ( $T_g$ ) when the motion of the chains is allowed. Indeed, CANs are thermoset polymers and their chain mobility is limited at a temperature lower than  $T_g$ . An exception to this behaviour is provided by vitrimers.

Vitrimers are CANs that show a gradual viscosity change that follows the Arrhenius model at a temperature above the  $T_g$ . They behave like silica vitreous and are coined *Vitrimers* by Leibler's group. The bond formation and the decrosslinking in this kind of CANs occur at the same rate and the exchange reactions are thermally activated. The exchange reaction rate follows an Arrhenius temperature dependence too.<sup>23</sup>

Vitrimers are organic strong glass formers made of atoms covalently bonded creating a network and are based on the reversible network topology freezing concept. Through bond exchange reactions the network can change its topology keeping constant in time the total number of bonds. When this occurs, the polymer relaxes and flows.<sup>23</sup>

For vitrimers two characteristic temperatures exist: the conventional  $T_g$ , below which a transition from elastic-state to a hard solid (a glass with modulus of about 1 GPa) is observed and the viscosity of the material changes abruptly and follows a WLF model, and the topology freezing transition temperature ( $T_v$ ), above which the reversibility is activated.<sup>23</sup>

$T_v$  can be defined also as the temperature at which “the mechanical relaxation time controlled by the exchange reaction rate becomes longer than the experimental time scale and on this time scale, the network topology is frozen.”<sup>23</sup> Below  $T_v$  the material appears as an elastic solid with a modulus that can vary from 1 MPa and 100 MPa depending on the crosslink density.

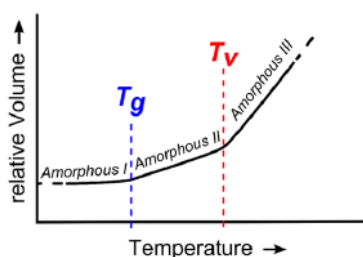


Figure 1. 8 V-T vitrimers characteristic<sup>23</sup>

Figure 1. 8 illustrates the trend of relative volume with respect to temperature and shows the two transitions that occur in vitrimers described above<sup>23</sup>.

Figure 1. 9 shows the trend of the viscosity versus temperature. Of note, when  $T > T_v > T_g$  the viscosity follows the Arrhenius law and it is governed by the kinetics of reversible bond breakage and reformation.

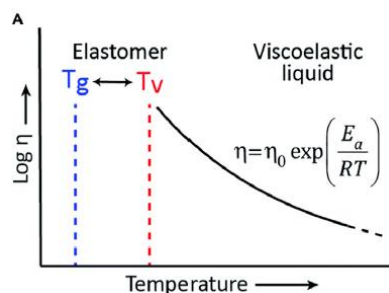


Figure 1. 9 Temperature dependence of viscosity for  $T_v > T_g$ <sup>23</sup>

In some cases,  $T_v$  is lower than  $T_g$  as represented in Figure 1. 10. The viscosity here first follows the WLF model near the  $T_g$  then, at higher temperature, the Arrhenius dependence on temperature can be observed.

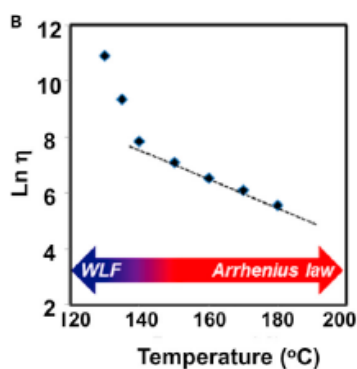


Figure 1. 10 Temperature dependence of viscosity for  $T_v < T_g$ <sup>22</sup>

$T_g$  is affected by crosslinking density and by the rigidity of monomer structure.  $T_v$ , instead, can be varied with the choice of dynamic bonds, catalyst and their concentration, and bond activation energy though the manipulation of the monomer structure. By changing  $T_v$  and  $T_g$  different processing and service temperature can be achieved.<sup>23</sup>

### 1.3 Diels-Alder Reaction

This reaction was already known in the 20<sup>th</sup> century and its discovery was attributed to Professor Diels and his student Alder who identified the products (4 and 6 of the schemes below) of the reaction between cyclopentadiene and quinone. (Figure 1. 11) They were rewarded with a reaction that bears their names and Noble Prize in Chemistry in 1950.<sup>24</sup>

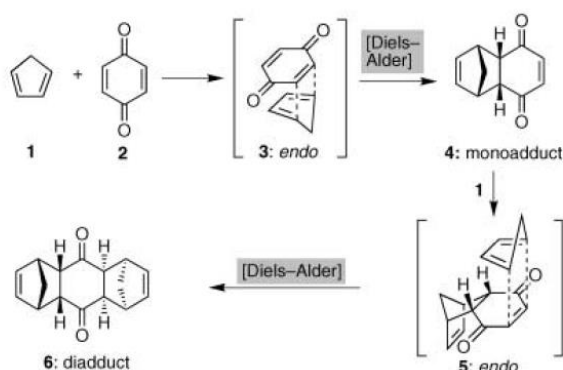


Figure 1. 11 Diels-Alder reaction between cyclopentadiene and quinone<sup>24</sup>

DA reaction is a cycloaddition of a conjugated diene and a substituted alkene also called dienophile. The product of this reaction is a six-membered ring as a result of the rearrangement of six  $\pi$ -electrons that leads to the formation of two  $\sigma$  bonds and one  $\pi$  bond. This reaction is called [4+2] cycloaddition, indeed six  $\pi$ -electrons are participating in this mechanism: four of the diene plus two of the dienophile.

When one of the two reactants is cyclic two different isomers can be formed, one endo oriented and the other exo oriented, depending on whether the substituents of the dienophile are oriented towards the diene or towards the other side, respectively. The endo product is usually favoured because of the secondary orbital interactions (endo-rule). Anyway, the ratio between the endo and the exo isomers can vary according to whether the reaction is kinetically or thermodynamically controlled.

Thanks to the endo-rule the stereochemistry of this type of reaction can be predicted.<sup>25</sup> In Figure 1. 12 of endo and exo products are reported:

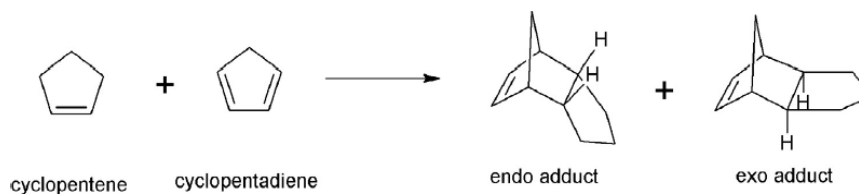


Figure 1. 12 Endo and Exo adduct of Diels-Alder reaction<sup>26</sup>

The reason why the endo product is preferred to the exo one is not precisely known nowadays, it is still object of discussion in literature but there are three aspects that can explain the endo-Rule: the secondary orbital interaction; the electrostatic attraction (and the closed shell repulsion) and the solvent effect.<sup>26</sup> Anyway, there are some methods to enhance the regioselectivity. One of these is based on the use of Lewis acids catalysts that affect the electronic behaviour of the diene/dienophile substituents. An example is the reaction between quinone and butadiene catalysed by  $\text{SnCl}_4$ . This Lewis acid reverses the electronic behaviour of oximes functional groups from electron-donating to electron-deficient and generating products that would not otherwise be observed.<sup>24</sup>

DA cycloaddition proceeds faster if a dienophile with electron withdrawing groups (as carbonyl or ketones) and a diene with electron donating groups (like alkyl chains) are utilized as reactants. This reaction is called “normal electron demand DA reaction”. An alternative reaction is the “reverse electron demand DA reaction” in which the electron distribution between the reactants is reversed and so in this case an electron-poor diene reacts with an electron-rich dienophile.

In Figure 1. 13 some examples of Dies-Alder reaction are reported.

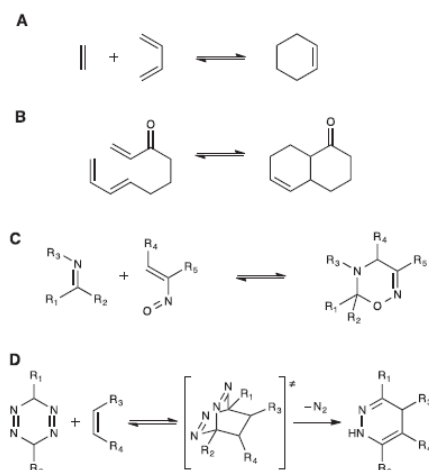


Figure 1.13 Examples of Diels-Alder reaction: a classical DA reaction A, an intramolecular DA reaction B, a hetero-DA reaction C and a reverse electron demand DA reaction D<sup>25</sup>

The second example in Figure 1.13 represents an intramolecular DA cycloaddition which occurs when diene and dienophile are part of the same molecule.

Another kind of DA reaction is the hetero-DA reaction which involves heteroatoms, as showed in the third example of the figure (C). Indeed, both diene and dienophile have the possibility to incorporate different hetero-atoms at any possible positions. The first hetero-DA reaction was carried out by Alder himself, who discovered that imine tautomer can be DA coupled to suitable dienes.

The last example represents a reverse electron demand cycloaddition (reaction D in Figure 1.13).<sup>25</sup>

Diels-Alder reaction belongs to click chemistry.<sup>27</sup> This chemistry was introduced by Sharpless and colleagues in 2001 who defined the requisites that a reaction must have in order to be considered a click reaction:

*“The reaction must be modular, wide in scope, give very high yields, generate only inoffensive byproducts that can be removed by nonchromatographic methods, and be stereospecific (but not necessarily enantioselective). The required process characteristics include simple reaction conditions (ideally, the process should be insensitive to oxygen and water), readily available starting materials and reagents, the use of no solvent or a solvent that is benign (such as water) or easily removed, and simple product isolation. [...] Click processes proceed rapidly to completion and also tend to be highly selective for a single product [...]”*<sup>28</sup>



DA reactions possess these criteria in fact DA cycloadditions can go on without the use of catalysts (although they are accelerated by Lewis acid catalyst), can proceed also at room temperature (even if in this case the kinetic reaction is slow), has no by products, can take place in water and so toxic solvent are not required and it has a high yield.

An important characteristic of the DA cycloaddition is its reversibility: at high temperature the retro DA reaction (rDA) is favoured giving a self-healing behaviour to polymers.<sup>25</sup>

### 1.3.1 Diels-Alder in Furan/Maleimide system

In the furan/maleimide couple, the furan acts as diene and the maleimide as dienophile. The scheme of the reaction is the following (Figure 1. 14):

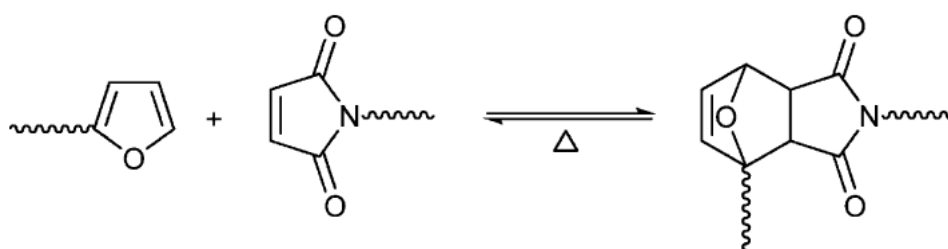


Figure 1. 14 DA reaction between Furan and Maleimide groups<sup>29</sup>

This couple represents a suitable system to build a large variety of macromolecules for the three reasons:

1. The retro Diels-Alder occurs at relatively low temperature: up to 60°C the left-to-right DA prevails while above about 110°C the rDA dominates,
2. Possible side products and thermal degradation mechanism can be neglected,
3. Furan reagents derive from renewable resources<sup>29</sup>

In the scheme above the endo and the exo isomers are not represented because they do not affect the formation and the thermal reversibility of this polymer in most situation. Anyway, an investigation on the role of endo/exo isomers in the retro-DA reaction has been carried out by J. Canadell et al.<sup>30</sup> on various DA adducts. The endo isomers were found to decouple at temperature 30-50°C lower than the exo ones, with

a small influence of the structure. In particular, typical retro DA temperatures for the endo products are around 90-100°C and for the exo isomers around 120-140°C.

Starting from different monomers containing the furan or the maleimide groups with different functionality, a large variety of polymer can be obtained

For instance, a linear DA polymer was obtained for the first time from bisfuran and bismaleimide monomer by G.C. Tesoro and V.R. Sastri.<sup>31</sup> In the synthesis of linear DA polyadduct two opposite approaches can be followed: the first has the aim of exploiting the thermoreversibility of these systems while with the second one a thermostable polymer is obtained through an aromatization reaction of the DA adduct. After the aromatization, the polymer is stable also at temperatures higher than the retro-DA temperature. An example of a polymerization between a difuran and a bismaleimide followed by an aromatization reaction, realized by Tesoro and Sastri, is reported in Figure 1. 15.

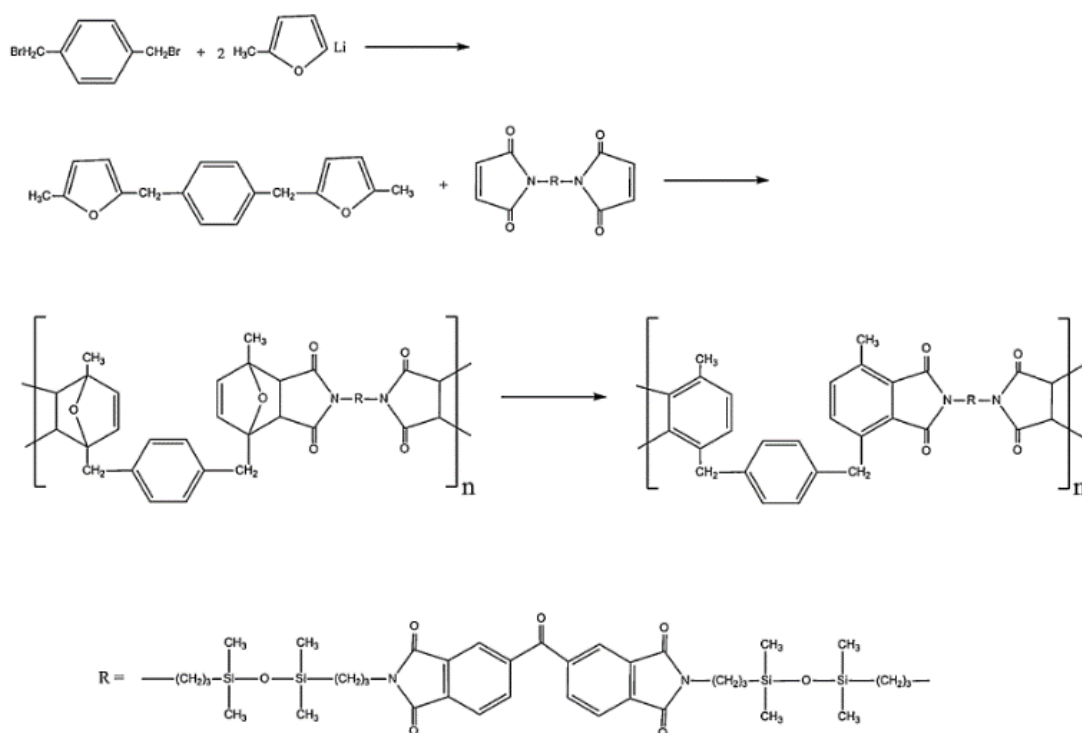


Figure 1. 15 Polymerization between a difuran and a bismaleimide<sup>31</sup>

Usually, in furan/maleimide system A-A and B-B monomers are used as in the above reaction but also A-B monomers can be synthesized like the 2-furfurylmaleimide (Figure 1. 16).

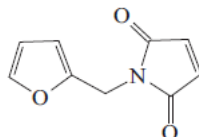


Figure 1. 16 2-furfurylmaleimide<sup>29</sup>

It was obtained from furfurylamine and maleic anhydride. This monomer did not polymerize with a simple DA cycloaddition and the lack of DA reactivity can be explained considering the electronic interaction between the two functional groups. The two heterocycles affect each other electronically so that the symmetry of the maleimide ring is perturbed since the two carbonyl groups of the maleimide ring are not equivalent. These two functional groups work as diene and dienophile when they lie further apart.<sup>32</sup> One of the first study about the retro-DA of a A-A B-B system is based on the evolution of the UV spectrum during polymerization and de-polymerization of the reaction sketched below (Figure 1. 17):

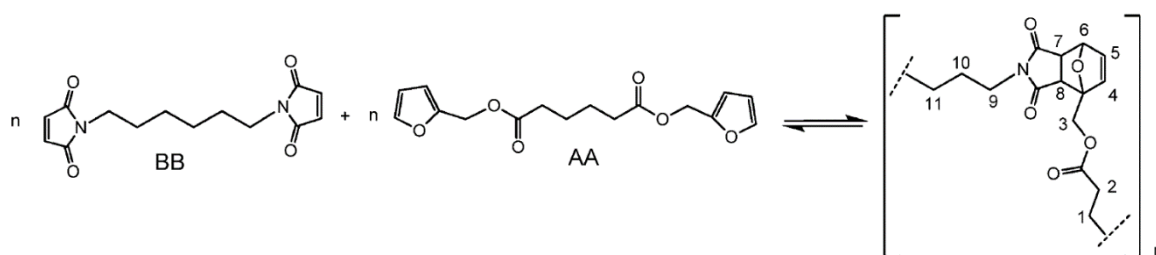


Figure 1. 17 DA reaction between an AA and BB monomer<sup>29</sup>

In the UV spectrum the decrease of the peak at 300 nm associated to C=O-C=C-C=O during the reaction can be observed, demonstrating the DA adduct formation (Figure 1. 18Figure 1. 17). This polymerization was carried out at 65°C and the retro-DA was found to occur at 110°C. During the de-polymerization the reverse trend was displayed on UV spectrum because of the decoupling of the adducts and the reformation of monomers.

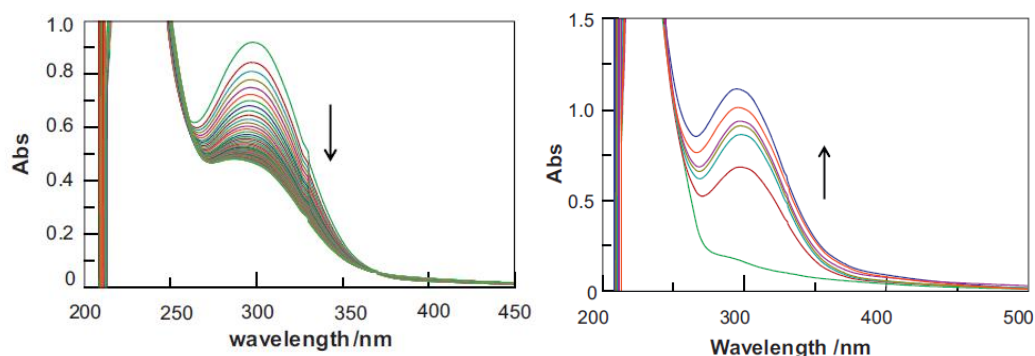


Figure 1.18 UV spectra during polymerization (left) and depolymerization (right)<sup>33</sup>

The first successful investigation on the thermoreversible polymerization of a furan/maleimide A-B monomer was based on the protected AB monomer, synthesized from  $\beta$ -alanine and furan maleic anhydride DA adduct. In fact, DA reaction can be used also to protect monomers from premature polymerization during storage and characterization. Then, by heating at 110°C the retro-DA takes place and the protection is removed. The system is successively cooled at 65°C to allow the polymerization (Figure 1.19).<sup>33</sup>

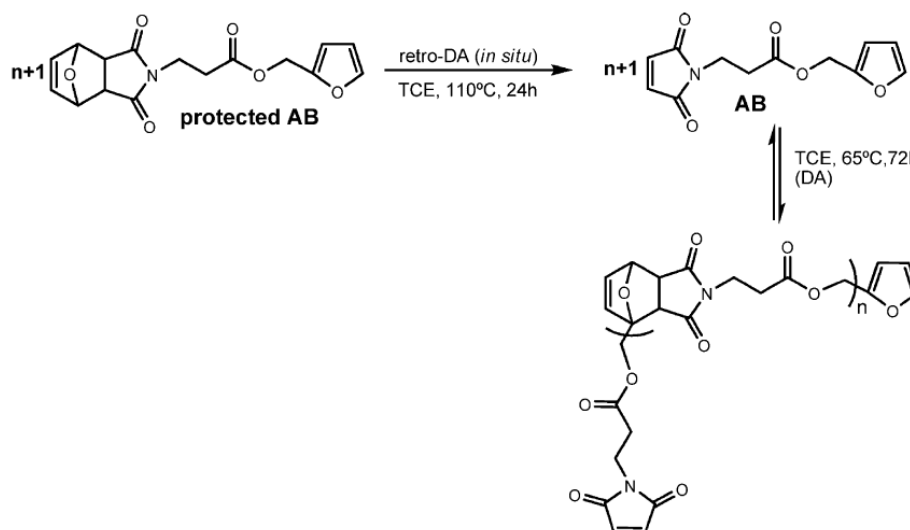


Figure 1.19 Polymerization of a furan/maleimide A-B monomer<sup>29</sup>

Thermal reversible non-linear polymers are obtained from multifunctional furan and maleimide monomers and are the first example of thermally mendable crosslinked materials. The mendability can be evaluated with a fracture toughness test and the

possibility of repairing cracks. By heating at 115-150°C and pressing the sample in the direction perpendicular to the crack the retro-DA takes place and furan and maleimide monomers are regenerated. Then, by cooling the network is formed again thanks to the formation of new DA adducts across the crack that disappears. Successively, Y.L. Liu and C.Y. Hsieh<sup>34</sup> developed a DA polymer starting from a tri-maleimide and a tri-furan and demonstrated its self-healing behaviour. A lot of investigations were dedicated to the study of epoxy network. The first research on this topic was made by Wudl et al. They realized a DA-epoxide bifunctional monomer, which is a system with two DA adducts end groups carrying pendant epoxy functionalities. They used this monomer as a component of a foam to test the possibility of removing foams with a hot solvent like butanol at 90°C, that favour the de-crosslinking of the network through the retro-DA. Another investigation showed that DA crosslinked film when intended by a hot tip underwent local depolymerization thanks to retro-DA, opening the possibility of using a DA network in maskless lithography. Optimizing the process parameters, a resolution of 20 nm can be achieved.<sup>35</sup>

Also reactions involving polymers carrying these two functional groups were realized and analysed. Three kinds of reactions are possible. In the first class, the reaction occurs between a polymer which includes one of the two heterocycles, and a multifunctional monomer containing the functional group not present in the polymer. For example, a DA polymer was obtained from multi-arm polylactic structures bearing furan groups and multifunctional maleimide and its thermoreversibility was verified.<sup>36</sup> The second case involves polymers with pendant furan and/or maleimide functional groups. Y. Chujo and co-workers<sup>37</sup> developed a DA polymer from two poly(oxazoline)s: one bearing furan groups and the other maleimide moieties with different degree of substitution. (Figure 1. 20) They found that the extent of the water swelling decreases as the degree of substitution grows since the crosslink density increases.

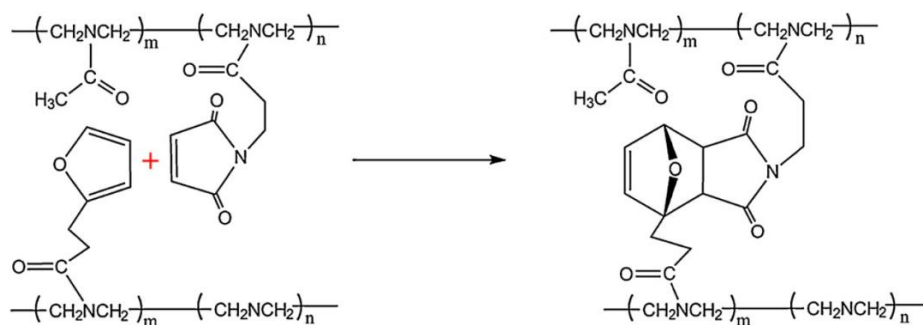


Figure 1. 20 Synthesis of a DA polymer from two poly(oxazoline)s<sup>37</sup>

If the crosslinked polymer is dipped in a hot solvent, after some hours the total solubilization is observed and <sup>1</sup>H NMR analysis confirmed the reformation of the two initial linear polymers through the retro-DA reaction.

In the third case furan and maleimide pendant groups are introduced onto the same polymer, as for example onto ethylene copolymer. The advantages of these systems stem from the fact that DA and retro-DA reaction can be performed in the bulk polymers with extrusion technologies.<sup>29</sup>

Furan/maleimide DA reaction can be exploited in different applications.

This couple of diene and dienophile can be used for example to reduce the surface tension: anionic surfactants, consisting of polar and non-polar moieties joined by furan/maleimide DA adduct, were synthesized by J.R. McElhanon et al<sup>38</sup>. The surface tension was found to increase upon heating above 95°C since the splitting of the two components through the retro-DA takes place.

Furan/maleimide DA adducts were also used to protect maleimide groups during polymerization to avoid side reactions between free radicals and maleimide moieties. At the end of the process upon heating the furans are all realised.<sup>39</sup>

To improve the electronic interaction between nanoparticles and macromolecules, organic-inorganic nanohybrids were generated by DA coupling a polymer bearing pendants furans groups and gold nanoparticles decorated with maleimide groups.

Furthermore, furan and maleimide couple was used to control the surface energy. Glass slide can be linked to furan groups through siloxane chemistry. When furans are DA

coupled with perfluorinated component bearing maleimides, the glass surface become hydrophobic. Then, refluxing toluene the maleimide compounds are removed and the surface returns to be hydrophilic.

The performance of polymer-based light-emitting-diodes can be improved thanks to DA reaction and its thermoreversibility. J.R. Reynold and co-workers<sup>40</sup> prepared a poly(fluorene) bearing pendant furan groups that crosslinked with two bismaleimides, one of which carried a red emitting donor-acceptor-donor moiety. As a result, emission and luminance were enhanced.

Healable polymers represent another application of furan/maleimide DA adducts. An example is the thermally reversible crosslinked polymer obtained by Weizman et al. from a tetra-furan and 1,10-(methylenedi-4,1-phenylene) bismaleimide which is characterized by self healing properties.<sup>41</sup>

The healing efficiency of furan/maleimide system can be improved with the use of plasticizers as benzyl alcohol. In a recent work, a non linear DA polymer (2M-2F3F) was obtained from an aromatic bismaleimide (1,1'-(methylenedi-4,1-phenylene), and two furan monomers: a difuran and a trifuran obtained from bisphenol A diglycidyl ether (DGEBA) and N,N-diglycidyl-4-glycidyyloxyaniline, respectively. Two samples were prepared, one with the 10% w/w of the plasticizers and the other without the benzyl alcohol. Scratches were made on the polymers surface. The healing in the sample with the additive was found to occur after 10 minutes at 120° in contrast to the sample prepared without the plasticizer in which after the same heating cycle the scratch was not completely healed. The healing efficiency of the sample with benzyl alcohol was preserved also after other cycles of scratching and healing. Mechanical tests on this sample were carried out studying the virgin, damaged and healed samples. After thermal cycle of 120°C/10 min the mechanical properties were partially recovered. The maximum stress was restored of 48% demonstrating a good thermoreversibility of the polymer network.

DSC and DMA analyses were conducted to find out the T<sub>g</sub> of the material and the temperature of the retro Diels-Alder reaction.

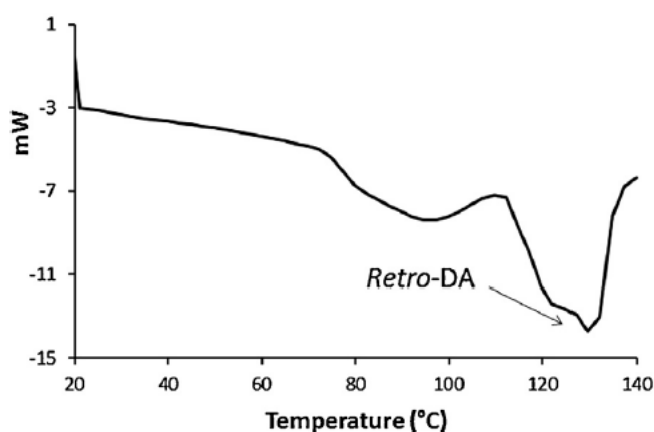


Figure 1. 21 DSC analysis of 2M-2F3F polymer<sup>42</sup>

Figure 1. 21 shows the DSC curve from which it is possible to find the T<sub>g</sub> of the material that corresponds to the first transition around 80°C and the temperature of the retro Diels-Alder reaction that coincides with the endothermic peak at 130°C.

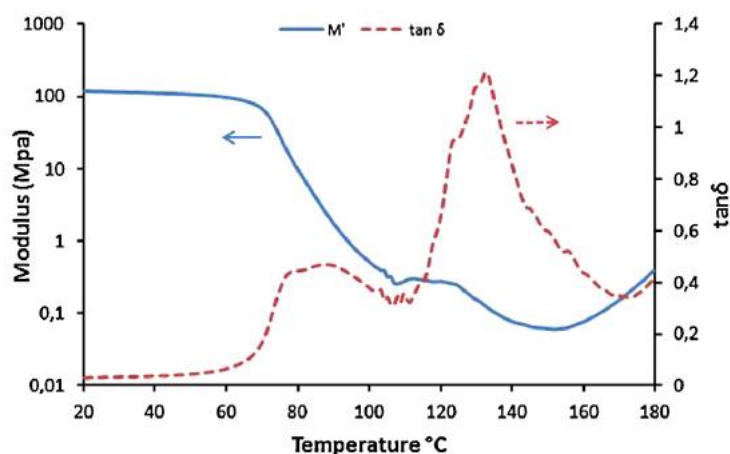


Figure 1. 22 DMA analysis of 2M-2F3F polymer<sup>42</sup>

The DMA analysis confirms this behaviour, indeed the  $\tan\delta$  curve reveals a peak around 130°C and a glass transition around 80°C (Figure 1. 22).<sup>42</sup>

In another work<sup>43</sup>, the kinetic of the DA reaction was studied. The reaction rate and the conversion rate of maleimide/furan DA polymers can be described with these formulas:

$$\frac{d[F]}{dt} = -k[F][M] + k'[DA]$$



$$\frac{dx(t)}{dt} = k[F_0](1 - x(t))^2 - k'x(t) = \frac{dQ}{dt} \frac{1}{\Delta_r H}$$

[F], [M] and [DA] are the concentration of furan, maleimide and of the DA product respectively,  $k$  and  $k'$  are the kinetic constants of the forward and retro-DA reaction,  $x(t)$  is the conversion,  $dQ/dt$  is the flux of heat and  $\Delta_r H$  is the reaction enthalpy.

This model was found to match the experimental data. At higher temperature the DA reaction proceeds faster but the retro DA becomes important and so the conversion will be lower, while at lower temperature the forward Diels-Alder reaction proceeds slower but with higher conversion.

The reaction enthalpy of the DA reaction is about -51.8 kJ/mol. This means that the new  $\sigma$  bond in the DA adduct is weaker than the typical covalent single C-C bond (368 kJ/mol) and so it will be preferentially broken in case of mechanical damage. (Therefore, the new C-C bond will break in a concerted process and furan and maleimide monomers will be reformed.)<sup>43</sup>

In the work of N.B. Pramanik et al.<sup>44</sup> a copolymer was synthesized from furfuryl methacrylate and butyl methacrylate via RAFT polymerization (reversible addition fragmentation chain-transfer). This copolymer reacted with the 1,1'-methylene-di-4,1-phenylene bismaleimide to obtain a crosslinked polymer. The self-healing behaviour of this material has been studied. The graph of DSC analysis shows also in this case that the retro DA occurs at 130°C.

To study the self-healing behaviour a notch in the surface of a film of this DA polymer has been generated with a blade. After heating at 130°C for 4 hours and then at 50°C for 24 hours, the crack was completely recovered. A mechanism to explain the healing process has been proposed. After crosslinking the polymer is characterized by a low chain mobility and a high hardness while, at high temperature, when the decrosslinking of the network occurs thanks to the retro-DA, the chain mobility increases. This leads to a reflow of the material and the healing occurs because of the reformation of the bonds through DA reaction.

Another demonstration of the DA reaction is given by solubility test. The obtained polymer was found to be insoluble in toluene at 30°C confirming the crosslinked nature of this material. Once heated a 130°C for 10 minutes it becomes soluble. It means that the polymer undergoes the retro-DA and the decrosslinking occurs.<sup>44</sup>

The utilization of renewable resources in polymer, the easy recycling and the biodegradability are becoming more and more important and so a biomass-based difuran has been synthesized by N. Teramoto et al.<sup>45</sup> In their study the difuran diene has been obtained from a reaction between trehalose, a disaccharide of glucose, and furfural, which was prepared through hydrolysis and dehydration of plants containing pentosans. Bismaleimidodiphenylmethane (BMIDP) and bismaleimidohexane (BMIH), two types of bismaleimides, were selected as dienophiles even if they are not renewable resources and so two different polymers were synthesized starting from the same biobased difuran: polymer 1 with the aromatic bismaleimide (BMIDP) and polymer 2 with the aliphatic one (BMIH).

To study the DA and the retro-DA GPC analysis was carried out (Figure 1. 23). The DA adduct 1 and 2 were formed at 70 and 55°C respectively because at that temperature the GPC graphs show the highest molecular weight. Increasing the temperature, the molecular weight decreases because the retro-DA competes with the DA.

To verify the retro cycloaddition polymer 1 and polymer 2 were heated in DMF at 140°C with a heating rate of 5°C/min. When the temperature was near 100°C part of the solution was taken out and analysed by GPC. The following graphs were obtained and compared with the ones of the starting monomers:

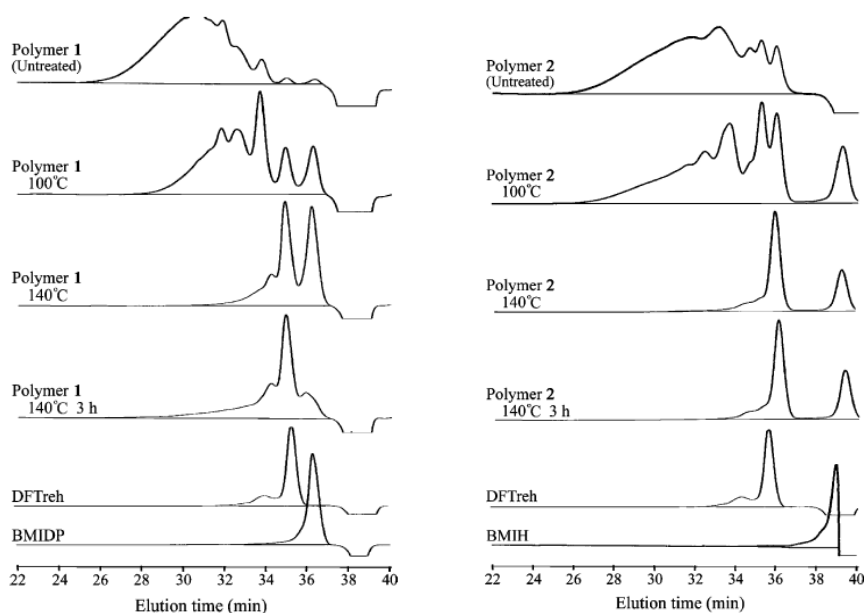


Figure 1. 23 GPC analyses of polymer 1 and polymer 2 compared with monomers<sup>45</sup>

When the temperature reaches 100 °C a shift of the molecular weight distribution towards lower molecular weight regions can be seen from the graphs, indicating that the retro-DA has already begun. At 140°C the retro cycloaddition is found to be almost completed, because the distributions above (Figure 1. 23) show the polymer decomposition into the corresponding monomers after 3 hours.

Therefore, the Diels-Alder cycloaddition meets two environmentally friendly aspects: first the polymerization proceeds under mild condition and usually without a catalyst, and second it is thermally reversible. In fact, the polymer obtained with the DA reaction can be decomposed into the starting monomers by increasing the temperature with the retro-DA.<sup>45</sup>

The importance of this particular couple of diene and dienophile is demonstrated also in the work of S. Magana et al.<sup>46</sup> in which they synthesized a thermoreversible crosslinked commercial polyethylene that have pendant furan and maleimide groups (Figure 1. 24.)

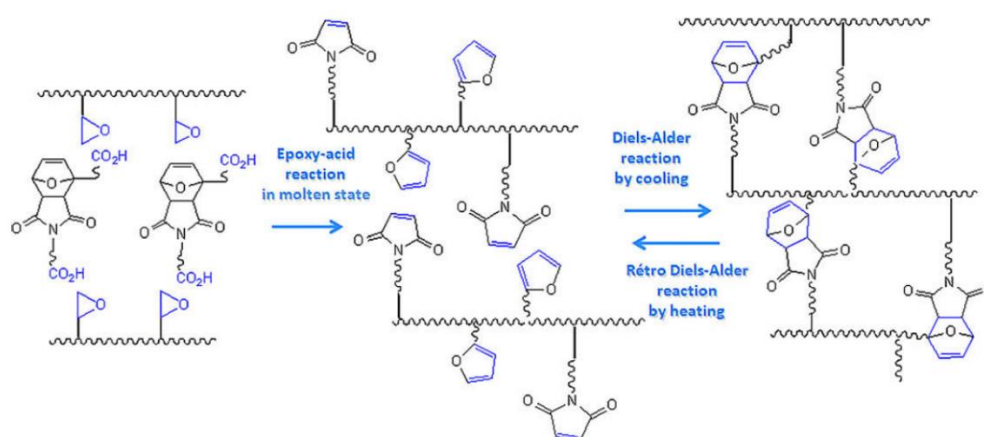


Figure 1. 24 Synthesis of a thermoreversible crosslinked commercial polyethylene<sup>46</sup>

The Diels-Alder and the retro DA were studied with FT-IR analysis monitoring the evolution of the intensity of the peak at  $1505\text{ cm}^{-1}$  and at  $700\text{ cm}^{-1}$  associated to C=C in furan and to the =C-H in maleimide respectively, versus temperature.

When the DA reaction occurs the absorption intensity of the C=C furan and =C-H maleimide should decrease while, when the retro-DA takes place, an increase of the intensity of these peaks is expected. The graph below (Figure 1. 25), that shows the evolution of  $I_R^*$  (the intensity of the peaks referred to the retro DA) versus the temperature confirm this trend. This trend indicates the regeneration of furan and maleimide groups and so it demonstrates the occurrence of the retro-DA.

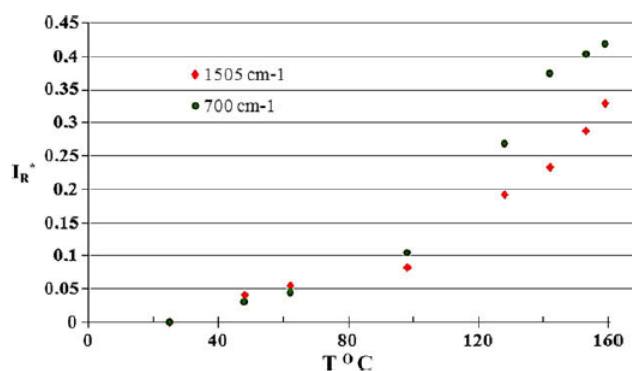


Figure 1. 25 Trend of the intensity of the peaks associated to furan and maleimide groups during rDA<sup>46</sup>

Upon cooling from  $140^{\circ}\text{C}$  to  $40^{\circ}\text{C}$  the intensity of C=C and =C-H was found to decrease indicating that the DA takes place. <sup>46</sup>

In a recent work a transparent DA-based acrylate for coating application was synthesized to overcome the issue of irreversible crosslinked nature of acrylic polymers, which are often used in coating industry because of their excellent durability, low cost and good adhesion. In order to obtain a colourless and transparent DA coating two aliphatic difunctional maleimides were synthesized: 1,6-bismaleimido hexane (C6) and 1,12-bismaleimido dodecane (C12). Each of the two dienophiles were mixed with furan functional polyacrylates, which were synthesized through free radical polymerization of FMA with one co-monomer among n-butyl methacrylate (BMA), 2-ethylhexyl methacrylate (EHMA) and lauryl methacrylate (LMA). In this way a crosslinking through DA cycloaddition between furan and maleimide is obtained. The coatings can be prepared with a thermal treatment after the deposition on a glass substrate.

The thermal reversibility of the DA coatings was studied with DSC technique (Figure 1. 26).

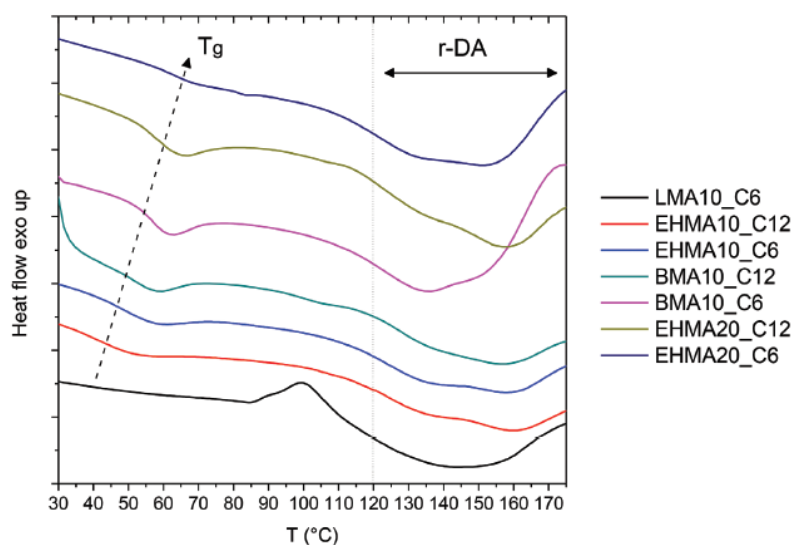


Figure 1. 26 DSC analyses of transparent DA-based acrylate polymers<sup>47</sup>

It can be noticed that all the samples show a single glass transition which is affected by the length of the maleimide: systems crosslinked with C6 are more rigid and therefore exhibit a higher  $T_g$ . The broad endothermic transition between 120°C and 170°C indicates the occurrence of the r-DA reaction.

Investigation of the self-healing character of the coatings was carried out producing scratches on the surface with a scalpel: after a thermal treatment at 150°C for 90 minutes followed by a slow cooling the cuts were found to be repaired.

Optical transparency and adhesion were studied in order to assess the suitability of these systems as transparent coatings. All DA coatings show a transmittance higher than 90% throughout the visible range, which is attributed to the amorphous nature of the DA polymeric networks.

The failure mode was found to be completely cohesive demonstrating an excellent coating-substrate adhesion. This kind of coating represents a promising platform for the development of self-healing system for optical applications.<sup>47</sup>

### **1.3.1.1 Bismaleimides**

Bismaleimides (BM) are often exploited with furan-functionalized monomers in order to obtain DA polymers. BM monomers contain two maleimide functional groups which are connected through an aromatic or aliphatic chain.

Most of the commercial BM contain multiple aromatic moieties which impart to the monomers high glass transition temperatures. These kind of bismaleimides are very widespread because of their good properties and of their low costs.<sup>48</sup>

A disadvantage of aromatic bismaleimide is related to their rigid structure. In fact, when fibers are incorporated in a resin consisting in furan-functionalized monomers crosslinked with aromatic bismaleimide, as in the work of G. Fortunato et al.<sup>21</sup>, the impregnation of the fibers in the matrix is not complete. This result in an inhomogeneous dispersion of the fibers in the matrix and in the formation of voids at the interface which leads to a low fiber/matrix adhesion. Moreover, aromatic bismaleimides exhibit a yellow color which make them useless in the preparation of DA based coating for optical application, where transparency is needed.<sup>47</sup>

To overcome these issue, aliphatic bismaleimides can be exploited. Aliphatic BM are less rigid than aromatic ones and are characterized by lower Tg. The drawbacks of this second class of BMs are their high costs and their low-yield synthesis often followed by long purification steps.

Figure 1. 27 shows some examples of the of commercial aromatic and aliphatic bismaleimides.

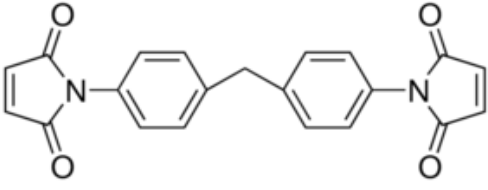
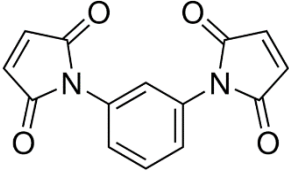
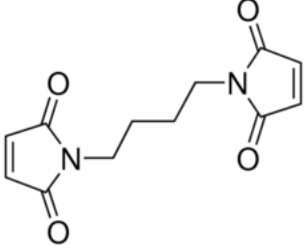
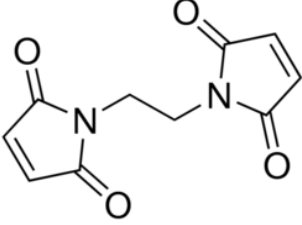
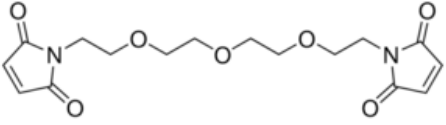
1,1'-(Methylenedi-4,1-phenylene)bismaleimide	
N,N'-(1,3-Phenylene)dimaleimide	
1,4-Di(maleimido)butane	
BMOE (bis-maleimidoethane)	
BM(PEG)3 (1,11-bismaleimido-triethyleneglycol)	

Figure 1. 27 Examples of Bismaleimides available on the market

An example of an aliphatic BM synthesis procedure was provided by Kossmehl in 1995<sup>49</sup>, who synthesized two aliphatic bismaleimides which differed in the length of carbon atom chain. The scheme of the reaction is depicted in Figure 1. 28, where R can be C<sub>6</sub>H<sub>12</sub> or C<sub>12</sub>H<sub>24</sub>:

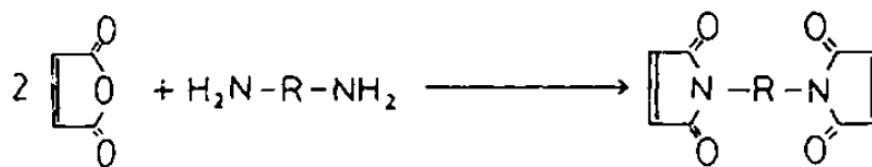


Figure 1. 28 Synthesis of aliphatic bismaleimide by Kossmehl<sup>49</sup>

The entire process is complex and can be divided in three steps: the actual reaction, the washing and the final purification of the product. Moreover, three catalyst are needed: nickel(II)acetate, acetic acid anhydride and triethylamine. The yield of the process was around 20/40%.

Another procedure was reported by Y. Stark et al.<sup>50</sup>, which prepared two aliphatic bismaleimides: the decane diol diester bismaleimide, obtained from maleimido hexanoic acid and decane diol (Figure 1. 29); and the dimer diester bismaleimide (Figure 1. 30) which was synthesized from the same acid and pripol 2033.

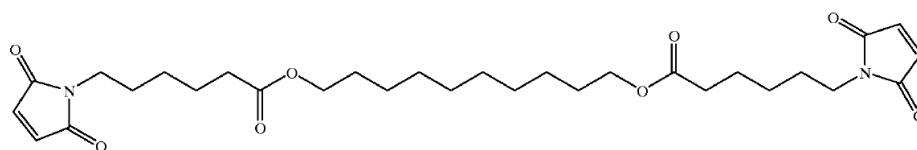


Figure 1. 29 Decane Diol Diester Bismaleimide<sup>50</sup>

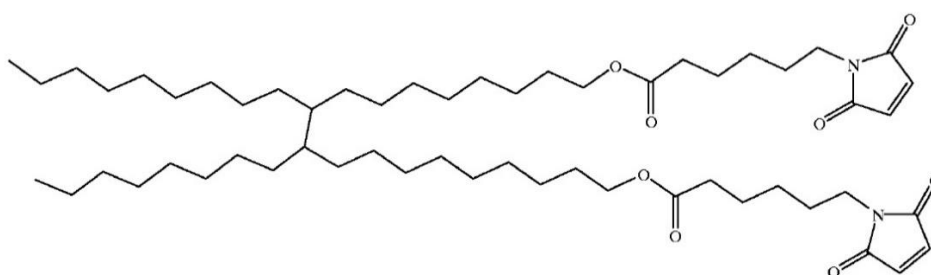


Figure 1. 30 dimer diester bismaleimide<sup>50</sup>

Also in this case, purification and washing steps are required. The reaction yield was around 58% for the decane diol diester bismaleimide and around 68% for dimer diester bismaleimide. Both reactions were catalysed by sulfuric acid, which is considered to be very dangerous and corrosive.



In this thesis a new aliphatic bismaleimide starting from 1,4-butanediol diglycidyl ether and maleimido hexanoic acid was obtained, with a yield around 85%. This reaction was catalyzed by pyridine, a less dangerous catalyst. In addition, the procedure was simple and did not required purification steps.

### **1.3.2 Diels-Alder in composite materials**

Diels-Alder chemistry was recently exploited in composite materials mainly in order to promote self-healing behaviour so that if the composite material is damaged, the matrix is able to repair the damage without substituting all the component.

In a recent work the healing behaviour of a composite polymer, made of a polyurethane derivative and unidirectional carbon fibers, was studied.

The matrix was synthesized in two different formulations by starting from a polyurethane derivative, furfuryl alcohol and N-(2-Hydroxyethyl)-maleimide.

The Tg of the material, the forward DA temperature and the rDA temperature were studied by DSC analyses and it was found that they correspond to 47°C, 96°C and 135°C, respectively.

The mechanical properties of the matrix and of the composite were studied too: mechanical properties of the composite base on a DA resin are comparable with the one of a composite made of commercial epoxy resins.

The studies of the healing behaviour showed a decrease of the healing efficiency with the increase of the healing cycles: after the first healing cycle the healing efficiency was 85% while after the second one it was around 73%.<sup>51</sup>

Due to the high viscosity of the polymeric matrix, the self-healing is usually slow. It was found in the work of C. Cai et al.<sup>52</sup> that, this issue can be overcome by using a nanocomposite material reinforced with graphene. The incorporated graphene, when it is in proximity of DA crosslinks, acts as an intrinsic localized thermal source. In fact, it was able to transform the absorbed infrared energy or microwave energy in heat energy, which enhanced the retro DA reaction speeding up the self-healing process. DSC

analyses indicated that the forward DA reaction occurred in a temperature range of 60–80°C while the retro DA one above 110°C. This system showed two other advantages: 1) 0,5 wt.% graphene could improve the strength of crosslinked epoxy resin matrix by more than two times; 2) the healing mechanism can be triggered by different approaches, including heat, IR light, and microwave, because of the multiple responsive nature of graphene.<sup>52</sup>

In the successive work of Cai et al., the same approach was used to provide to the material also a shape memory behaviour. In fact, this work was focused on the shape memory of composites, in addition to self-healing, and enhanced mechanical properties. The incorporation of Diels–Alder bonds also gave to the material a solid state plasticity through topological network rearrangement, thus leading to versatile shape adaptability.<sup>53</sup>

The scheme of the studied chemical principle is reported in Figure 1. 31:

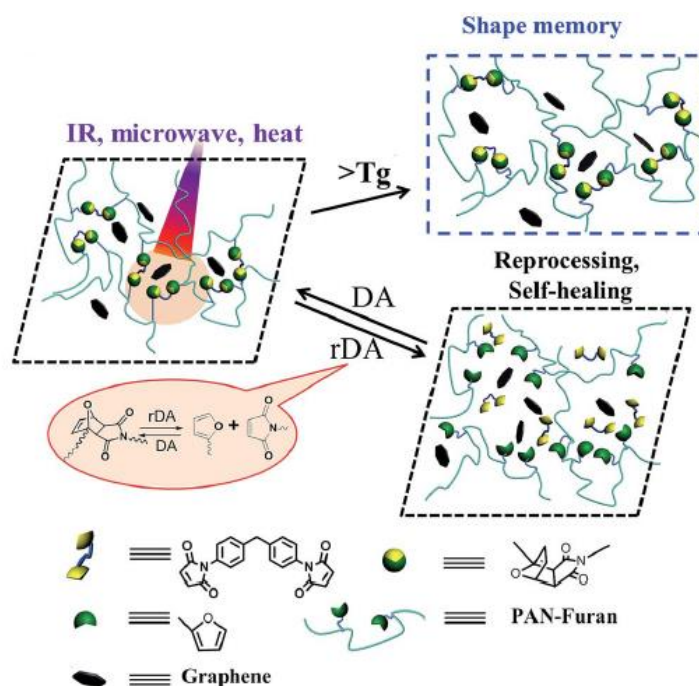


Figure 1. 31 Schematic diagram of the shape memory, healing and reprocessing mechanism by triggering glass transition and rDA reaction in thermally reversible DA-crosslinked PAN-DA/GR nanocomposites via multiple approaches including heat, microwave and IR light<sup>53</sup>

Mechanical properties of composite can be improved also by adding fullerene C60 as demonstrated by J. Chen et al. They prepared a reversibly crosslinked composite made

of aromatic polyamide (fPA) with pendant furan groups and fullerene. DA adducts were formed at moderate temperature between furan groups and fullerene which led to an increase of the mechanical and thermal properties. Tensile test showed that with the addition of 0,3% wt C60 the average modulus, the tensile strength and the elongation at break were improved compared to the mechanical properties of polyamide without fullerene. These improvements were attributed to the crosslinking between fPA and C60 which could spread the applied load across the whole network more efficiently, by dissipating more external energy. DMA analyses were in agreement with these results since they showed an increase of both the storage modulus and the Tg with the addition of a small amount of C60. In fact, a consequence of the crosslinking is the restriction effect on thermal motion of polymer chains. Recyclability of C60/fPA composite was assessed by dissolving the composite in 1-methyl-2-pyrrolidone and successively casted on a glass plate. Recycled composite exhibited mechanical properties comparable with the original material with a recovery efficiency higher than 95%. In addition, the crosslinking also improved the high temperature shape memory properties and in particular, the shape recovery rate and the recovery ratio increased by increasing the amount of C60.<sup>54</sup>

DA chemistry based on furan/maleimide adduct can be used also to enhance the interfacial adhesion between matrix and fibres. A.M. Peterson's group developed a composite made of a furan-functionalized epoxy-amine matrix which is crosslinked with maleimide-functionalized glass fibers in order to provide remendability at the interface between polymer and glass. A strong interface is obtained through the formation of DA adducts at room temperature, and upon heating above 90°C, a decoupling between fibres and matrix is observed, with the reformation of the original furan and maleimide groups. Healing was studied with single fiber microdroplet pull-out testing. The healing efficiency was around 41% and it was independent of the distance of displacement. For some species the recovery of the properties was shown to be of 100%. Up to five healing cycles were investigated demonstrating that, with maleimide functionalized glass fibers

incorporated in a furan functionalized network, it is possible to extend the fatigue life of composite materials.<sup>55</sup>

In addition to thermal reversibility, Diels-Alder reaction can be exploited in composite polymer to impart also recyclability, with the recovery and reuse of both fibers and resin in contrast to other technologies for composite recycling which are focused only on the recovery of fibers.

For the first time the recovery and the reuse of the matrix as DA coating was studied in a recent research. A DA resin was prepared from three monomers: a bifunctional furan compound (2F), a three functional furan compound (3F) and an aromatic bismaleimide (BM). This material was used as binder for different classes of carbon fibers to obtain a composite polymer.

Thermal reversibility was proved with DSC measures and by repeatedly reprocessing the crosslinked polymer by grinding and re-molding with compression molding up to 5 times. DSC analyses were recorded for the fresh sample and for the sample recycled 5 times. Both curves showed an endothermic transition between 120°C and 180°C related to r-DA reaction, proving the ability of the system to retain the thermal reversibility.

Two kinds of composite polymers were prepared: reinforced with nonwoven mat (DA/mat) or with unidirectional fibers (DA/UD). By SEM analysis it was noticed that for the polymer reinforced with nonwoven mat the impregnation of the fibers in matrix was good, but the fiber/matrix adhesion was not ideal since the formation of some voids in the matrix phase could be observed. In the DA/unidirectional composite the impregnation of fibers was not homogenous and in some region the fibers were not well dispersed in the matrix.

Tensile tests were made to study the mechanical properties of the composites which were compared with the ones of a composite prepared with commercial epoxies (Figure 1. 32).

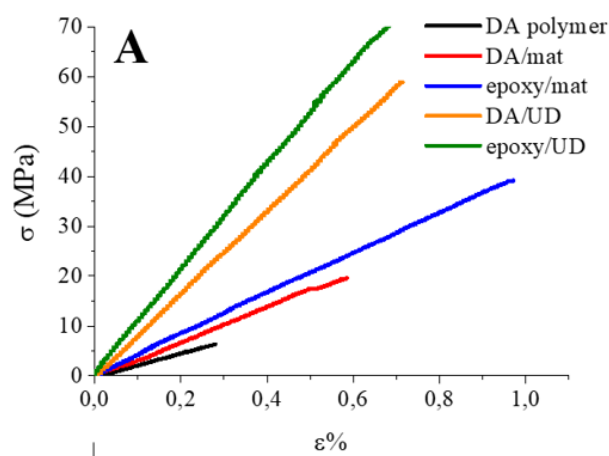


Figure 1.32 Mechanical properties of the different composite materials compared with the one of a composite based on a commercial epoxy resin<sup>21</sup>

It was observed that all samples broke without plastic deformation. Moreover, composites, reinforced with unidirectional fibers, had a higher tensile strength compared to DA/mat and epoxy/mat, if the stress was applied in the same direction of the fibers.

The recovery of the fibers was performed with a solvolysis approach for three classes of carbon fibers: milled, non-woven mat and unidirectional fibers. The sample was immersed in different solvent and then the system was heated at 120-125°C to allow r-DA reaction to take place.

The nonwoven mat reinforcement, after being recovered, was reused in a composite obtained with hot pressing between two layer of DA matrix. The recycled composite is characterized by a Young modulus of 3,2 GPa which corresponded to the 97% of the initial value and by a maximum stress lower than 5 MPa compared to the virgin composite (8MPa instead of 13MPa).

In all sample the purity of recovered fibers was very high and comparable with the one obtained from low or high temperature solvolysis.

In addition, the recovered DA polymers can be reused as smart polymer. The swelled DA polymer in DMF was heated to achieve complete de-crosslinking. Then, the solution was poured on a pre-heated glass substrate. After evaporation of the solvent, the coating was treated at 50°C to allow DA reaction to occur. To study the healing behavior, scratches were made on the surface. After a thermal treatment at high temperature followed by a slow cooling the cuts disappeared completely.<sup>21</sup>

# ***2. Materials***

## 2.1 Furfurylamine

Furfurylamine is a primary amine that comes from a reaction between the furfural and ammonia. This reaction is called reductive amination and it takes place when ketones or aldehydes are converted to amines. This occurs through the formation of an intermediate, an imine, that is treated with a reducing agent to form the amine. Furfurylamine contains also a furan group and is able to react with epoxy resins. The primary amine of furfurylamine can open the epoxy rings introducing furan groups in the resin. Furfurylamine is a yellow liquid with an ammonia odour. Its chemical structure is reported in Figure 2. 1.

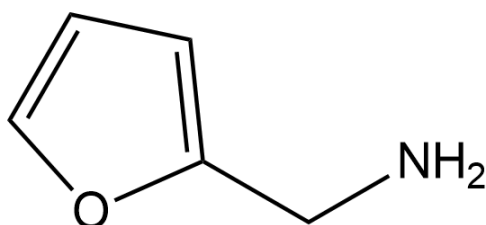


Figure 2. 1 Chemical structure of Furfurylamine

Table 2. 1 chemical properties of Furfurylamine

Molecular weight	97,12 g/mol
Density	1,10 g/cm <sup>3</sup>
Melting point	-70°C
Boiling point	145°C

## 2.2 Epoxy resins

Epoxy resins are thermosetting polymers that are obtained from epoxy monomers. This occurs through the curing process: the set of reactions that leads to the formation of the polymer network, the resin.

There are a lot of molecules that can be used as curing agent as for examples: amines, polyamines, isocyanate and anhydrides. The choice of the resin and of the curing agent depends on the process selected, on the required properties and on the application. Moreover, the kinetics, the glass transition temperature of the final material and the reaction mechanism are affected by the molecular structure of the curing agent.

The obtained resins can be represented as a 3D covalent polymer network that affect the properties of thermosetting of the material. These kinds of polymers, contrary to thermoplastic polymers, characterized by linear chains, can not be reprocessed and does not melt.

Epoxy monomers can be classified as aromatic or aliphatic and glycidyl or non glycidyl epoxies. The presence of an aromatic ring in the starting monomer makes the oxirane group very reactive. This effect is due to the strong electron-withdrawing effect of the bond between the aromatic ring and the oxygen of the ether.

Epoxy resins are employed as adhesive, surface coating, fibres reinforced plastics and electronics components because of their good insulating properties, their high chemical, thermal and corrosion resistance, and their great mechanical properties.<sup>56</sup>

In this work four different epoxy resins precursors were used: two aromatics, bisphenol A diglycidyl ether (DGEBA) and N,N-diglycidyl-4-glycidyoxyaniline DGGO, and two aliphatics, 1,4-butanediol diglycidyl ether (1,4BDE) and trimethylolpropane triglycidyl ether (TMPTE). All were purchased by Sigma-Aldrich.

DGEBA is produced by the alkylation of bisphenol A with epichlorohydrin. It is solid at room temperature and its chemical structure is reported in Figure 2. 2:



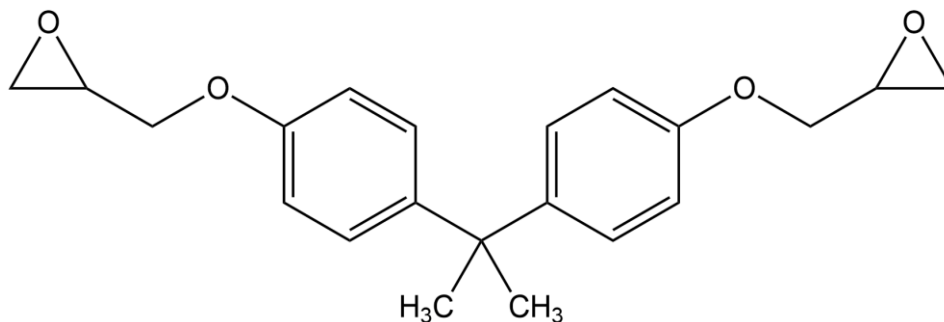


Figure 2. 2 Chemical structure of DGEBA

Table 2. 2 Chemical properties of DGEBA

Molecular weight	340,419 g/mol
Density	1,16 g/cm <sup>3</sup>
Melting point	40-44°C

DGGO is liquid at room temperature and it is characterized by three epoxy rings (Figure 2. 3):

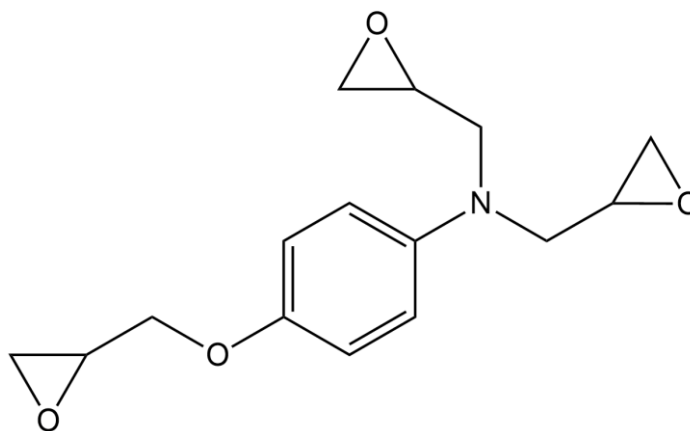


Figure 2. 3 Chemical structure of DGGO

Table 2. 3 Chemical properties of DGGO

Molecular weight	277 g/mol
Density	1,22 g/cm <sup>3</sup>
Boiling point	420,18 °C

1,4BDE is liquid at room temperature and his chemical structure is reported in Figure 2. 4:

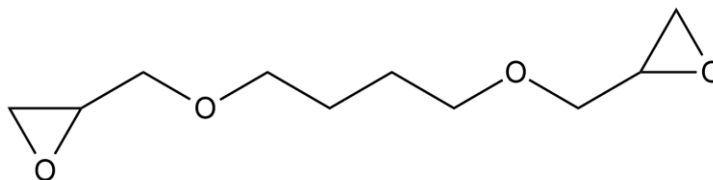


Figure 2. 4 Chemical structure of 1,4BDE

Table 2. 4 Chemical properties of 1,4BDE

Molecular weight	202,25 g/mol
Density	1,1 g/cm <sup>3</sup>
Boiling point	266°C

TMPTE is a viscous liquid at room temperature and contains three epoxy rings (Figure 2. 5):

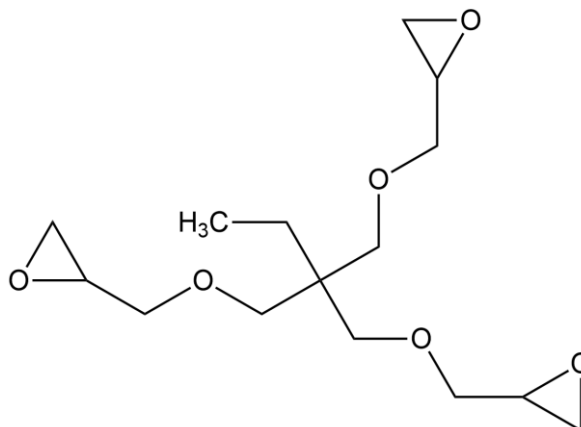


Figure 2. 5 Chemical structure of TMPTE

Table 2. 5 Chemical properties of TMPTE

Molecular weight	302,36 g/mol
Density	1,157 g/cm <sup>3</sup>
Boiling point	410,7 °C

## 2.3 Maleimido hexanoic acid

Maleimido hexanoic acid (MHA) is a carboxylic acid composed by two functional groups, the carboxylic and the maleimide, joined by a hydrocarbon chain.

The functional group of carboxylic acids is the carboxyl one that contains carbonyl and hydroxyl groups.

Carboxyl acids are characterized by:

- a higher boiling point with respect to other organic compound with a similar molecular weight;
- the formation of hydrogen bond when they interact with water, in fact they are more soluble than other compounds like alcohols or ethers. Their solubility in water decreases with the increases of molecular weight.
- Two regions with different polarity: the hydrophilic carbonyl group and the hydrophobic hydrocarbon chain. The longer hydrocarbon chain, the lower the solubility in water.<sup>57</sup>

Maleimide is a five-member ring with nitrogen on the top and two carbons double bounded to oxygens. The carbon-carbon double bond in the group is characterized by a high reactivity indeed maleimides act as diphenyl in the Diels-Alder reaction.

The structure of the maleimido hexanoic acid is reported in Figure 2. 6:

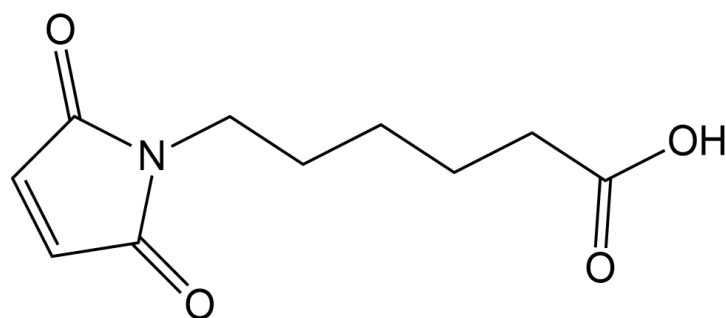


Figure 2. 6 Chemical structure of maleimido hexanoic acid

Table 2. 6 Chemical properties of maleimido hexanoic acid

Molecular weight	211,21 g/mol
Melting temperature	87-92 °C

## 2.4 Aromatic Bismaleimide

In this experimental work, a compound with two maleimide functional groups which are linked through a chain consisting of two phenyl rings were used: the 1,1'-(Methylenedi-4,1-phenylene) bismaleimide.

This bismaleimide appears as a solid yellow powder at room temperature. Its chemical structure is reported in Figure 2. 7.

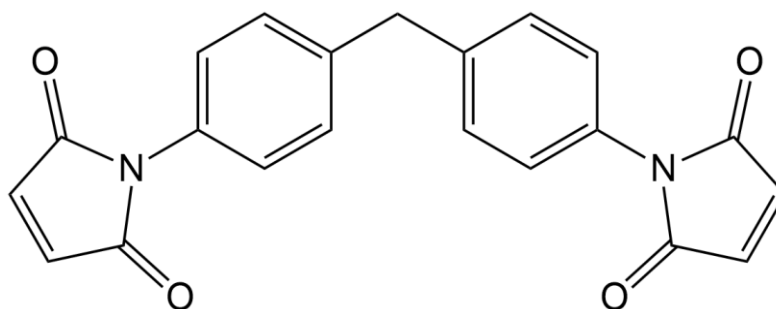


Figure 2. 7 Chemical structure of 1,1'-(Methylenedi-4,1-phenylene) bismaleimide

Table 2. 7 Chemical properties of 1,1'-(Methylenedi-4,1-phenylene) bismaleimide

Molecular weight	358,35 g/mol
Melting temperature	156 °C

## 2.5 Pyridine

Pyridine is a heterocycle organic compound that belongs to azine group which includes six atoms heterocycle components where at least one of them is nitrogen.

Pyridine can be produced from coal tar or synthesized by condensation of ketones or aldehydes with ammonia. It can be used as solvent of organic compounds, as denaturant for ethylic alcohol, as insecticide for plants or as catalyst. In this work it was used to catalyse the reaction between epoxy rings and carboxylic groups.

It is a highly flammable, weakly alkaline, water-miscible liquid which at room temperature is colourless and characterized by an unpleasant smell. The chemical structure is reported in Figure 2. 8:

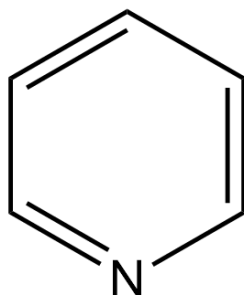


Figure 2. 8 Chemical structure of Pyridine

Table 2. 8 Chemical properties of Pyridine

Molecular weight	79,1012 g/mol
Density	0,978 g/cm <sup>3</sup>
Boiling point	115 °C
Melting temperature	-42 °C

## 2.6 Solvents

### Methanol

Methanol (CH<sub>3</sub>OH) is the simplest of alcohols and consists in a methyl group linked to a hydroxyl group. It is a polar, colourless, flammable and volatile liquid with a boiling point of 64,7 °C.

It was used as solvent in the furan compounds synthesis.

### Toluene

Toluene is also known as methyl benzene, indeed it consists of a methyl group linked to a phenyl group. It is a colourless and water-insoluble liquid with a boiling point of 111 °C. It was used as solvent in the bismaleimide synthesis. Its chemical structure is represented in Figure 2. 9:

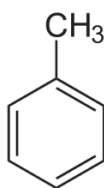


Figure 2. 9 Chemical structure of toluene

### Dimethylformamide

Dimethylformamide (DMF) is the amide of dimethyl amide and formic acid. It is a colourless liquid characterized by a boiling point of 153 °C, one of the highest boiling point among all the solvent. In this work it was used to verify the crosslinking/decrosslinking of the DA polymers. The chemical is reported in Figure 2. 10.

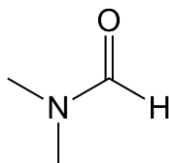


Figure 2. 10 Chemical structure of DMF

## **2.7 Carbon fibers**

Two kinds of carbon fibers were utilized: non-woven and woven.

The non-woven mats are mat characterized by a weight per square meter of 20 g/m<sup>2</sup>, while woven carbon fibres have a textile with a weight per square meter equal to 200 g/m<sup>2</sup>. Non-woven carbon fibers were purchased by TFP Global and unidirectional carbon fibers were provided by ZOLTEK Carbon Fibers.

## **2.8 Glass fibers**

Common woven unidirectional glass fibers, with a good mechanical resistance were used with a weight per square meter equal to 50 g/m<sup>2</sup>.

They were purchased by Prochima.

# ***3. Methods***



## 3.1 Synthesis

### 3.1.1 Bismaleimide synthesis (BM)

BM synthesis was based on the work<sup>58</sup>, where an aliphatic BM was synthesized from MHA and 1,4-butanediol, catalysed with sulfuric acid. The reactants and the catalyst were mixed in toluene in a three necks flask where nitrogen was supplied too. The solution was kept under stirring and heated to reflux: the water produced was collected in the dean stark trap. Successively, purification steps were needed. In this thesis a new procedure was found which require a simple equipment, short reaction steps and it is not followed by purification steps.

Maleimidohexanoic acid was dissolved in toluene at 50°C in a one-necked flask. 1,4-butanediol diglycidyl ether and pyridine, the catalyst, were added after complete dissolution. Pyridine was added with a concentration of 0,01% with respect to the moles of epoxies. The solution was kept under magnetic stirring for one hour and then it was transferred in a foil of Polytetrafluoroethylene. It was left under fume hood for three hours to make the solvent evaporate and successively it was put in a vacuum oven for one hour to ensure the complete removal of toluene. The mixture was therefore put in a beaker, heated gradually up to 130°C and stirred for 1 hour. The product was transferred in a tared Teflon and put in oven at 130°C to let the residual epoxy rings react. The scheme of the reaction is reported in Figure 3. 1:

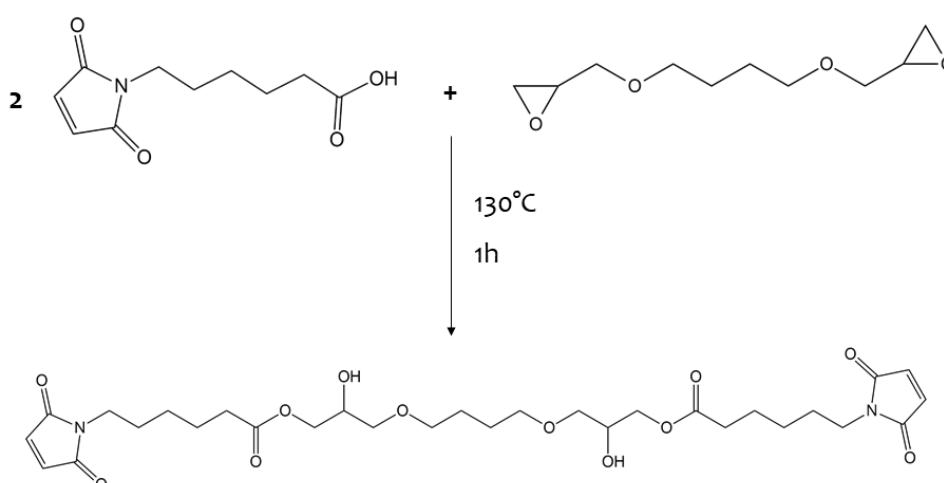


Figure 3. 1 reaction scheme of the synthesis of bismaleimide

Table 3. 1 bismaleimide synthesis

	<b>MW [g/mol]</b>	<b>mass [g]</b>	<b>moles [mol]</b>
<b>MHA</b>	211,12	3,34	0,016
<b>1,4BDE</b>	202,3	1,6	0,008
<b>BM aliphatic</b>	624,54	4,94	0,008

### 3.1.2 Furan Compounds Synthesis

DGEBA and DGGO were both functionalized with furfurylamine to obtain a bifunctional and a trifunctional aromatic furan compound. These two components were synthesized following the procedure reported in work<sup>21</sup>.

The same procedure was exploited in this experimental thesis for the first time in order to obtain aliphatic bifunctional and trifunctional furan compounds, starting from furfurylamine and two aliphatic precursors: 1,4BDE and TMPTE, respectively.

The equipment used for these syntheses was a three-necked flask immersed in an oil bath and connected to a bubble condenser. The system was kept under inert nitrogen atmosphere by using a rubber balloon. In all the syntheses methanol was used as solvent. The used quantity of solvent was 10 ml each 6 g of reacting epoxy resin.

The precursors were mixed in stoichiometric quantities: 1 mole of amine for each mole of epoxy group in the precursors.

### 3.1.2.1 Aromatic Bifunctional Furan (Aromatic 2F)

DGEBA was weighted into a three-necked flask. Methanol was added and the solution was stirred for 15 minutes with a magnetic stirring. After three cycles of evacuation and backfilling with nitrogen, inert atmosphere was obtained. Then the stoichiometry quantity of furfuryl amine was added with a sterile syringe to the flask. The mixture was kept at 85°C for five hours under magnetic stirring. The final product was poured, after cooling, in a previously tared one-necked flask so that it was possible to remove methanol and unreacted furfurylamine under vacuum in an oven at 120°C. The scheme of the reaction is reported in Figure 3. 2.

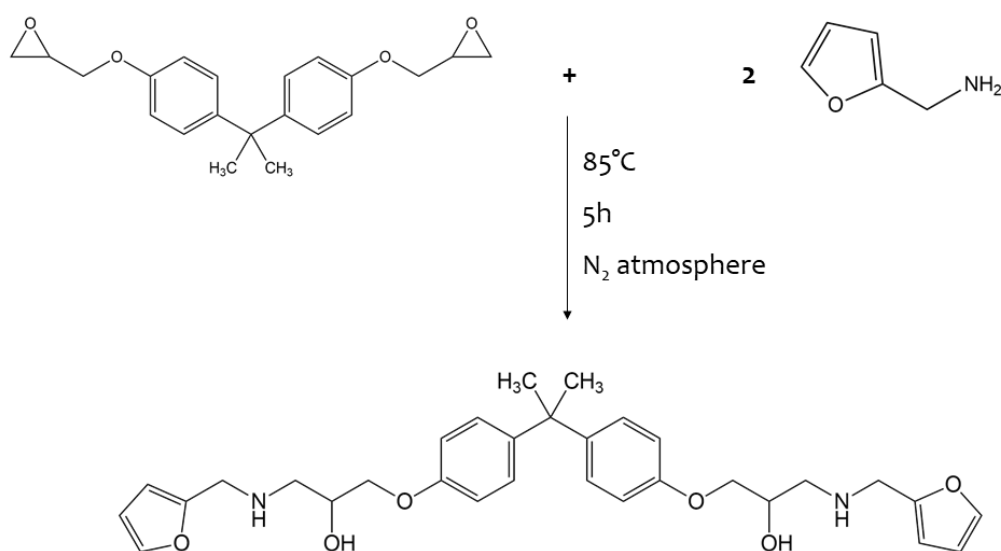


Figure 3. 2 2F Aromatic synthesis

Table 3. 2 2F aromatic synthesis

	<b>MW [g/mol]</b>	<b>mass [g]</b>	<b>moles [mol]</b>
<b>DGEBA</b>	340,2	6,00	0,02
<b>FA</b>	97,12	3,42	0,04
<b>Aromatic 2Furan</b>	534,66	9,42	0,02

### 3.1.2.2 Aromatic Trifunctional Furan (Aromatic 3F)

The functionalization of DGGO with furfurylamine by using the same above mentioned procedure leads to the formation of aromatic 3-Furan. The scheme of the reaction was reported in Figure 3. 3:

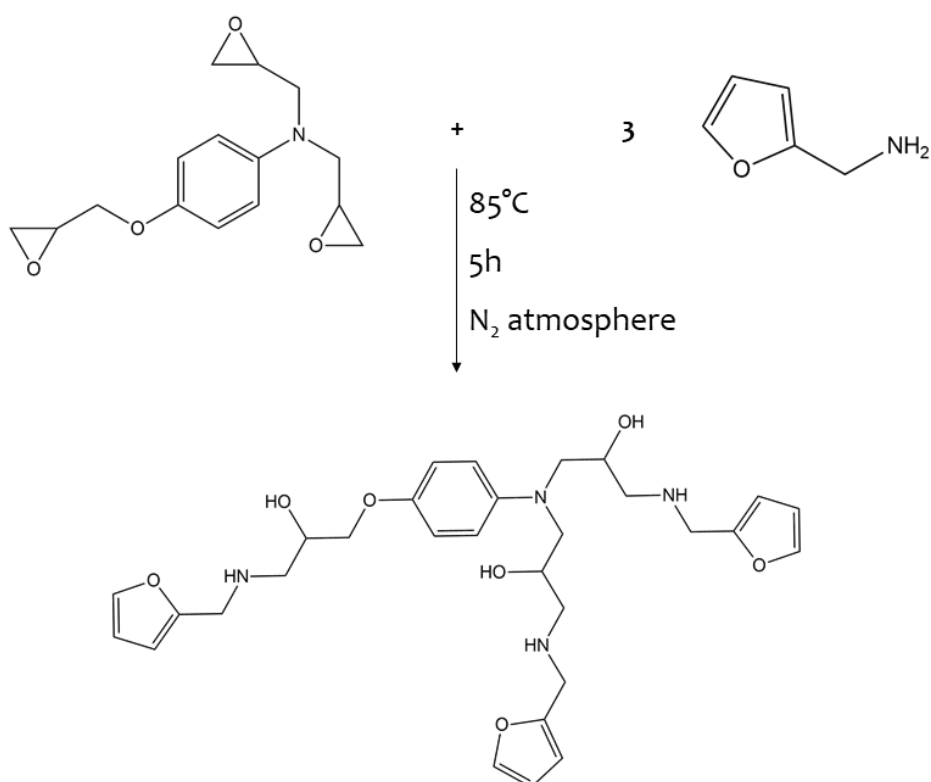


Figure 3. 3 3F Aromatic synthesis

Table 3. 3 3F aromatic synthesis

	<b>MW [g/mol]</b>	<b>mass [g]</b>	<b>moles [mol]</b>
<b>DGGO</b>	277,32	6,30	0,02
<b>FA</b>	97,12	3,42	0,06
<b>Aromatic 3Furan</b>	568,68	12,3	0,02

### 3.1.2.3 Aliphatic bifunctional furan (aliphatic 2F)

The functionalization of 1,4BDE to obtain aliphatic 2F was performed with the same procedure too. The reaction scheme is depicted in Figure 3. 4:

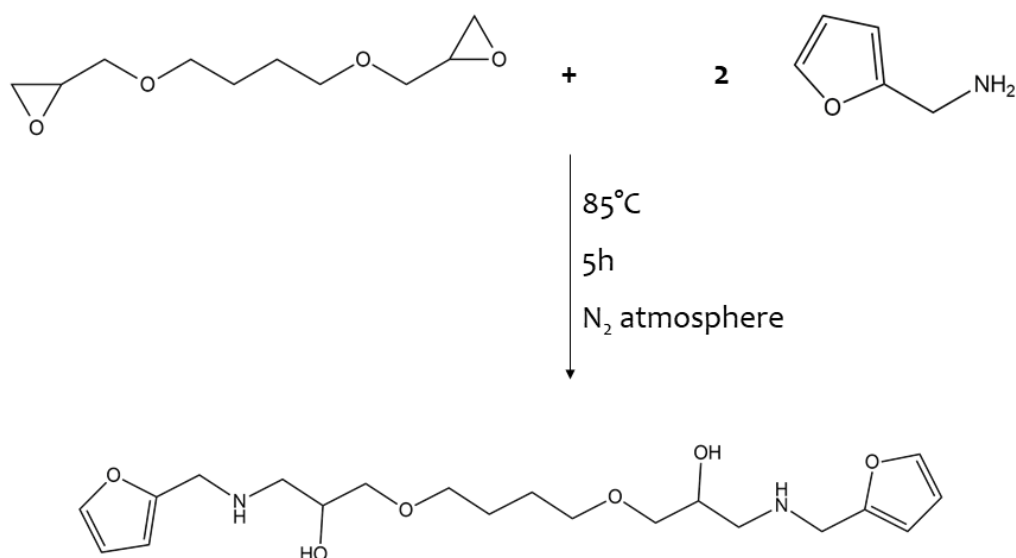


Figure 3. 4 Reaction scheme of the functionalization of 1,4BDE to obtain aliphatic 2F

Table 3. 4 functionalization of 1,4BDE to obtain aliphatic

	<b>MW [g/mol]</b>	<b>mass [g]</b>	<b>moles [mol]</b>
<b>1,4BDE</b>	202,3	6,00	0,03
<b>FA</b>	97,12	5,76	0,06
<b>Aliphatic 2Furan</b>	396,54	11,76	0,03

### 3.1.2.4 Aliphatic Trifunctional Furan (aliphatic 3F)

With the same method it is possible to obtain also aliphatic 3-Furan from TMPTE. The scheme of the reaction is reported in Figure 3. 5:

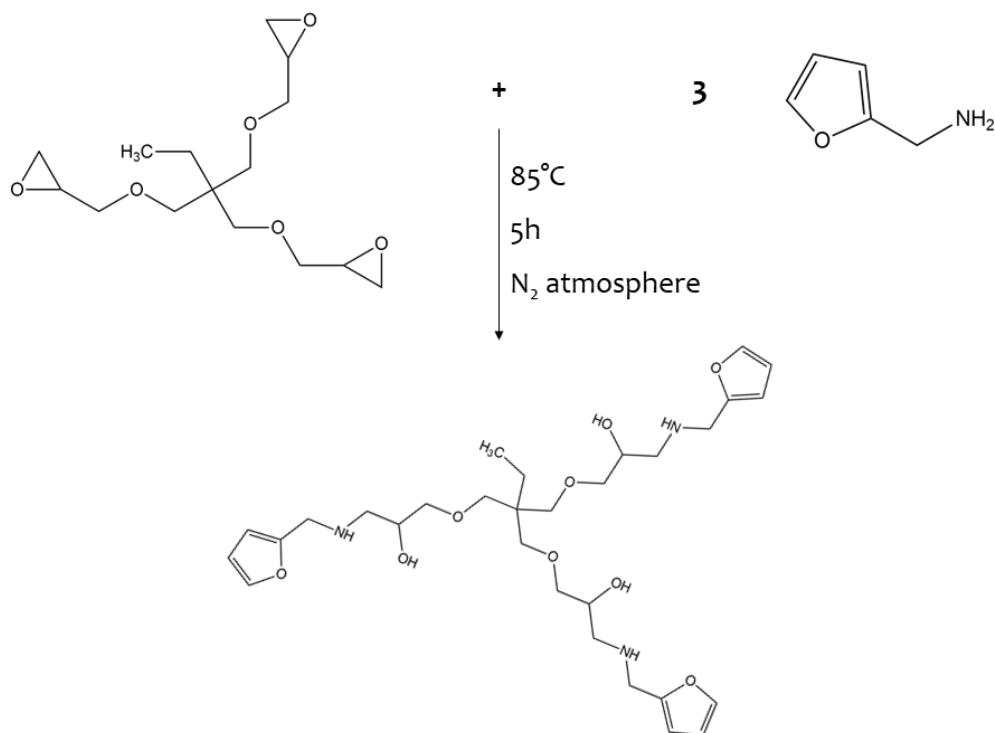


Figure 3. 5 reaction scheme of the functionalization of TMPTE to obtain aliphatic 3F

Table 3. 5 functionalization of TMPTE to obtain aliphatic 3F

	<b>MW [g/mol]</b>	<b>mass [g]</b>	<b>moles [mol]</b>
<b>TMPTE</b>	302,6	6,00	0,02
<b>FA</b>	97,12	5,78	0,06
<b>Aliphatic 3Furan</b>	593,72	11,76	0,03

### 3.1.3 Dies-Alder Polymers

In this study, the Diels-Alder reaction occurs between a furan group, that acts as diene, and a maleimide group, that acts as dienophile.

A bifunctional furan compound (2F), a trifunctional furan (3F) compound and the bismaleimide were mixed in stoichiometric ratio in order ensure that all the furan functional groups react with all the maleimide functional groups.

In this work four Diels-Alder polymers were obtained (Table 3. 6):

Table 3. 6 DA polymers

Aliphatic 2F	Aliphatic 2F	Aromatic 2F	Aromatic 2F
+	+	+	+
Aliphatic 3F	Aromatic 3F	Aliphatic 3F	Aromatic 3F
+	+	+	+
Aromatic BM	Aliphatic BM	Aliphatic BM	Aliphatic BM
↓	↓	↓	↓
<b>DA polymer S0</b>	<b>DA polymer S1</b>	<b>DA polymer S2</b>	<b>DA polymer S3</b>

Different average functionalities ( $f_{av}$ ) were considered in order to find the highest value of  $T_g$  for each DA polymer.  $f_{av}$  equal to 2,2; 2,5 and 2,8 were selected for DA polymer 1,2 and 3. An average functionality equal to 3 was considered only for DA polymer 1, since for this system it was found out that the  $T_g$  increased with  $f_{av}$ .

DA polymer so was studied only with a  $f_{av}$  equal to 2,2. In fact, it was demonstrated that So could be synthetized only with the use of a solvent, which is not the aim of this thesis and therefore no further studies were taken forward.

The average functionality of a polymer obtained from two precursors can be calculated with this formula:

$$f_{av} = \frac{mol\ 2F * n2F + mol3F * n3F}{mol2F + mol3F}$$

Where  $mol\#F$  is the number of moles of the considered furan compound and  $n\#F$  is the number of functional groups of the considered furan compound.

4 mol of 2F and 1 mol of 3F were mixed to have a stoichiometric ratio of 4:1 needed to have an average functionality of 2,2 and so the formula above can be rewritten in this way:

$$f_{av} = \frac{4 \text{ mol} * 2 + 1 \text{ mol} * 3}{4 \text{ mol} + 1 \text{ mol}} = 2.2$$

The number of moles of bismaleimide is given by half of the total moles of furan groups since BM has two maleimide functional groups. The total moles of furan functional groups are equal to 11 and so the total moles of bismaleimide needed are 5,5.

$$\text{mol } 3F : \text{mol } 2F : \text{mol } BISM = 1 : 4 : 5.5$$

In order to have an  $f_{av}$  equal to 2.5 a stoichiometric ratio mol3F:mol2F of 1:1 is required and so 1 mol of 2F was mixed with 1 mol of 3F:

$$f_{av} = \frac{1 \text{ mol} * 2 + 1 \text{ mol} * 3}{1 \text{ mol} + 1 \text{ mol}} = 2.5$$

The total number of moles of bismaleimide in this case is 2,5 since the total moles of furan groups are 5:

$$\text{mol } 3F : \text{mol } 2F : \text{mol } BISM = 1 : 1 : 2.5$$

To obtain a  $f_{av}$  of 2,8, 1 mol of 3F was mixed with 0,25 mol of 2F:

$$f_{av} = \frac{0,25 \text{ mol} * 2 + 1 \text{ mol} * 3}{0,25 \text{ mol} + 1 \text{ mol}} = 2.8$$

In this case the moles of bismaleimide are 1,75 and so:

$$\text{mol } 3F : \text{mol } 2F : \text{mol } BISM = 1 : 0,25 : 1,75$$

When  $f_{av}=3$  only the 3 Furan is present in the polymer. 1 mole of 3F corresponds to 1,5 moles of bismaleimide:

$$\text{mol } 3F : \text{mol } BISM = 1 : 1,5$$



For each DA polymer, mass and moles of reactants are summarized in Table 3. 7, Table 3. 8, Figure 3. 9 and Table 3. 10.

Table 3. 7 DA polymer S<sub>0</sub> synthesis

<b>DA polymer S<sub>0</sub></b>				
		<b>Aliphatic 2F</b>	<b>Aliphatic 3F</b>	<b>Aromatic BM</b>
$f_{av}=2,2$	<b>MW [g/mol]</b>	396,54	593,72	358,35
	<b>Mass [g]</b>	1,3358	0,5000	1,6598
	<b>Moles [mol]</b>	0,0034	0,0008	0,0046

Table 3. 8 DA polymer S<sub>1</sub> synthesis

<b>DA polymer S<sub>1</sub></b>				
		<b>Aliphatic 2F</b>	<b>Aromatic 3F</b>	<b>Aliphatic BM</b>
$f_{av}=2,2$	<b>MW [g/mol]</b>	396,54	568,68	624,54
	<b>Mass [g]</b>	1,39460	0,50000	3,02013
	<b>Moles [mol]</b>	0,00352	0,00088	0,00484
$f_{av}=2,5$	<b>Mass [g]</b>	0,34865	0,50000	1,37278
	<b>Moles [mol]</b>	0,00088	0,00088	0,00220
$f_{av}=2,8$	<b>Mass [g]</b>	0,08716	0,50000	0,96095
	<b>Moles [mol]</b>	0,00022	0,00088	0,00154
$f_{av}=3$	<b>Mass [g]</b>	0	0,50000	0,82367
	<b>Moles [mol]</b>	0	0,00088	0,00132

Table 3. 9 DA polymer S2 synthesis

<b>DA polymer S2</b>				
		<b>Aromatic 2F</b>	<b>Aliphatic 3F</b>	<b>Aliphatic BM</b>
$f_{av}=2,2$	<b>MW [g/mol]</b>	534,66	593,72	624,54
	<b>Mass [g]</b>	1,80105	0,50000	2,89275
	<b>Moles [mol]</b>	0,00337	0,00084	0,00463
$f_{av}=2,5$	<b>Mass [g]</b>	0,45026	0,50000	1,31489
	<b>Moles [mol]</b>	0,00084	0,00084	0,00211
$f_{av}=2,8$	<b>Mass [g]</b>	0,11257	0,50000	0,92042
	<b>Moles [mol]</b>	0,00021	0,00084	0,00147

Table 3. 10 DA polymer S3 synthesis

<b>DA polymer S3</b>				
		<b>Aromatic 2F</b>	<b>Aromatic 3F</b>	<b>Aliphatic BM</b>
$f_{av}=2,2$	<b>MW [g/mol]</b>	534,66	568,68	624,54
	<b>Mass [g]</b>	1,88035	0,50000	3,02013
	<b>Moles [mol]</b>	0,00352	0,00088	0,00484
$f_{av}=2,5$	<b>Mass [g]</b>	0,47009	0,50000	1,37278
	<b>Moles [mol]</b>	0,00088	0,00088	0,00220
$f_{av}=2,8$	<b>Mass [g]</b>	0,11752	0,50000	0,96095
	<b>Moles [mol]</b>	0,00022	0,00088	0,00154

The two furan components were mixed in a beaker under magnetic stirring at 130°C. Then the corresponding quantity of bismaleimide was added and the system was stirred at 130°C for 10 minutes. The reaction was carried out without solvent. The obtained polymer was transferred in a previously tared teflon container and put in oven at 50°C for 2 hours so that the Diels-Alder reaction takes place.

The reaction schemes are reported in Figure 3. 6, Figure 3. 7 and Figure 3. 8, where

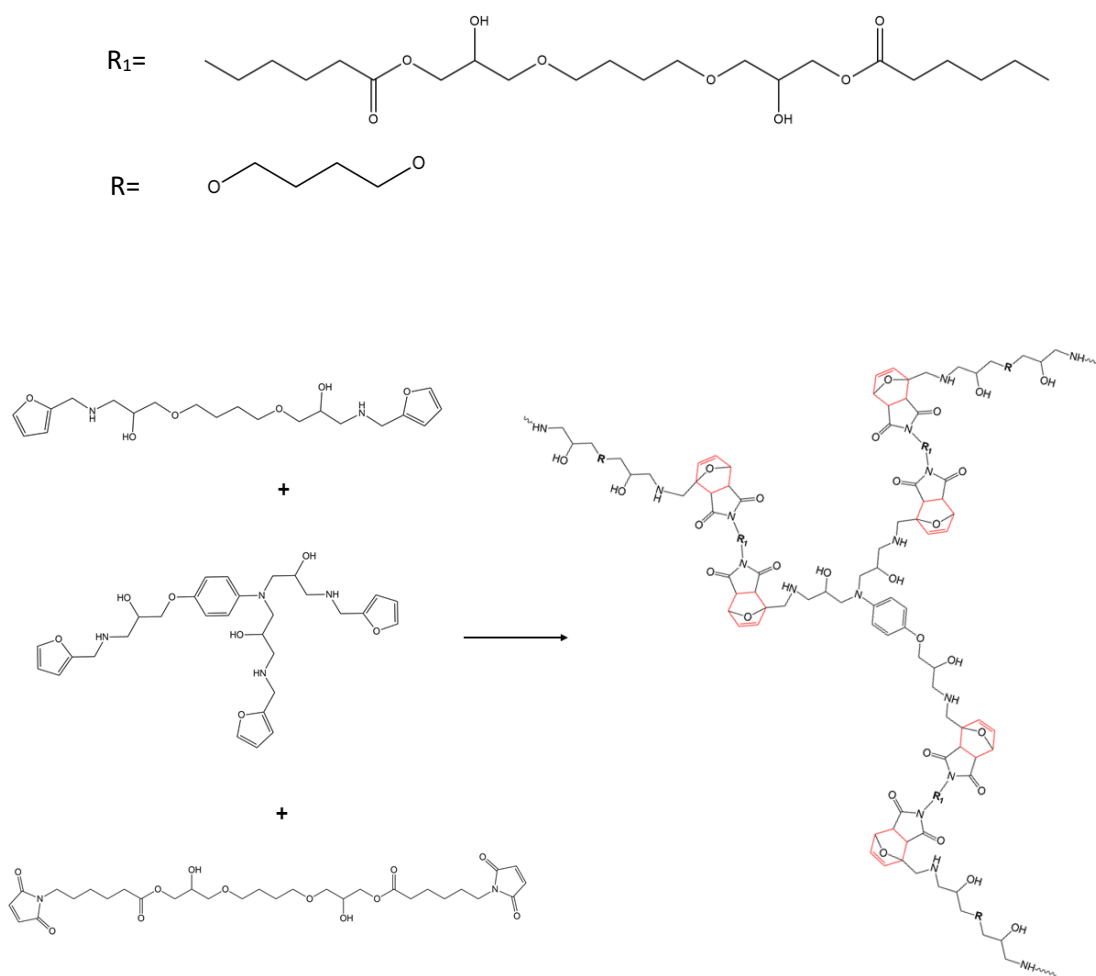


Figure 3. 6 Reaction scheme of the synthesis of DA polymer 1

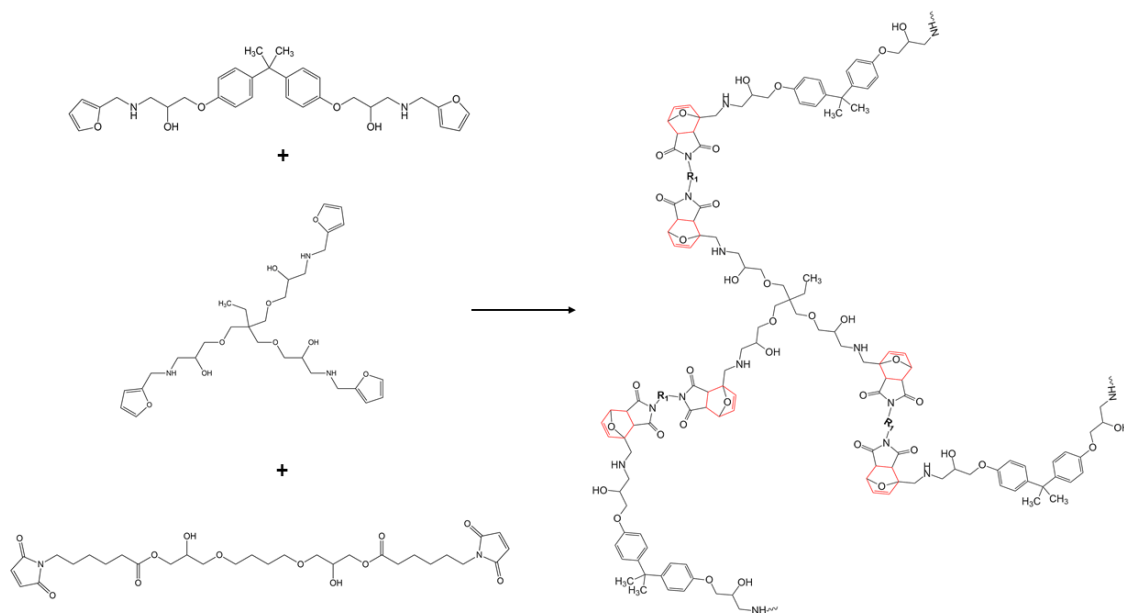


Figure 3. 7 Reaction scheme of the synthesis of DA polymer 2

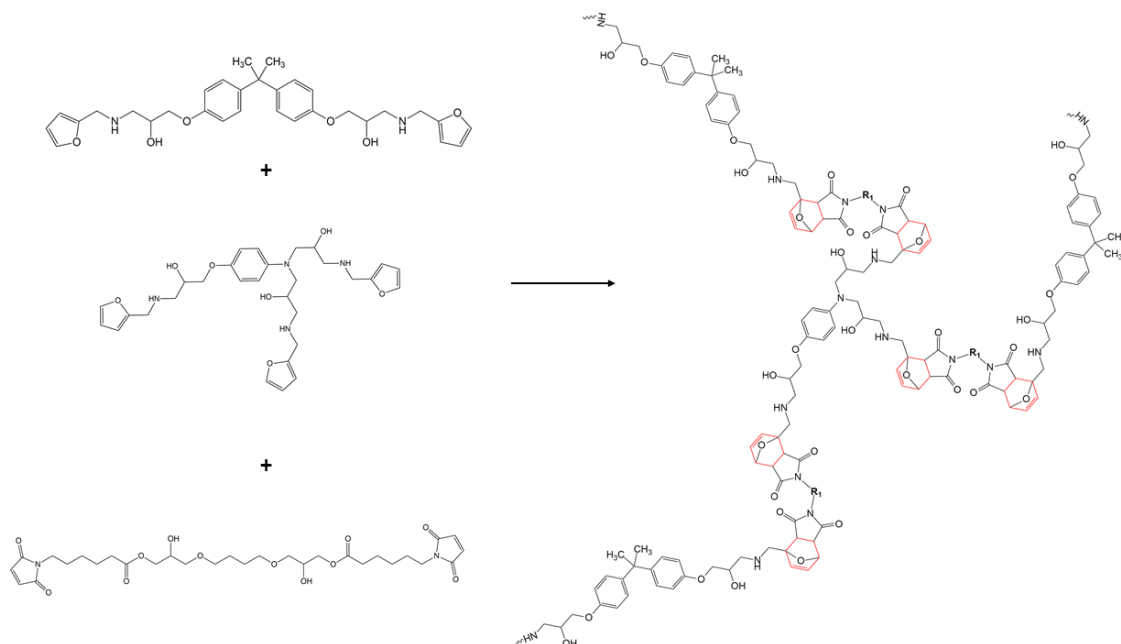


Figure 3. 8 Reaction scheme of the synthesis of DA polymer 3

The red bonds in the pictures correspond to the new formed bonds through DA reaction.

### 3.2 $^1\text{H}$ NMR Spectroscopy

$^1\text{H}$  NMR Spectroscopy is a characterization technique that is used to get information about the structure of molecules.

The concept behind this technique is that each charged particle in motion produce a magnetic field. This occurs at the macroscopic scale, because of the motion of electrons along a conductive material that produces electrical current, and at the atomic scale where electrons and protons can be seen as charged particles which rotate around their own axis.

Hydrogen nucleus  $^1\text{H}$ , the isotope with mass 1, is a charged particle so it can produce a magnetic field that will have a random orientation if there is not any external field applied.

When an external magnetic field is applied  $B_0$ , the orientation of the field produced by the hydrogen atom will be parallel or antiparallel with respect to the external one, and so two different energy levels are generated: a low energy state and a high energy state, respectively (Figure 3. 9).

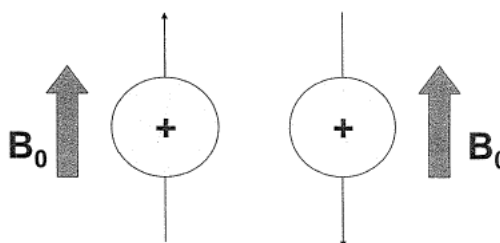


Figure 3. 9 orientations of the magnetic field of the hydrogen atom due to the application of an external magnetic field

If the protons are irradiated with a suitable magnetic radiation, they can adsorb energy and can jump from the lower energy state to the higher energy state: the resonance phenomena. Then the nucleus will release their energy and come back to the lower energy level.

If the hydrogen atoms are isolated, the resonance phenomena will occur at the same frequency for all the atoms, and so the different hydrogens will be indistinguishable in an NMR spectrum.

When the hydrogen atoms are bounded to other atoms, the magnetic field they are subjected to is given by the sum of the external radiation plus the local field, that is related to the presence of other charged particles around the atoms. The resonance phenomena for protons surrounded by different atoms occurs at different frequency.

In very electronegative atoms valance electrons are very close to the nucleus, so the magnetic field generated by these electrons will affect a little the total magnetic field felt by the hydrogen atoms near them. In this case the hydrogen nucleus felt a higher magnetic field and so the resonance phenomena will occur at higher resonance frequency.

If hydrogens atoms are close to less electronegative atoms, the total radiation they are subjected to will be lower because valance electrons have a high shielding effect. The resonance phenomena will occur at lower frequency.

In an NMR spectrum the chemical shift is reported on x axis. The chemical shift takes into account that nuclei surround by different atoms have different resonance frequencies. The intensity of the signal is reported on the y axis.

To obtain an NMR spectrum the sample is dissolved in a solvent without hydrogens. The solution is put in a cylindrical tube that is introduced between the magnets. The tube will rotate around its own axis so that the sample feels a homogenous magnetic field. A detector reports the absorption when a proton jumps from a level to another.

An important characteristic of the NMR spectra is the multiplicity of the peaks. This is related to the fact that the nuclei under consideration are influenced by the total field and by the magnetic fields produced by near protons, which can be oriented in different ways. The general rule states that the signal of a proton is divided by n hydrogens in n+1 peaks. The multiplicity is given by the number of hydrogens around the protons under examination plus 1.

Considering a methyl group that has only one hydrogens atom nearby  $H_a$ , it will be subjected to the total field  $B_{eff}$  and to the field created by  $H_a$ . The field generated by  $H_a$   $\beta$  can be parallel or antiparallel with respect to  $B_{eff}$  (Figure 3. 10). In the sample of methyl group under examination half of the molecules will felt a field given  $B_{eff}+\beta$  and the other

half will resent of a field equal to  $B_{\text{eff}}\beta$  and so the signal is divided in to two peaks that has the same intensity (Figure 3. 11).<sup>59</sup>

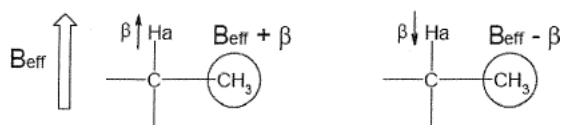


Figure 3. 10 Orientation of  $\beta$  with respect to  $B_{\text{eff}}$

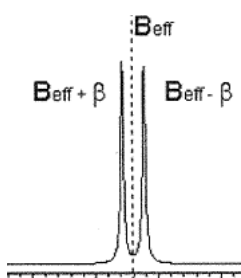


Figure 3. 11 Signal given by the methyl group above

In this thesis work, Chemical Draw, a simulation program for  $^1\text{H}$  NMR spectra was used to predict the spectra of obtained products.

### 3.3 Differential scanning calorimetry (DSC)

Differential scanning calorimetry is a fast and simple dynamic experimental technique that detects the transition temperatures, such as the melting temperatures or the crystallization temperatures. With this technique it is possible to identify the exothermic and endothermic transitions of a material.

The calorimeter consists of a heat flux plate with a temperature sensor, a computer controller, a recorder and two crucibles made by alumina. One of the two crucibles is empty and is used as reference, the other one contains 10-20 mg of the material under examination.

The general law referred to DSC is:

$$dQ = m c_p dT$$

Where  $m$  is the mass of the sample,  $c_p$  is its specific heat,  $T$  is the temperature and  $Q$  is the heat.

During the experiment the heat is provided or removed from the sample at constant speed, usually at 10 or 20 °C/min. If the weight of the sample is known, the result of the analysis is the heat flux that is proportional to the specific heat of the material. The instrument measures the heat absorbed by the sample during the thermal cycle.

For each transition three values of temperatures are given:  $T_{g\text{onset}}$  that correspond to the starting point of the sigmoid;  $T_{g\text{flex}}$  corresponding to the inflection point of the profile and  $T_{g\text{mid}}$  that is the average temperature between  $T_{g\text{onset}}$  and  $T_{g\text{flex}}$ . This last temperature is considered to be the glass transition temperature.

In this work the analyses were carried out by utilizing three thermal ramps and the chosen heating/cooling rate was 20°C/min to detect the glass transition temperature and 10°C/min to find the melting temperature.

DSC analyses were performed by means of a DSC/823e-Mettler Toledo: the calorimeter is calibrated with Indium and n-hexane.

Table 3. 11 DSC parameters

<b>Material</b>	<b>Heating/cooling rate</b>	<b>Ramp temperature</b>
<b>Bismaleimide</b>	20°C/min	-50°C-> 150°C
		150°C->-50°C
		-50°C->150°C
<b>Furan compounds</b>	10°C/min	-50°C-> 180°C
		180°C->-50°C
		-50°C->180°C
<b>Diels-Alder polymers</b>	20°C/min	-50°C-> 180°C
		180°C->-50°C
		-50°C->180°C



### 3.4 Thermogravimetric analysis (TGA)

TGA is a fundamental technique used to assess polymer degradation temperature and its general thermal behaviour. The instrument continuously records the mass of the sample of material as a function of temperature and time. It is composed by a thermal precision balance, an oven, a pipeline for gases to guarantee an inert or reactive atmosphere and a computer to have instrument feedback and to control the system. The result is the thermal decomposition curve. The plot presents on the axis of abscissae the temperature and on the axis of ordinates the percentage mass variation.

With TGA analysis it is possible to determine eventual residual solvent (or moisture) in the sample. In this case after an initial weight loss, TGA profiles reach a plateau to some constant weight level until the polymer degradation temperature range is reached.

A typical application is to investigate the thermal stability of a material: if a species is thermally stable in a defined temperature range, no mass changes will be detected.

TGA is also used to study the stability of a given material with the increase of temperature. When the material starts to degrade, a variation of mass is measured by the instrument and so a peak in the derivative of the weight loss is present.

In this thesis work, TGA was performed by using a XSTAR TG/DTA 6300 (Seiko Instruments Inc.) in a range of temperature between 25 °C and 800 °C with a temperature variation in time of 20 °C/min in air.

### 3.5 Fourier Transformed Infra-Red Spectroscopy (FT-IR)

The aim of Fourier Transformed Infra-Red Spectroscopy is to identify functional groups or to get the structure of the molecules, by measuring how much light is absorbed by the sample at each wavelength.

This is a simple and analytical technique that results from transitions between quantized vibrational energy levels: when a photon is absorbed a transition from the vibrational ground state to an excited vibrational state occurs.

Molecules with  $N$  atoms have  $3N$  degrees of freedom, of which three represent the translational motion along three mutual perpendicular directions both for complex and linear molecules. The degrees of freedom associated to the rotational motion are 3 for complex molecules and 2 for linear molecules. The remaining,  $3N-6$  for complex molecules or  $3N-5$  for linear molecules, are associated to the vibrational motion and so coincide with the number of vibrational modes. For each mode atoms vibrate at a characteristic frequency and so the absorption occurs only at a specific frequency.

There are two classes of vibrations: stretching vibrations involving bond length changes and bending vibrations that correspond to variations of the angle of the bond. Stretching vibrations are characterized by higher frequency with respect to bending vibrations because more energy is needed to stretch a bond than to deform it. Stretching vibrations could be symmetric or asymmetric depending on whether atoms vibrate at the same time or out of phase. Bending could be symmetric or asymmetric and it can occur on the same plane of the bond or out of the plane of the bond, so four different modes are possible: scissoring, rocking, twisting and wagging, respectively (Figure 3. 12).

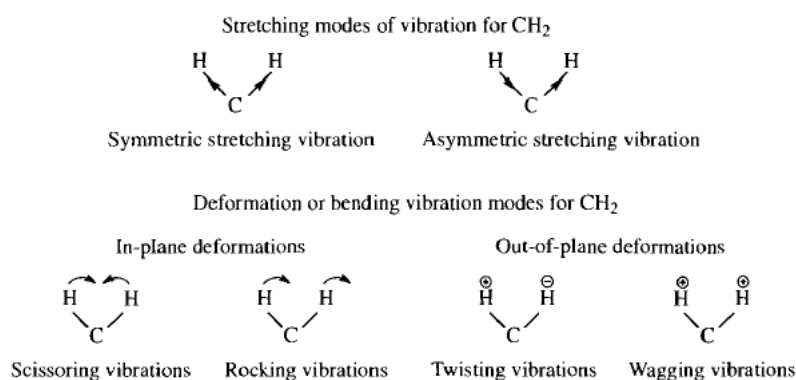


Figure 3. 12 Stretching and bending mode of vibrations

FT-IR instrument is composed of:

- A polychromatic source, as a tungsten filament lamp, that is directed towards the sample and the reference
- A reference that detects the peak associated to the environment
- A chopper through which the signal of both the reference and the sample are transmitted (In some instrument, like the one used for this thesis the chopper is absent.)
- A monochromator that receive the signal after it has crossed the chopper (it is a grid that exploits the phenomena of destructive interference and so only some wavelengths are allowed to go on)
- A detector that transmits the information to a computer.

The result of this analysis is the IR spectrum. On the abscissa axis the wavelength expressed in  $\text{cm}^{-1}$  is reported while on the ordinate axis is displayed the intensity of the peaks. If the sample is transparent to the radiation, the IR spectrum will be a horizontal line, on the contrary the absorption of a photon gives rise to a peak.

The IR spectra is divided in three regions. The far IR region (Wavenumber range:  $650\text{-}200\text{ cm}^{-1}$ ) contains information about heavy atoms, weak bonds such as hydrogen bonds and C-H out of plane bending vibrations. The peaks in the fingerprint region (Wavenumber range:  $1300\text{-}650\text{ cm}^{-1}$ ) are used to distinguish one molecule from another that contains similar functional groups, in fact the peaks in this region depend on the movement of the entire molecule. The presence of functional groups with a molecular

mass lower than 20 g/mol is pointed out in the functional group region at long wavelength (Wavenumber range: 4000-1300  $\text{cm}^{-1}$ ).

In this work IR analyses were performed for liquid and solid samples. Liquid samples were spread between two NaCl disks. Solid samples were grinded, mixed with KBr and pressed into thin disks with a manual hydraulic press. NaCl and KBr were selected because they are transparent to infrared radiation and so they do not absorb in those regions. Analyses were made in absorption mode. The spectra were collected by making 64 scans in the wavelength range 400-4000  $\text{cm}^{-1}$  with a resolution of 4  $\text{cm}^{-1}$ . IR analyses were carried out with a Nicolet 760-FTIR nexus spectrometer supported by the software Omnic™.



Figure 3. 13 Nicolet 760-FTIR nexus spectrometer

### 3.6 Solubility test

This test was performed in order to prove the crosslinking at low temperature and the decrosslinking at high temperature.

If the polymer has crosslinked it will not be soluble in any solvent demonstrating the occurrence of the Diels-Alder reaction.

At high temperature (around 110°C) the retro Diels-Alder reaction takes place. This leads to the decrosslinking with the reformation of the starting monomers, and the polymer becomes soluble. A ratio solid material:solvent of 1g:10ml was selected and dimethyl formamide was used as solvent because of its high boiling point (153 °C).

Gelification test was carried out by dissolving a small quantity of the DA polymer in DMF so that the r-DA reaction occurs and then letting it cool until room temperature. With cooling the DA reaction takes place and so gelification occurs.

### 3.7 Gel content measurement

Gel content test was performed to find the degree of crosslinking. Indeed, with this technique it is possible to investigate the gel percentage which is directly related to the degree of crosslinking: the higher the gel percentage, the higher the degree of crosslinking.

The polymeric sample, after being weighed ( $W_i$ ), is immersed in a solvent (THF in this thesis) which is able to dissolve the monomers, and kept under magnetic stirring. The fraction of not crosslinked material was expected to detach from the piece and dissolve in the solvent. After 24 hours, the solvent was filtered and the solid remaining on the filter, which corresponds to the crosslinked fraction of the sample, was dried in a vacuum oven at 50°C. Then, it was weighed at daily intervals until a constant value was reached (obtaining the final weight  $W_f$ ). So, at the end of the process, it was possible to measure the quantity of dissolved material and by weighing the final mass of the solid sample it is possible to find the gel percentage.

The gel percentage, or degree of crosslinking, was calculated with the following equation:

$$GC\% = \frac{W_f}{W_i} * 100$$

# ***4. Results and Discussion***

## 4.1 Aliphatic bismaleimide synthesis and characterization

A new procedure to obtain an aliphatic bismaleimide (BM) was defined after some attempts. First the reaction was carried out without catalyst (BM 1° attempt): 1,4BDE and MHA were dissolved in toluene and the solution was kept under stirring at 110°C for seven hours with no success, probably because epoxy and carboxylic groups are not very reactive since they are linked to aliphatic chains. To get through this issue, a thermal treatment was performed at 130°C after solvent evaporation (BM 2° attempt), but the reaction did not proceed even in this case as confirmed by IR analyses. Consequently, a catalyst was needed. Amines, according to a previous work<sup>60</sup>, can catalyse the reaction between epoxy groups and carboxyl groups. Pyridine was selected, in fact it has the highest catalytic activity compared with all the other amines. MHA, 1,4BDE and pyridine were mixed in toluene at 110°C for 7 hours, but again from IR spectra it was possible to see that the reaction did not occur (BMo). Finally, it was found out that by combining the addition of the catalyst and a thermal treatment the reaction occurred. In fact, after the evaporation of the solvent, by mixing at 130°C the solution (BMo) for another hour, the reaction proceeded as confirmed by IR and <sup>1</sup>H NMR analyses. On the basis of these attempts, it could be concluded that the thermal treatment in toluene was not enough to allow the reaction between -COOH and epoxy groups to occur, likely due to the high distance between the molecules in the solvent. After the evaporation step, the molecules were closer to each other letting the reaction to proceed. Moreover, the solvent had some effect too. In fact, if the mixing in toluene was bypassed, both with pyridine and without it, an insoluble product was obtained. As a result, the solvent could lead to a solvation of the carboxylic groups which favour the reaction with epoxy groups.

Later, an additional step was added: to let the residual epoxy rings react, the product was transferred in a tared Teflon and put in oven at 130°C for another hour.



Table 4. 1 Sums up the four attempts:

Table 4. 1 Attempts to defined bismaleimide reaction procedure: Mixing: in toluene at 110°C, Catalyst: pyridine, Thermal treatment: mixing after solvent evaporation at 130°C

	Mixing	Catalyst	Thermal Treatment
<b>BM 1° attempt</b>	✓		
<b>BM 2° attempt</b>	✓		✓
<b>BMo</b>	✓	✓	
<b>BM</b>	✓	✓	✓

The scheme of the difined reaction procedure is represented in Figure 4. 1.

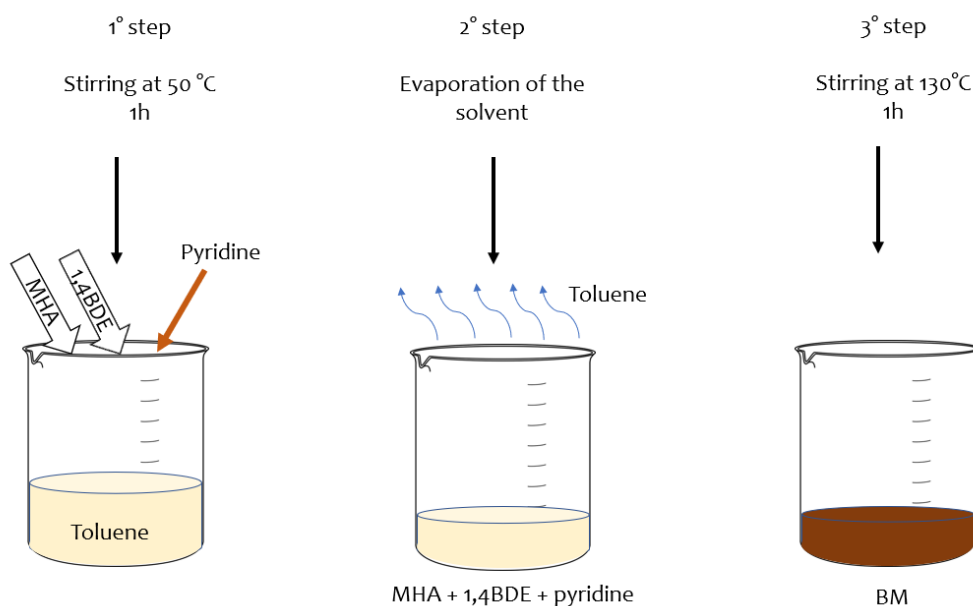


Figure 4. 1 Schematic picture of the synthesis of the aliphatic bismaleimide

Other attempts were performed with the aim of decreasing the amount of unreacted epoxy groups and in order to avoid possible reactions between epoxies. For these reasons, different ratio between 1,4BDE moles and MHA moles were considered (epoxy moles:acid moles), increasing gradually the amount of acid moles: 1:1,5 (BMA); 1:2 (BMB); 1:2,5 (BMC) and 1:3 (BMD). These reactions took place as the one with a ratio of 1:1, but in all the cases a small quantity of unreacted epoxies was always present.

All the reactions explained above are summarized in Table 4. 2.

Table 4. 2 Bismaleimides reactions

	ratio -COOH:CH-O-CH <sub>2</sub> -	MW [g/mol]	Mass [g]	Functional group moles [mol]
<b>BM 1° attempt</b>	1:1			
MHA		211,12	1,6698	0,0079
1,4BDE		202,3	0,8000	0,0079
<b>BM</b>	1:1			
MHA		211,12	1,6698	0,0079
1,4BDE		202,3	0,8000	0,0079
Pyridine		79,1	0,0063	7,91E-05
<b>BMA</b>	1,5:1			
MHA		211,12	2,5046	0,0119
1,4BDE		202,3	0,8000	0,0079
Pyridine		79,1	0,0063	7,91E-05
<b>BMB</b>	2:1			
MHA		211,12	3,3395	0,0158
1,4BDE		202,3	0,8000	0,0079
Pyridine		79,1	0,0063	7,91E-05
<b>BMC</b>	2,5:1			
MHA		211,12	4,1744	0,0198
1,4BDE		202,3	0,8000	0,0079
Pyridine		79,1	0,0063	7,91E-05
<b>BMD</b>	3:1			
MHA		211,12	5,0093	0,0237
1,4BDE		202,3	0,8000	0,0079
Pyridine		79,1	0,0063	7,91E-05

Once BM was selected, a scaling up of the reaction was made with success by doubling the quantities of reagents as reported in Table 4. 3.

Table 4. 3 Scaling up of the bismaleimide reaction

		<b>MW [g/mol]</b>	<b>Mass [g]</b>	<b>Moles [mol]</b>
1)	<b>MHA</b>	211,12	1,6698	0,0079
	<b>1,4BDE</b>	202,3	0,8000	0,0040
	<b>Pyridine</b>	79,1	0,0063	7,91E-05
2)	<b>MHA</b>	211,12	3,3395	0,0158
	<b>1,4BDE</b>	202,3	1,6000	0,0079
	<b>Pyridine</b>	79,1	0,0125	0,0002

All reactions were monitored with FT-IR analysis and the products were analysed with <sup>1</sup>H NMR and DSC techniques.

#### 4.1.1 FT-IR

IR spectra of 1,4BDE was compared with the one of the final products.

Peak corresponding to -C-O-C- stretching at  $1110\text{ cm}^{-1}$  was selected as the reference one<sup>61</sup>, in fact it was expected to remain constant as the reaction proceeded. Epoxy peak at  $915\text{ cm}^{-1}$  was monitored<sup>21</sup> to verify the occurrence of the reaction, since epoxy rings opened and reacted with the carboxylic groups of MHA, so it meant that the epoxy peak was expected to decrease.

Figure 4. 2 represents IR spectra of the reaction carried out without any catalysts after seven hours of mixing (BM 1° attempt) and after the thermal treatment at  $130^{\circ}\text{C}$  (BM 2° attempt). From it, it was possible to observe that epoxy peak at  $915\text{ cm}^{-1}$  did not decrease and so the reaction did not take place.

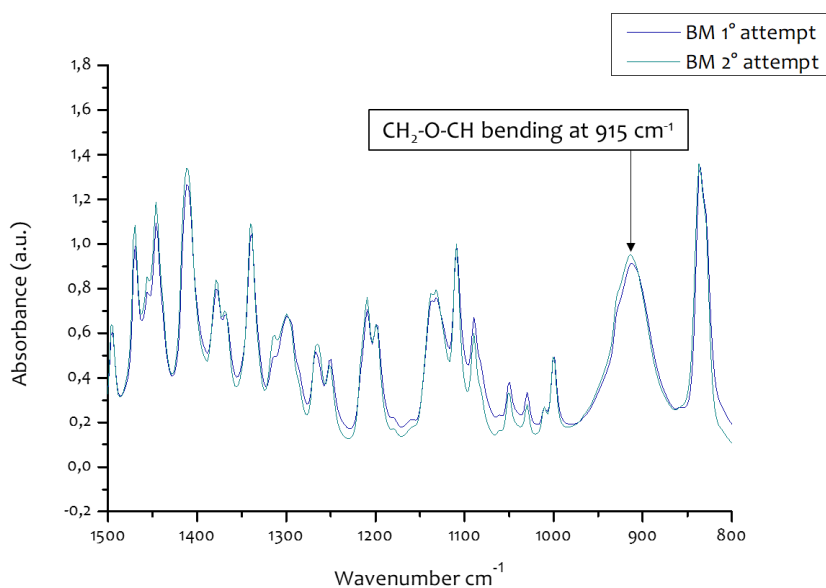


Figure 4. 2 IR spectra of the reaction carried out without catalyst

Spectra of the reaction executed with the catalyst but in absence of a thermal treatment are depicted in Figure 4. 3, where it is possible to observe that, even in this case, the absorption band associated to the epoxy peak does not decrease but it remains more or less constant from  $t_1$  (after one hour of mixing at  $110^{\circ}\text{C}$ ) to  $t_7$  (after seven hours of mixing at  $110^{\circ}\text{C}$ ).

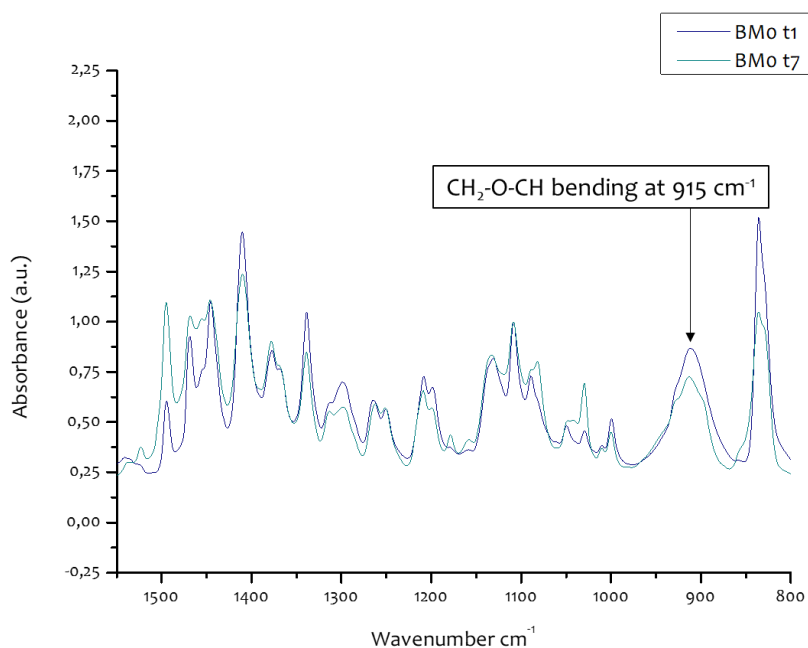


Figure 4. 3 IR spectra of the reaction carried out with Pyridine but with no thermal treatment

Considering the reaction catalysed with pyridine and followed by a thermal treatment, a decrease of the absorption band of epoxies could be observed in the IR spectra as depicted in Figure 4. 4, where *BM t1* is the IR spectrum of the product after being mixed at 130°C for 1 hour and *BM tf* is the spectrum of the product after being 1 hour in oven at 130°C. We can observe, normalizing the graph, that the peak associated to epoxy groups decreased from *t1* to *tf*, demonstrating that epoxy ring opened and reacted.

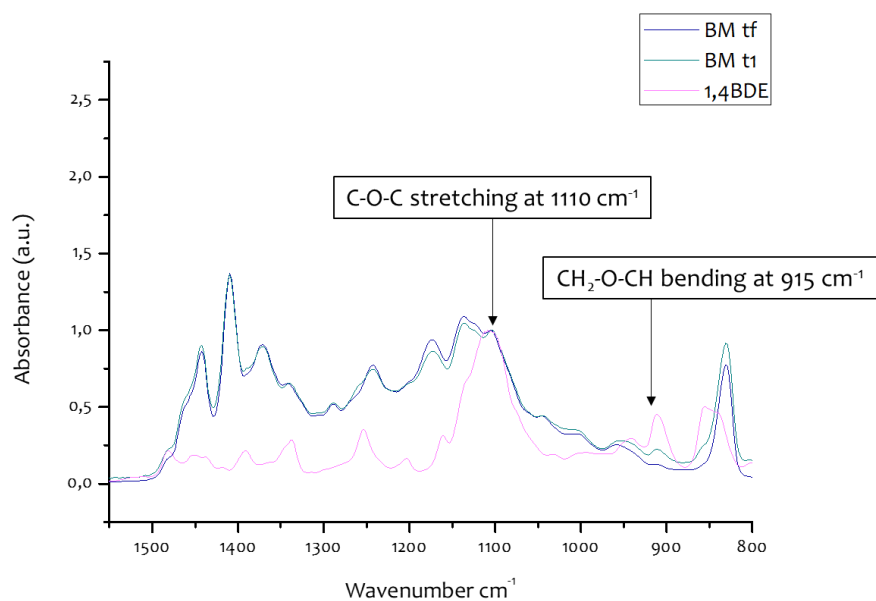


Figure 4. 4 IR spectra Bismaleimide reaction with pyridine and thermal treatment

IR spectra of bismaleimides A, B, C, and D are reported in Figure 4. 5 and compared with the one of 1,4BDE:

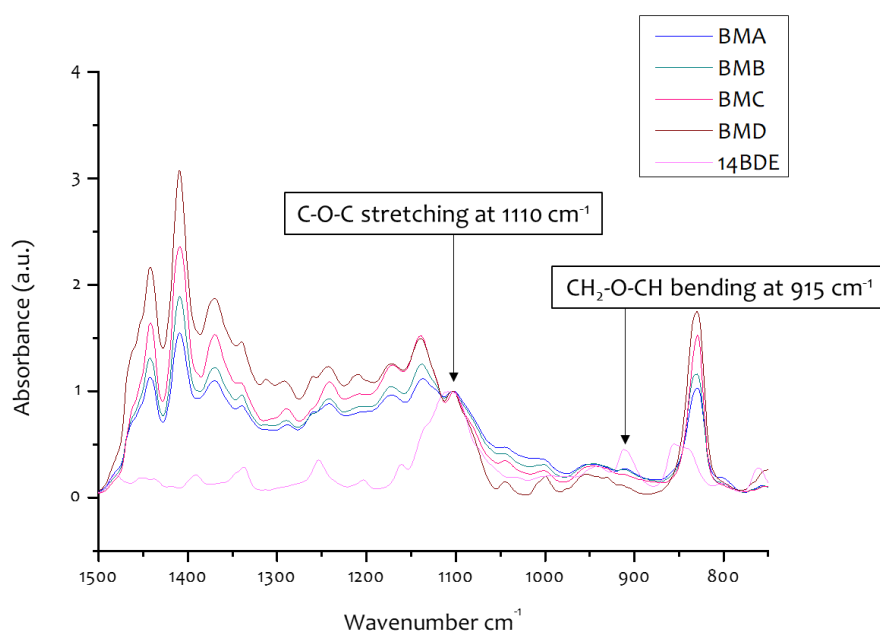


Figure 4. 5 IR spectra of Bismaleimides BMA, BMB, BMC and BMD

The decrease of the epoxy peaks could be observed in all the products as in the previous case when a ratio of 1:1 was selected.

All the products were characterized with DSC and <sup>1</sup>H NMR technique.

#### 4.1.2 $^1\text{H}$ NMR

NMR analyses were performed only on BMO and BM and their spectra were normalized and compared among them and with reactants spectra to evaluate the success of the reaction.

The spectrum of MHA (Figure 4. 6) was normalized by setting the area of the signal at 1.6 ppm equal to 4, which was associated to the signal given by the hydrogens 3 in Figure 4. 6. The signal at 6.68 ppm corresponded to the two hydrogen of the maleimide group. The area below this signal was expected to be 2 but it could be seen from the MHA spectrum that it was lower (1.86).<sup>62</sup>

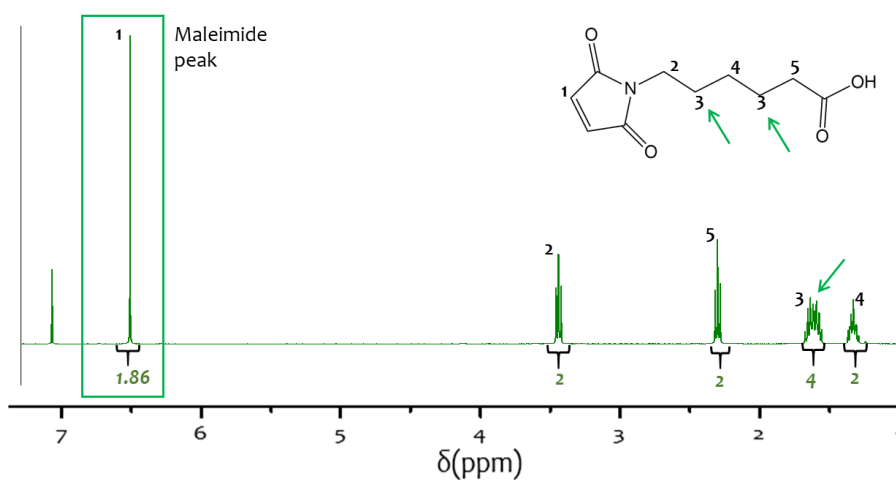


Figure 4. 6  $^1\text{H}$  NMR spectra of MHA

1,4BDE spectrum (Figure 4. 7) was normalized with respect to the peak at 1.66 ppm that was associated to hydrogen 7 in the 1,4BDE molecule in Figure 4. 7, which must not change during the reaction. The area of this peak was set equal to 4 that corresponds to the number of hydrogens which gave the same signal.<sup>63</sup>

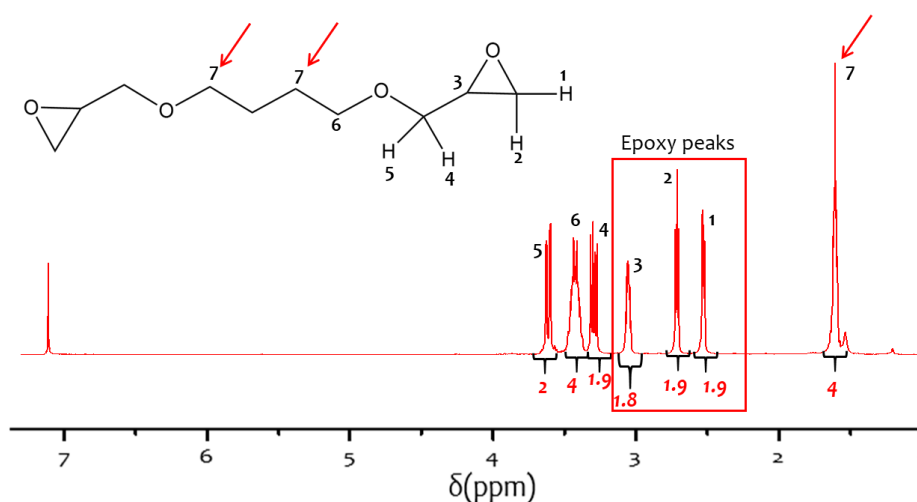


Figure 4.7  $^1\text{H}$  NMR spectra of 1,4BDE

Observing and normalizing the spectrum of BMO (Figure 4.8), it was possible to notice that this graph was given by the sum of the spectra of MHA and 1,4BDE, showing that the reaction did not proceed without the thermal treatment at  $130^\circ\text{C}$ . This spectrum was normalized setting the area of the peak at 1.6 ppm equal to 12 since the signal in this point is given by the sum of the signals of hydrogens 3 of the acid in Figure 4.6 and of hydrogens 7 in Figure 4.7. Comparing the spectrum in Figure 4.8 with 1,4BDE spectrum, it was possible to note that signals present at 4.1 ppm, which probably correspond to the formation of new bonds, were very weak, proving that the amount of carboxylic and epoxy groups which reacted was very low. In addition, it could be observed that most of the epoxy rings were still present in the final product: epoxy peaks, associated to signals at 2.6 ppm, 2.7 ppm and at 3.1 ppm, are clear both in the product spectrum and in 1,4BDE one. Moreover, the total integrated area of these peaks in Figure 4.8 was equal to 4.7 ppm. As a result, considering that the total area of epoxy peaks in 1,4BDE spectrum was 5.6, the percentage of reacted epoxies was 16%: only a small amount of epoxy rings opened and reacted with  $-\text{COOH}$  groups. The maleimide peak at 6.68 ppm was taken into consideration too. The area of this peak in Figure 4.8 is equal to 3.6, while it should be 3.72 (1.86, the area of the same peak in MHA spectrum multiplied by 2), which means that the percentage of maleimide groups in the product is 97%; the remaining 3% of maleimide groups maybe reacted with each other.



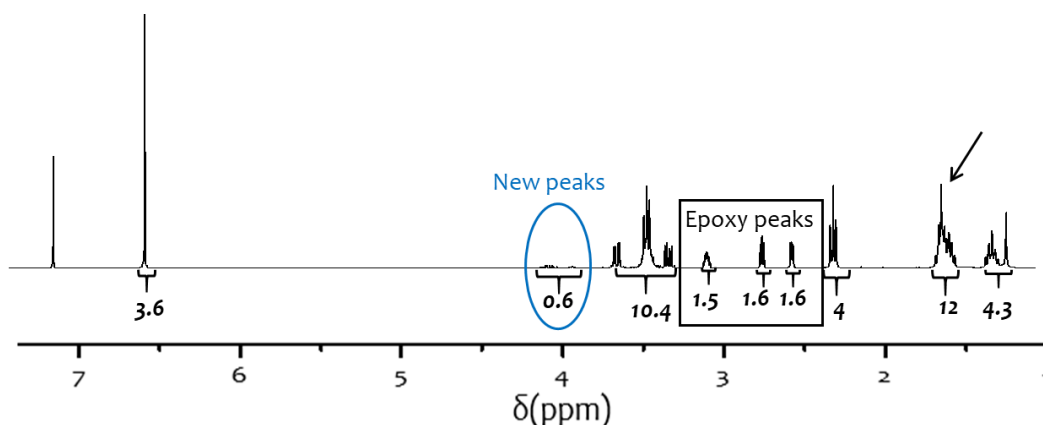


Figure 4. 8  $^1\text{H}$  NMR spectra of the product of the reaction carried out with catalyst and no thermal treatment

Figure 4. 9 represents the spectrum of the bismaleimide BM. This spectrum was normalized in the same way as spectrum in Figure 4. 8. From this graph it was possible to observe new signals at 4.1 ppm and at 3.9 ppm, probably associated to hydrogens involved in the formation of the new bonds or to hydrogens near these new bonds. In addition, epoxy peak, which were evident in the 1,4BDE spectrum at 2.6 ppm, 2.7 ppm and 3.1 ppm, decreased in the product spectrum: the total area below these peaks in the reactant spectrum was equal to 5.6 while in the BM spectrum was around 2: the percentage of reacted epoxies was 64%. As a consequence, the addition of Pyridine and the thermal treatment favoured the opening of the epoxy rings and the reaction with the carboxylic groups.

In this case the percentage of maleimide groups in the final products was 81% since the area below the maleimide peak was equal to 3, instead of 3.72. in this case, a higher amount of maleimide groups reacted with each other, maybe the high temperatures favoured also this reaction but in small quantities.

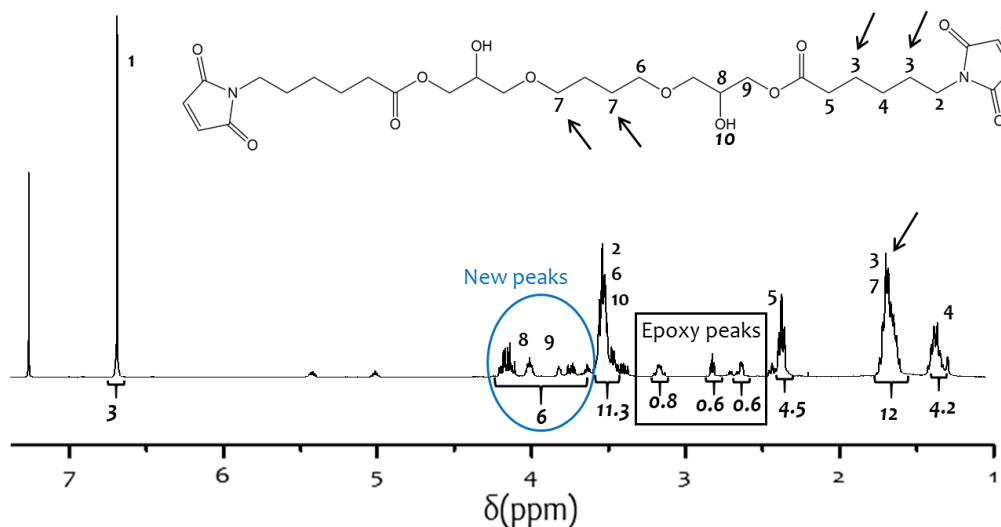


Figure 4.  $^9\text{H}$  NMR of Bismaleimide (BM)

NMR spectra of the bismaleimides obtained with different ratio between epoxy groups and carboxylic groups were reported in Figure 4. 10. NMR spectra of BMA and BMB were normalized setting the area of the peak at 1.6 equal to 16 and 20, respectively. These values are given by the sum of all the hydrogens which gave the same signals. For example, for BMA, a ratio COOH:epoxy groups of 1,5:1 was considered and therefore the hydrogens which gave the same signal for MHA were 12 (hydrogen 3 in Figure 4. 6) and for 1,4BDE were 4 (hydrogens 7 in Figure 4. 7).

It was possible to notice that unreacted epoxies were always present, and that the area of the peaks associated to new bonds was lower with respect to the one found for the bismaleimide with a ratio carboxylic groups/epoxy groups of 1:1.

The percentage of maleimide groups in BMA and BMB were 82% and 85%, respectively: the amount of maleimide groups which reacted with each other in this case is comparable with BM but the amount of residual epoxy groups is higher compared to BM spectrum. It could be concluded that with other ratios than 1:1 -COOH:epoxies, other reactions could occur.

BMD and BMC  $^1\text{H}$  NMR analysis were not performed because they were completely insoluble in chloroform, the solvent utilized in this technique.

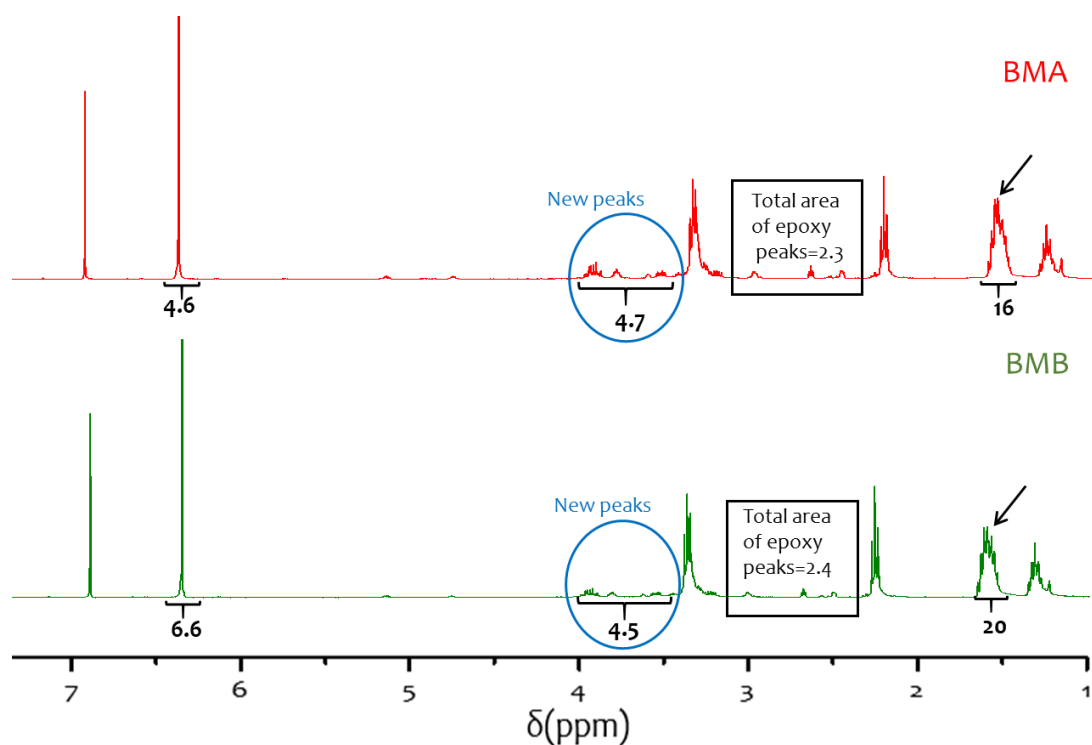


Figure 4.  $^{10} \text{H}$  NMR spectrum of BMA and BMB

Table 4. 4 shows the reacted epoxy groups for each bismaleimide, which was calculated dividing the total area of unreacted epoxies by the total area of epoxy peak in 1,4BDE spectrum which is 5,66, and the percentage of maleimide groups, evaluated as the ratio between the effective area (the predicted one) of the peak at 6.68 and the real one (calculated by integrating  $^1\text{H}$  NMR spectra):

Table 4. 4 quantification of reacted epoxies

	<b>total area of unreacted epoxies</b>	<b>%reacted epoxies</b>	<b>%maleimide groups</b>
<b>BMo</b>	4,7	16%	95%
<b>BM</b>	2	64%	84%
<b>BMA</b>	2,3	59%	82%
<b>BMB</b>	2,4	57%	85%

Assuming that all MHA reacted, it could be concluded that not all the epoxides were reacted likely due to secondary reactions. For example, esterification reactions could occur between some carboxylic acid groups and -OH<sup>64</sup> groups linked to the aliphatic BM, leading to the formation of some multifunctional maleimide. Moreover, from Table 4. 4 it could be observed that increasing the amount of MHA, the percentage of reacted epoxies decreased, which could mean that with an excess of -COOH groups, the reaction between carboxylic and -OH groups is favoured. However, the decreased of reacted epoxies from BM to BMB is small and so not particularly notable. Furthermore, the amount of maleimide groups in the obtained products is always lower than expected, which could mean that some maleimide polymerized with other maleimide groups. This could denote that the final product could be composed by some monofunctional maleimide.

As a result, the product could be a mixture composed mostly of bifunctional maleimides but also of some multifunctional and monofunctional maleimide.

BMC and BMD were not taken into considerations since they were not soluble or only partially soluble and so it meant that they crosslinked, but in this thesis a soluble aliphatic bismaleimide was needed for further experiments.

Bismaleimide with a ratio 1:1 was selected to obtain the Diels-Alder polymers. In fact, BMA, BMB and BM showed some unreacted epoxy groups but, according to <sup>1</sup>H NMR spectrum of the BM obtained with a ratio of 1:1, it was found that the total area of new peaks was higher than in the other spectra. So, in the bismaleimide prepared with a stoichiometry ratio of 1:1, a higher number of new bonds between carboxylic and epoxy groups were likely to be formed. In addition, from Table 4. 4 it can be observed that BM showed the higher number of epoxies which are linked to MHA.

### 4.1.3 DSC

DSC analyses were carried out with a heating/cooling rate of 20°C/min and by utilizing three thermal ramps: from -50°C to 150°C; from 150°C to -50°C and from -50°C to 150°C. From DSC analysis of BM some considerations could be made:

- 1) The third temperature run (which is represented in Figure 4. 11) was equal the first one, which meant that MHA and 1,4BDE reacted; in fact no peak related to the melting of the reactant was observed in the first run.
- 2) Other transitions were not detected and so it could be deduced that the degree of purity was high. In addition, the product could be considered stable up to 150°C.
- 3) The glass transition temperature was well below room temperature; in fact the obtained product was a viscous liquid.

DSC graph of the bismaleimide BM is reported in Figure 4. 11, where it could be noticed that the  $T_g$  is around -35,88°C.

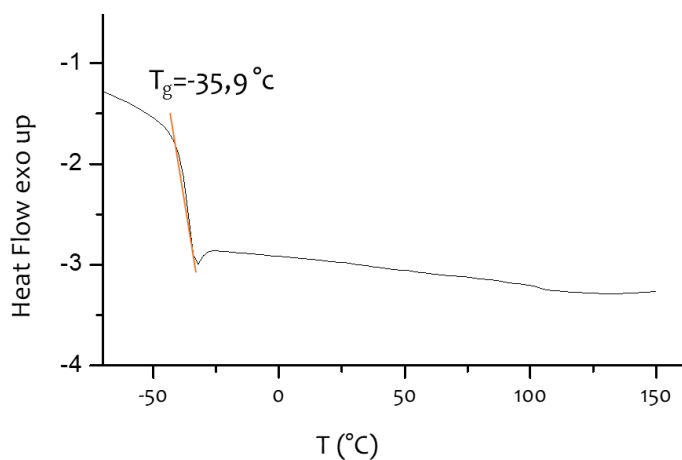


Figure 4. 11 DSC of Bismaleimide

From the DSC graph of the product BMo (obtained with the catalyst but no thermal treatment), two peaks in the first part of the graph could be noticed, as depicted in Figure 4. 12, where the first run of the DSC of BMo is depicted.

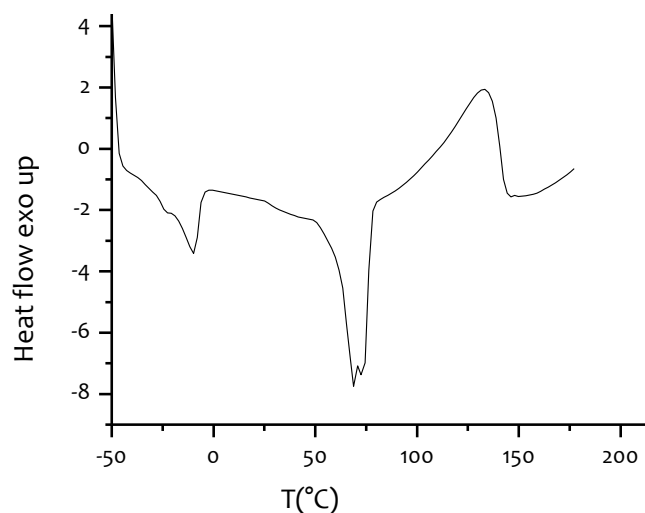


Figure 4. 12 DSC of BMO

In order to explain these peaks, DSC analyses were performed also on the two reactants (Figure 4. 13). In MHA graph, a fusion peak around 80/90 °C was observed and in the one of 1,4BDE a fusion peak was detected around -20°C. These two fusion peaks corresponded to the two peaks found in Figure 4. 12 which proved that the reaction without catalyst did not proceed.

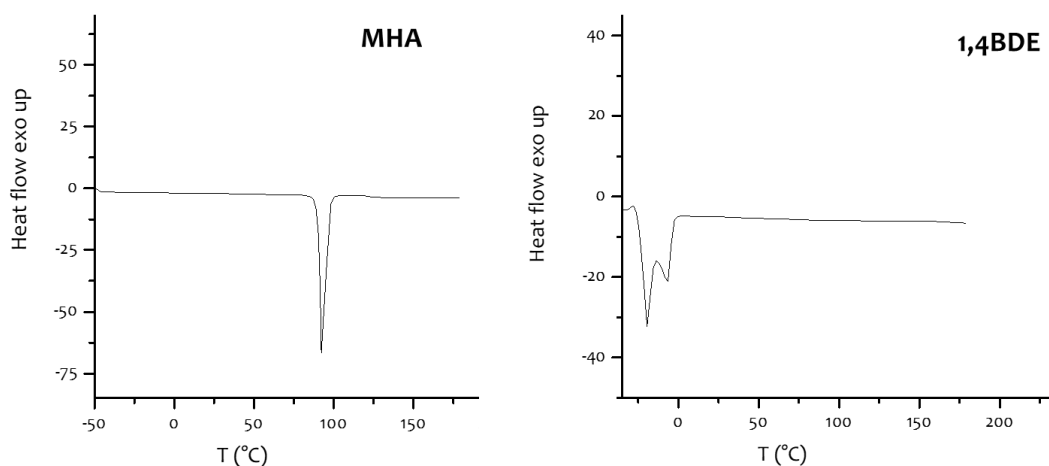


Figure 4. 13 DSC of MHA and 1,4BDE

The third temperature run of DSC of BMA, BMB, BMC and BMD are showed in (Figure 4. 14). These graphs were similar to DSC graph of BM and had similar  $T_g$  values. Also in this

case, in the first run the melting peak of MHA was not present, demonstrating the success of the reactions.

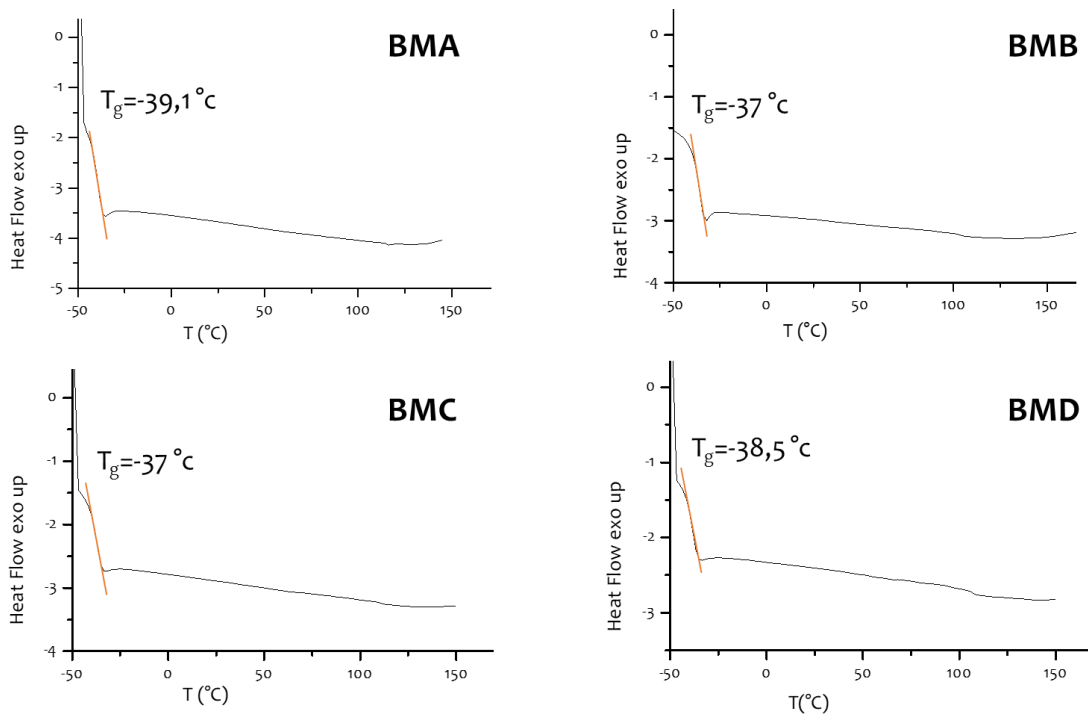


Figure 4. 14 DSC of BMA, BMB, BMC and BMD

Anyway, the T<sub>g</sub> of BM, the selected product to obtain the DA polymer, was far below the room temperature in accordance with the consistency of the products which was viscous fluid. Taking into account the final application of these molecules, DSC analyses confirmed the possibility to implement them in a solvent-free process being the glass transition temperature so below room temperature.

## 4.2 Synthesis and characterization of furan compounds

Furan compounds were obtained from the reaction between an epoxy resin (1,4BDE, TMPTE, DGEBA or DGGO) and the furfuryl amine as reported in chapter 3.1.2. In this thesis two new aliphatic furan compounds were synthesized with the same procedure already known for aromatic 2F and aromatic 3F.

Epoxy resin was mixed with Methanol at 50°C. After obtaining an inert atmosphere with three cycles of evacuation and backfilling with nitrogen, FA was added with a syringe through a silicon cap. The solution was kept under magnetic stirring at 85°C for 5 hours. Successively methanol and the unreacted FA were removed with a thermal treatment in a vacuum oven. A scheme of the reaction is represented in Figure 4. 15.

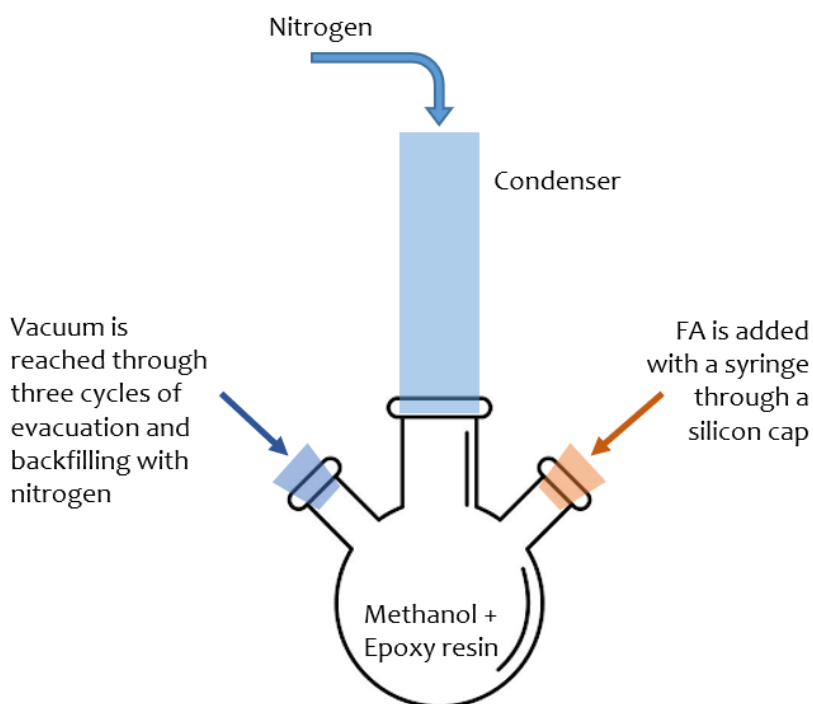


Figure 4. 15 Schematic representation of furan functionalization

A qualitative study was made by monitoring the reactions with FT-IR technique while a quantitative analysis was carried out by examining  $^1\text{H}$  NMR spectra of the components. To detect thermal transitions DSC analyses were performed too on all the products.



#### 4.2.1 FT-IR

To monitor furan functionalization reactions, peak at  $915\text{ cm}^{-1}$  was selected, which is associated to the bending of  $\text{CH}_2\text{-O-CH}$  of the epoxy groups. When the reaction took place, the epoxy rings opened and reacted with NH group of the furfuryl amine. Consequently, the peak at  $915\text{ cm}^{-1}$  should, in principle, decrease as the reaction goes on.

For IR spectra of aliphatic furan compounds, the peak at  $1110\text{ cm}^{-1}$ , which corresponds to C-O-C bonds<sup>61</sup>, was selected as the reference one, to compare them with the spectra of the corresponding reactants.<sup>61</sup>

Comparing IR spectra of 1,4BDE and aliphatic 2F (Figure 4. 16), it could be noticed that the absorption band associated to epoxy groups was shifted and decreased in the product spectrum.

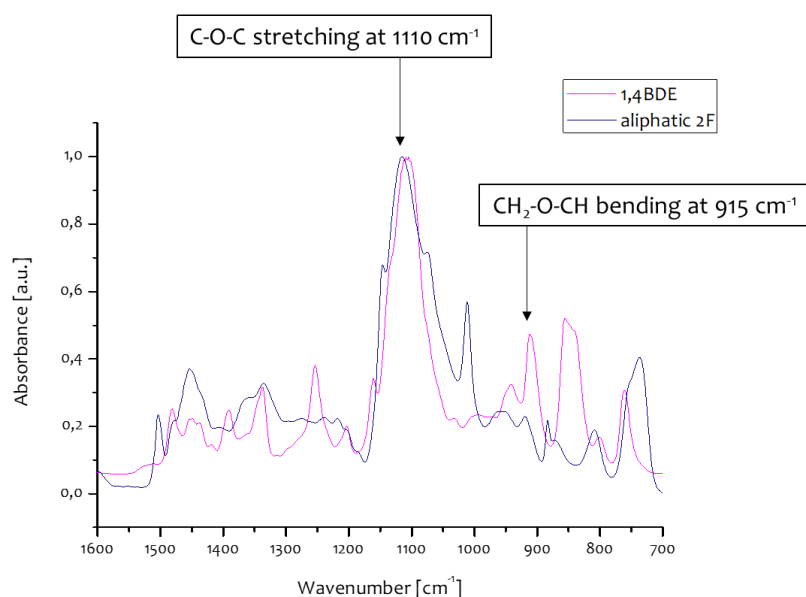


Figure 4. 16 IR spectra of 1,4BDE and aliphatic 2F

The same decrease of epoxy absorption band was observed also comparing IR spectra of TMPTE and aliphatic 3F (Figure 4. 17).

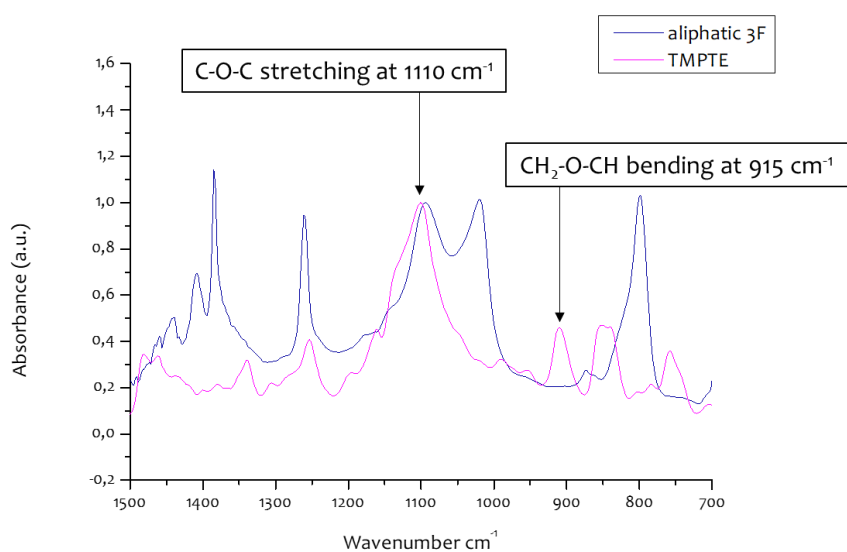


Figure 4. 17 IR spectra of TMPTE and aliphatic 3F

As regards spectra of DGEBA, DGGO and aromatic furans (Figure 4. 18 and Figure 4. 19), the peak at 1182  $\text{cm}^{-1}$ , which corresponds to C-O stretching of the carbon belonging to the aromatic ring, was selected as the reference one.

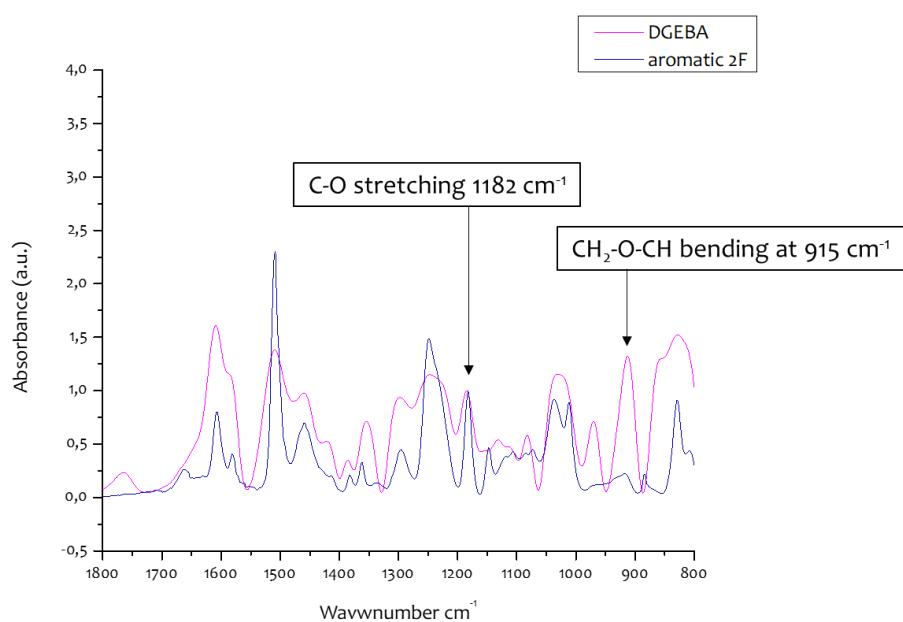


Figure 4. 18 IR spectra of DGEBA and aromatic 2F

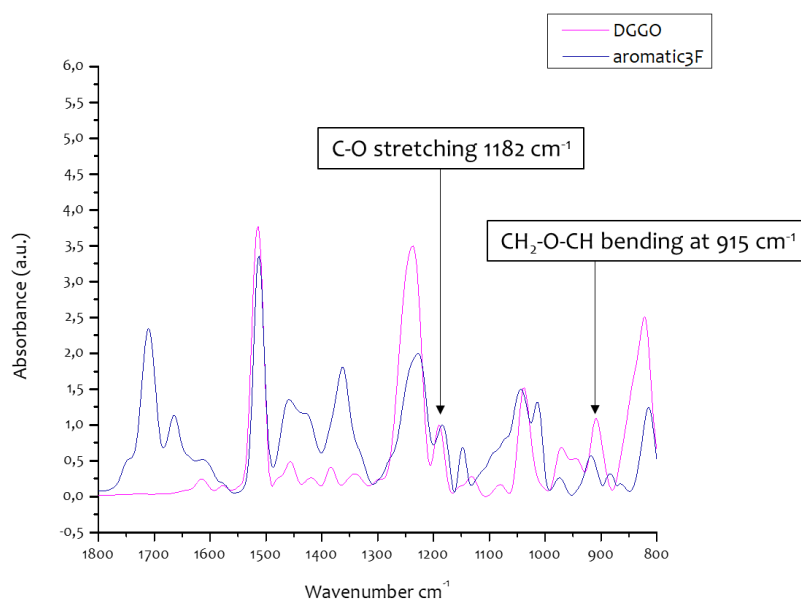


Figure 4. 19 IR spectra of DGGO and aromatic 3F

As expected, the peak at 915 cm<sup>-1</sup> was present in all the starting monomers and then disappeared or decreased in the final product, demonstrating the success of the reactions.

Successively, to make a quantitative analysis, NMR spectra of the products were studied.

### 4.2.2 $^1\text{H}$ NMR

$^1\text{H}$  NMR analysis confirmed that the reaction took place. Also in this case, the furan modified compound spectrum was compared to the ones of initial epoxy monomers.

The spectra of 1,4BDE and aliphatic 2F are reported below:

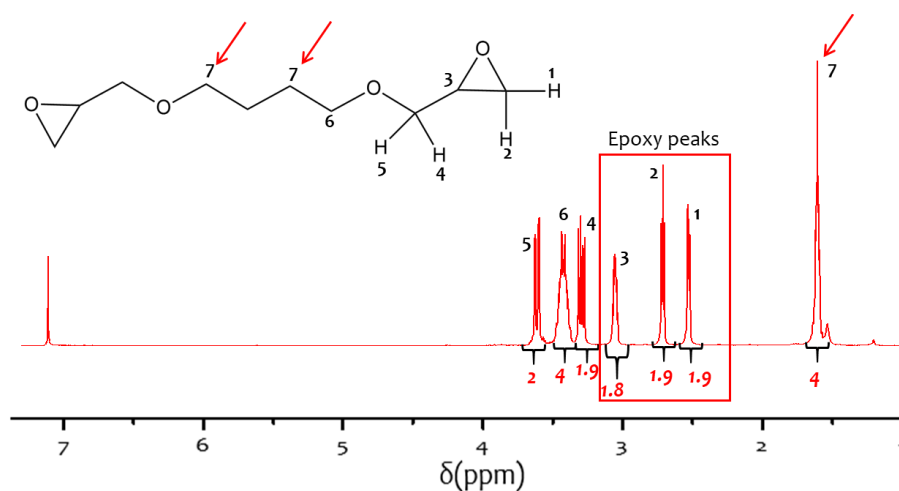


Figure 4. 20  $^1\text{H}$  NMR spectrum of 1,4BDE

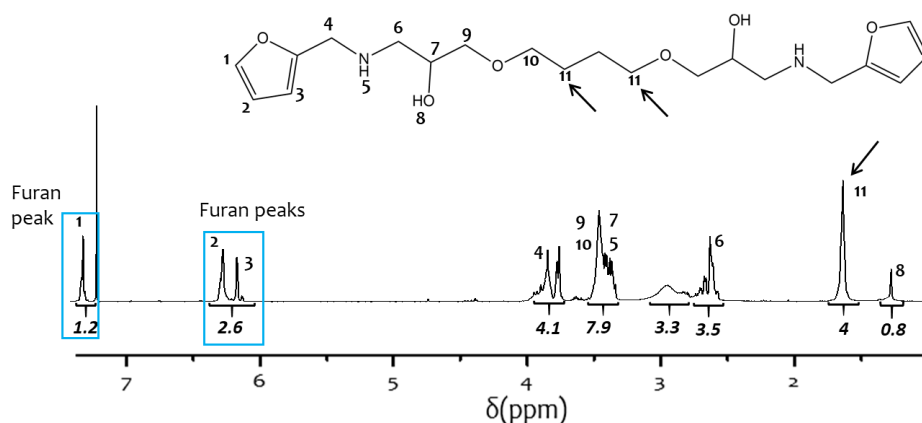


Figure 4. 21  $^1\text{H}$  NMR spectrum of aliphatic 2F

1,4BDE spectrum<sup>63</sup> (Figure 4. 20) and Aliphatic 2F spectrum (Figure 4. 21) were normalized with respect to the peak at 1.66 ppm that was associated to hydrogen 11 in the molecular structure of Aliphatic 2F (Figure 4. 21) or to hydrogen 7 for 1,4BDE, which was not expected to change during the reaction. The area of this peak was set to 4 that corresponds to the number of hydrogens which gave the same signal.

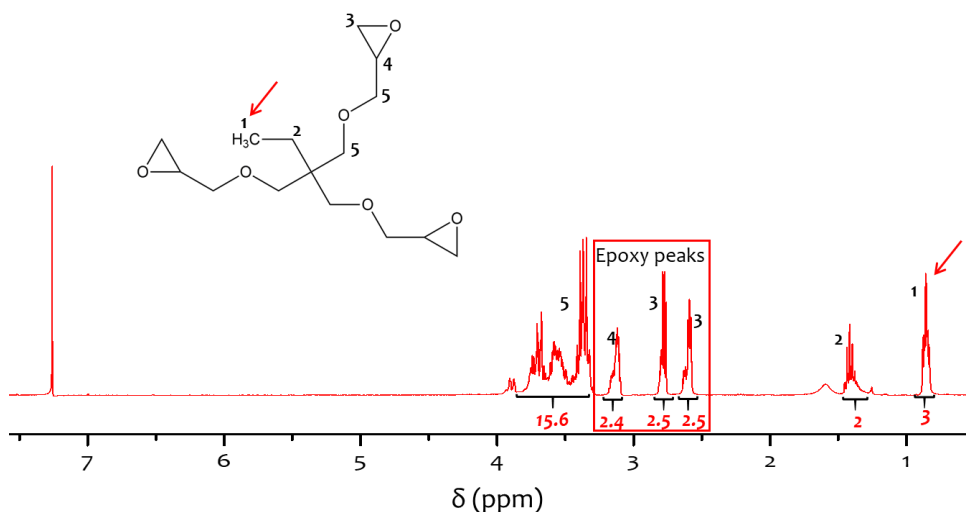
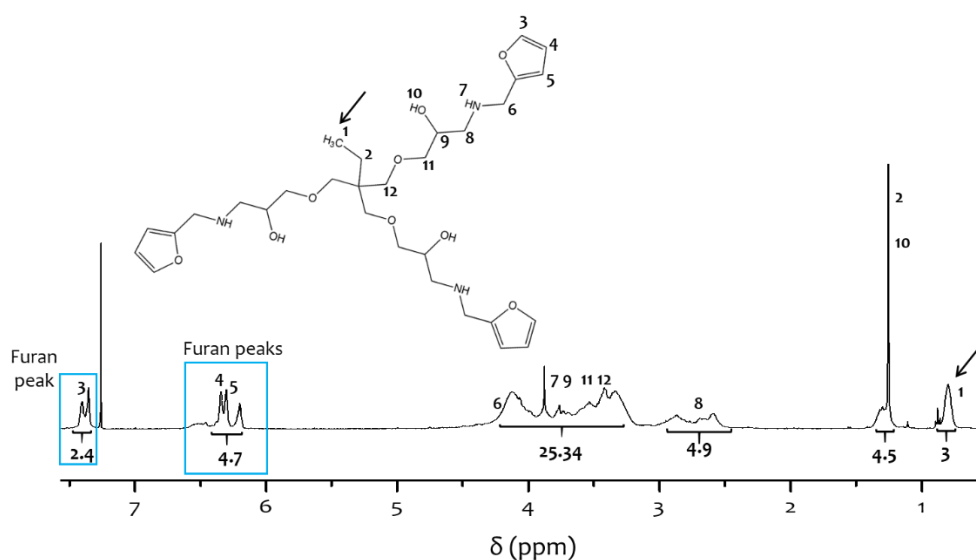
Peaks at 3.1 ppm, 2.6 ppm and 2.7 ppm in 1,4BDE spectra corresponded to hydrogens of the epoxy rings. These peaks were expected to decrease or disappear when the reaction occurred. The total area of epoxy peaks was around 5,7, instead of 6 (since there are 3 hydrogens for each epoxy group). On the base of this consideration, the functionality of 1,4BDE was recalculated and it was equal to 1,9 (instead of 2). As a consequence, FA which could react with epoxy groups was 1,9 too.

Peaks at 6.1 ppm, 6,2 ppm and 7,3 ppm in Figure 4. 21 were associated to the hydrogens of furan groups (1,2 and 3 in Figure 4. 21). It was assumed that, after the thermal treatment in oven, the furfurylammine still present in the product was the one which was chemically linked to 1,4BDE. The predicted total area below these peaks should be around 5,7: the amount of FA which was linked to epoxies was 1,9 that if multiplied by 3 gives the number of hydrogen of the furan groups which should be present, but actually the area was around 3.8. Then, the percentage of reacted furan was calculated: it was around 67%. Therefore, it could be concluded that the functionality of aliphatic 2F was lower than the one expected, namely 2.

In addition, from the spectra of aliphatic 2F it could be seen that the signal at 3.1 ppm disappeared while peaks at 2.6 ppm and 2.7 ppm seemed shifted, which proved that some epoxy groups reacted. The wide peak at 2.5 ppm and the new peaks between 3.4 ppm and 4 ppm in the 2F aliphatic spectrum could be associated to the signal given by hydrogens involved in the formation of new bonds.

In this part of the spectrum, it was not easy to distinguish the new peaks from the epoxy peaks, so a quantitative analysis on unreacted epoxy groups was not possible.

Similar considerations could be derived from spectra of TMPTE and aliphatic 3F, which are depicted in Figure 4. 22 and Figure 4. 23 below<sup>65</sup>:

Figure 4. 22  $^1\text{H}$  NMR spectrum of TMPTEFigure 4. 23  $^1\text{H}$  NMR spectrum of aliphatic 3F

Peak at 0.8 ppm, corresponding to the signal of the hydrogens of the methyl group, was selected as the reference one to normalize both spectra above. The total area of the epoxy peaks in TMPTE spectrum was equal to 7,4. As in the previous case, it was lower than the predicted one, which was 9, and so the functionality of TMPTE was recalculated too: it was 2,5 instead of 3. The furan peaks at 6.2 ppm, 6.3 ppm and 7.3 ppm were present in the aliphatic 3 furan spectra too. Here the total area of furan signals was 7,1. Considering that FA which could react with epoxy group was equal to 2,5, the expected

area of furan peaks was 7,5. So, the amount of furan which reacted was around 95%. Even in this case, the functionality of the product was lower than the one predicted.

As for aliphatic 2F, epoxy peaks at 3.1 ppm disappeared in the final product, while signal at 2.6 ppm and 2.7 ppm decreased and shifted, demonstrating the occurrence of the reaction. In the aliphatic 3F spectrum the peaks around 4 ppm could be associated to the signal of hydrogens involved in the formation of new bonds, but also in this case it was difficult to distinguish new peaks from epoxy peaks and to associate them precisely to hydrogens belonging to new bonds..

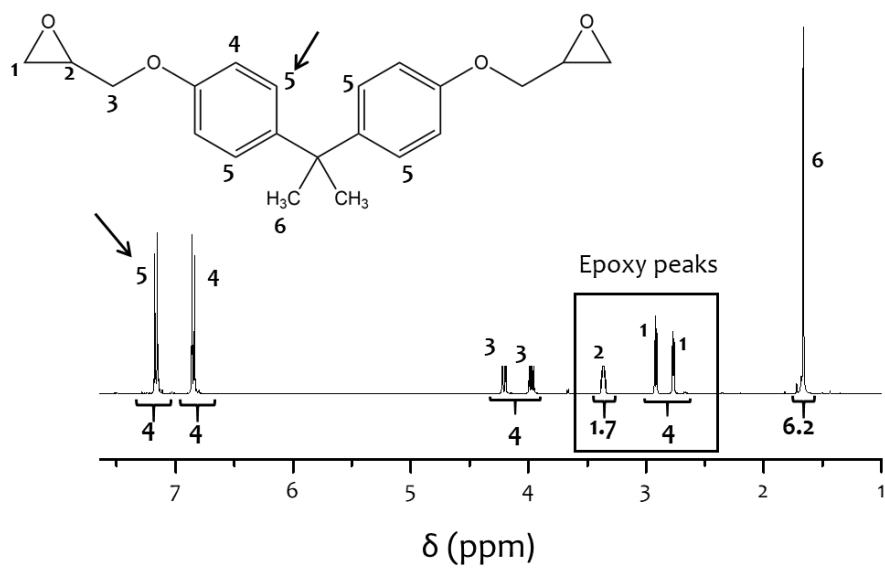
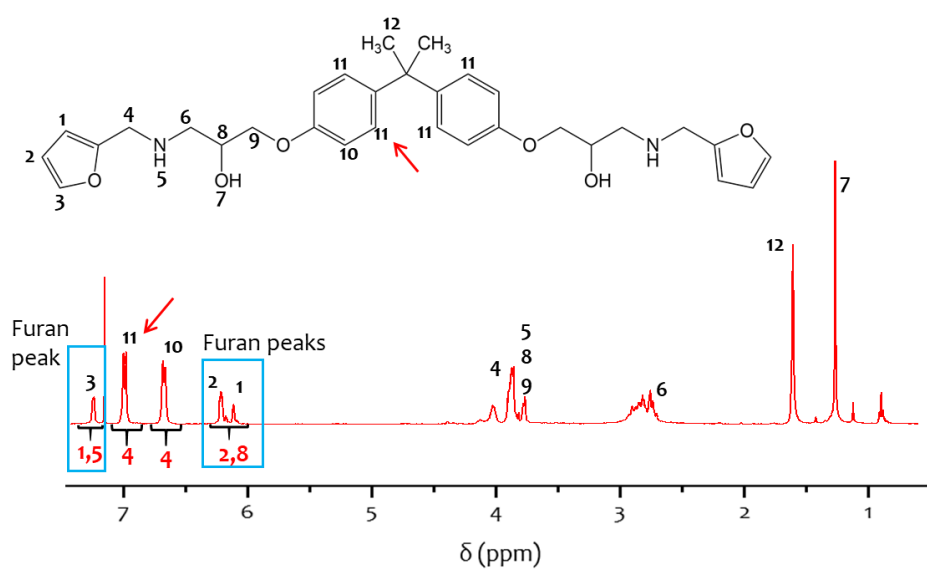
<sup>1</sup>H NMR spectra of DGEBA<sup>66</sup>, aromatic 2F, DGGO and aromatic 3F are depicted in Figure 4. 24, Figure 4. 25, Figure 4. 26 and Figure 4. 27. In the spectra of the products the appearance of furan peaks (peaks 1,2 and 3 in the molecular structure of the products in Figure 4. 24 and in Figure 4. 26) and a decrease of the epoxy peaks could be observed, demonstrating the formation of aromatic 2F and 3F.

Spectra of DGEBA and of aromatic 2F were normalized setting the area of the peak corresponding to hydrogen 5 in Figure 4. 24 or hydrogen 11 in Figure 4. 25 equal to 4.

As regard the spectra of DGGO and aromatic 3F, peak at 6,7 ppm was selected as the reference one: the area below this peak was set equal to 4.

Also in this case a quantitative analyses of the amount of reacted furan groups was carried out. Considering that the area below furan peaks in DGEBA spectrum was equal to 5,7 instead of 6, the functionality of DGEBA was found to be 1,9. Consequently, the area of furan peaks in the spectrum of aliphatic 2F was expected to be 5,7, but actually it was 4,3: the amount of furan groups which reacted was 75%.

The calculated functionality of DGGO was 2,6 (instead of 3) since the epoxy peaks area in this case was 7,9. The total area of furan peaks in aromatic 3F spectrum was 7,8, while the expected one was 7,9. The amount of furan groups which reacted in this case was 98%. So, it could be deducted that the functionality was lower than the one predicted also for aromatic 2F and 3F.

Figure 4. 24 <sup>1</sup>H NMR of DGEBAFigure 4. 25 <sup>1</sup>H NMR of aromatic 2F



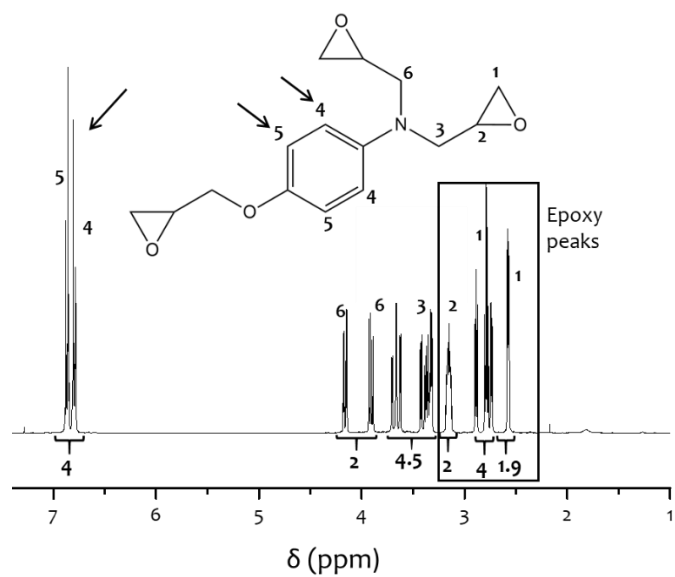
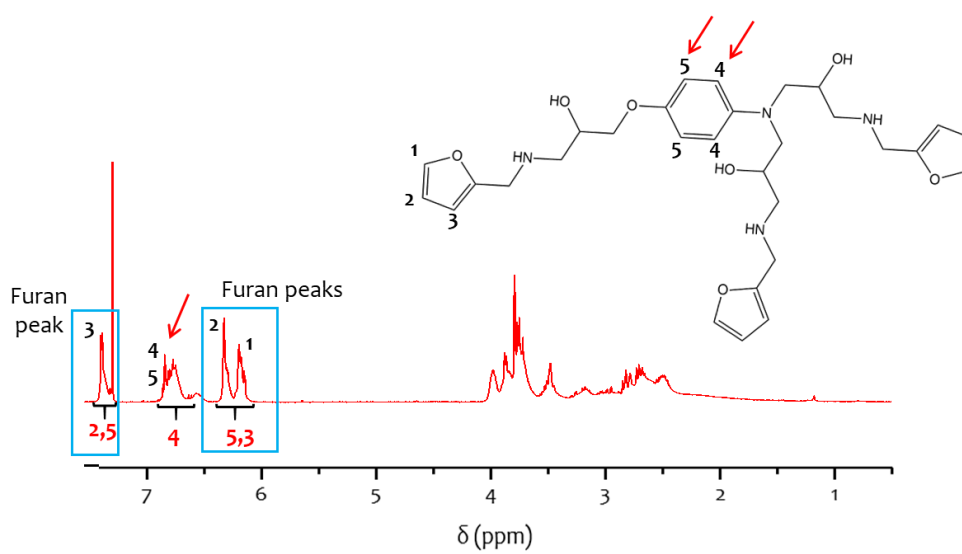
Figure 4. 26  $^1\text{H}$  NMR of DGGOFigure 4. 27  $^1\text{H}$  NMR of aromatic 3F

Table 4. 5 and Table 4. 6 and summarizes the functionalities of the reactants and the amount of furan which reacted for the different compounds:

Table 4. 5 predicted and effective functionalities

	<b>predicted functionality</b>	<b>effective functionality</b>
<b>1,4BDE</b>	2	1,9
<b>TMPTE</b>	3	2,5
<b>DGEBA</b>	2	1,9
<b>DGGO</b>	3	2,6

Based on these considerations and evaluating the expected and effective area of furan peaks, the percentage of furan groups which reacted was calculated:

Table 4. 6 % reacted furan groups

	<b>predicted area of furans peaks</b>	<b>effective area of furans peaks</b>	<b>% reacted furans</b>
<b>Aliphatic 2F</b>	5,7	3,8	67%
<b>Aliphatic 3F</b>	7,5	7,1	95%
<b>Aromatic 2F</b>	5,7	4,3	75%
<b>Aromatic 3F</b>	7,9	7,8	98%

It can be observed that, the percentage of reacted furan groups for aromatic 2F was higher than the one for aliphatic 2F as well as the % of reacted furan groups for aromatic 3F was higher than the one for aliphatic 3F. This could be due to the higher reactivity of epoxy groups linked to an aromatic ring compared to the reactivity of epoxy ring linked to an aliphatic chain.

### 4.2.3 DSC

DSC analyses are reported in Figure 4. 28.

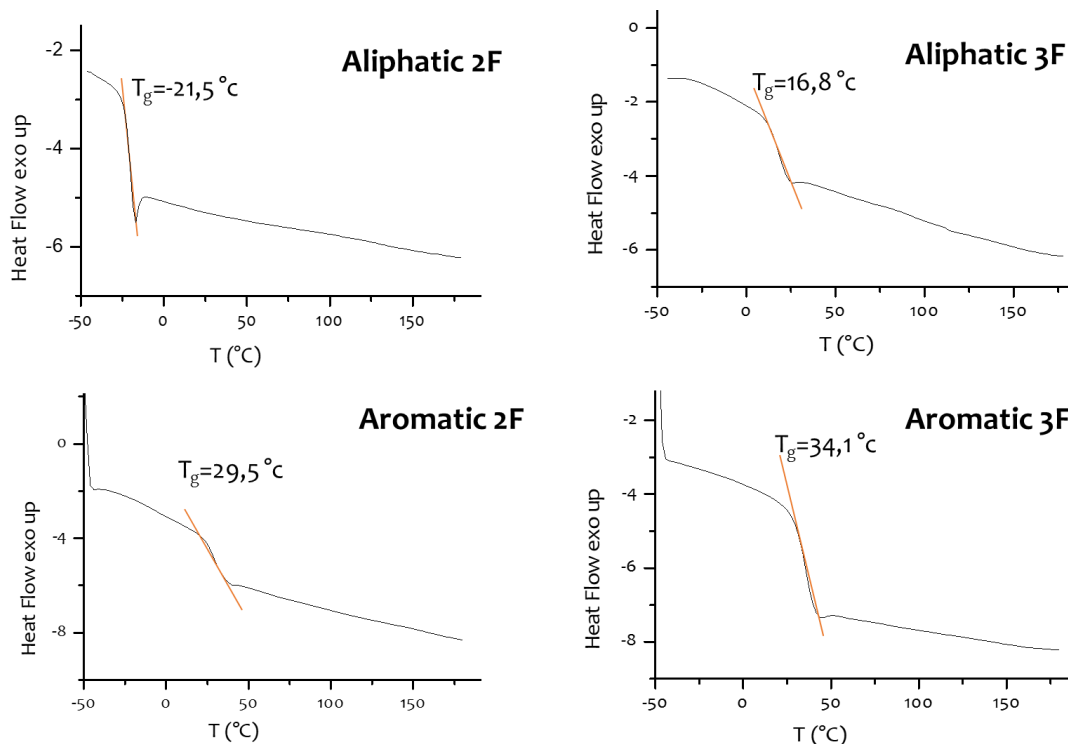


Figure 4. 28 DSC of Furan compounds

DSC analyses were performed to find the glass transition temperatures of the different furan functionalized compounds, that correspond to the midpoint between the onset and the inflect points, which are reported above.

It could be noticed that the  $T_g$  of aliphatic furan compounds were lower than the  $T_g$  of the corresponding aromatic furan components. In fact, aromatic compounds are more rigid than aliphatic ones.

Moreover, the  $T_g$  of trifunctional components were higher than the  $T_g$  of bifunctional furans. The reason of this could be associated with the chemical structure of trifunctional components, which had higher steric hindrance than bifunctional ones.

### 4.3 DA polymers synthesis and characterization

The aim of this thesis was to obtain a crosslinked DA polymer without any solvents to be employed as DA matrix for composite materials. For this reason, aliphatic furan components and an aliphatic bismaleimide were synthesized. In fact, aliphatic molecules are less rigid than the aromatic ones. Therefore, an aliphatic matrix is expected to allow better impregnation of the fibers compared to an aromatic one. On the other hand, the disadvantages of aliphatic compounds are their low values of  $T_g$ , which prevents their use from some applications, and their poor mechanical properties. Based on these considerations, a DA polymer made of only aliphatic monomers was excluded and a mixture of aliphatic and aromatic compound was taken into account.

A bifunctional furan compound and a trifunctional furan compound were mixed in a beaker under magnetic stirrer at 130°C. Then, the corresponding quantity of bismaleimide was added and the system was stirred at 130°C for 10 minutes. The reaction was carried out without solvent. The obtained polymer was transferred in a previously tared teflon and put in oven at 50°C for 2 hours so that the Diels-Alder reaction took place.

DA polymers synthesized in this thesis could be also obtained through casting, to provide to the material a particular shape, in this case a rectangular one.

This was possible since the polymers at 80°C had a low viscosity and so could be transferred from the beaker, where the mixing between furan components and the aliphatic bismaleimide occurred, to the mold.

The molds were then put in an oven at 130°C for 20 minutes. Successively, they were cooled down to favour the formation of DA adducts.

A first attempt was carried out by using 1,1'-(Methylenedi-4,1-phenylene) bismaleimide, a commercially available aromatic bismaleimide, which reacted with aliphatic 2F and aliphatic 3F (So). This system showed DA adduct formation and dissociation, since it was insoluble at room temperature and soluble at high temperature. Moreover, by means of DSC analyses, this material revealed also a high glass transition temperature. Even

though this system appeared promising, it was not possible to produce it without solvent; in fact, the aromatic bismaleimide could not be dissolved in the mixture of aliphatic 3F and 2F. Only with the use of a solvent it was possible to obtain a homogeneous mixture. This problem was due to the aromatic bismaleimide which is solid at room temperature and have a very high melting temperature.

Therefore, only the aliphatic bismaleimide, which is a viscous liquid at room temperature, was taken into account in the formulation of new materials to be employed in composite materials.

Three DA polymers were obtained without solvents, reported in Table 4. 7.

Table 4. 7 DA polymers obtained without the usage of solvents

Aliphatic 2F	Aromatic 2F	Aromatic 2F
+	+	+
Aromatic 3F	Aliphatic 3F	Aromatic 3F
+	+	+
Aliphatic BM	Aliphatic BM	Aliphatic BM
↓	↓	↓
<b>DA polymer S1</b>	<b>DA polymer S2</b>	<b>DA polymer S3</b>

For the purpose of this project, which aims to be a basis for an in-depth research on DA systems processed without solvent and capable of acting as a matrix for composite materials, only the theoretical functionality of each molecule was considered.

For each system different  $f_{av}$  were considered as explained in section 3.3.

All the polymers were characterized with solubility tests and DSC analyses. The three polymers with highest  $T_g$  were analysed also with FT-IR, gel content and TGA techniques.

### 4.3.1 Solubility tests

Solubility tests were performed to assess the occurrence of the Diels-Alder and of the retro DA reaction. A ratio polymer:solvent equal to 1g:10ml was selected.

All polymers were insoluble at room temperature; therefore DA reactions took place leading to the formation of a crosslinked network.

The retro DA reaction was found to start between 110°C and 115°C: by heating and stirring DA polymers immersed in DMF at those temperatures, a uniform solution was obtained, since the polymer became soluble in the solvent.

An example is reported is reported in Figure 4. 29 and Figure 4. 30.



Figure 4. 29 Solubility test at low temperature



Figure 4. 30 Solubility test at high temperature

Another proof the thermal reversibility was given by the gelification test. Each material was dissolved in DMF (40,5 wt%) at 110/115°C. Then the samples were put in oven at 50°C until gelification occurred (Figure 4. 31). Upon heating the systems at rDA temperature, they became again liquid.



Figure 4. 31 Gelification

### 4.3.2 DSC

DSC analyses were performed in order to find the glass transition temperatures and to assess the thermoreversibility and so the occurrence of the effective retro-DA reactions. In addition, the three polymers with the highest  $T_g$  were selected for further analyses and experiments.

The analyses were performed on all the DA polymers.

First DSC analysis was performed on polymer S<sub>0</sub> with a  $f_{av}=2,2$ . The use of the aromatic bismaleimide allowed to obtain a polymer with higher  $T_g$ . In fact, the  $T_g$  of polymer S<sub>0</sub> was around 90°C, higher than the  $T_g$  of polymers obtained with aliphatic BM. Instead, the retro DA peak, in this case, appeared at lower temperature. For the polymer crosslinked with the aromatic BM, this peak was around 130°C, while for polymers obtained with the aliphatic one it was around 140°C.

DSC thermographs of DA polymers S<sub>1</sub>, S<sub>2</sub> and S<sub>3</sub> are reported in Figure 4. 32, Figure 4. 33 and Figure 4. 34. In all the cases it was possible to see an endothermic transition in the temperature range 120-150 °C, which correspond to the rDA peaks reported in the figures below. This transition is commonly attributed to the retro Diels-Alder reaction (rDA) as showed in the section 1.4.1.



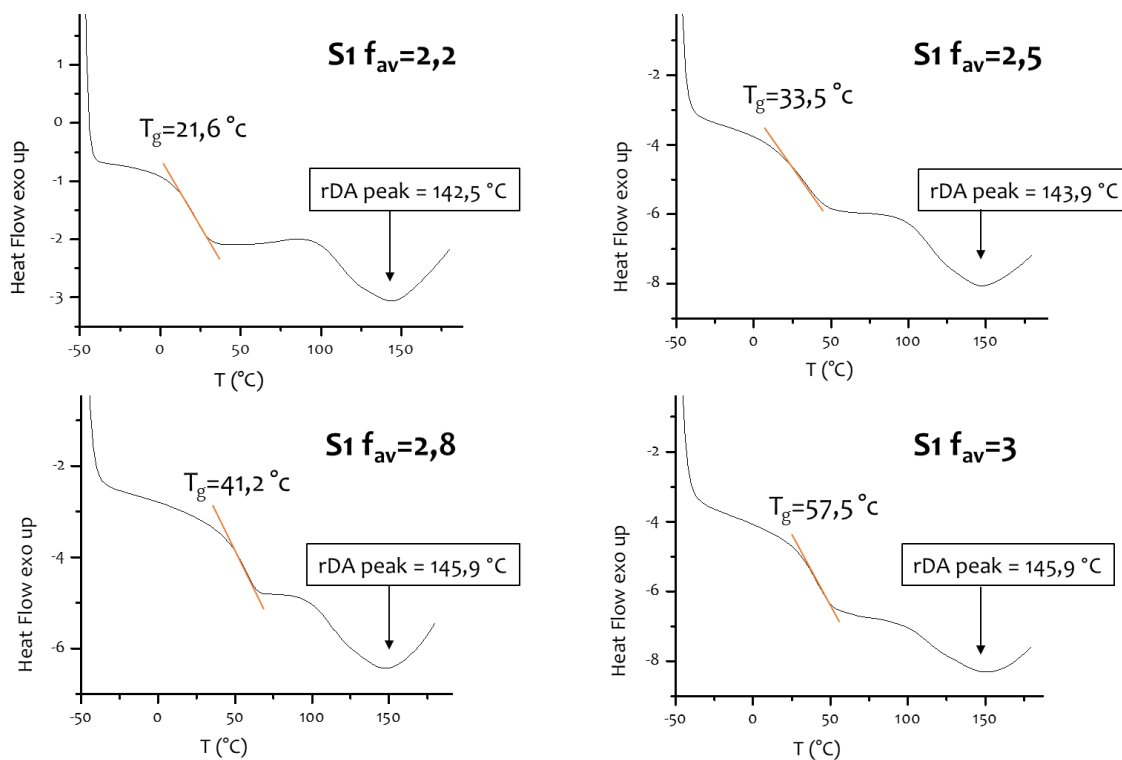


Figure 4.32 DSC of DA polymers 1

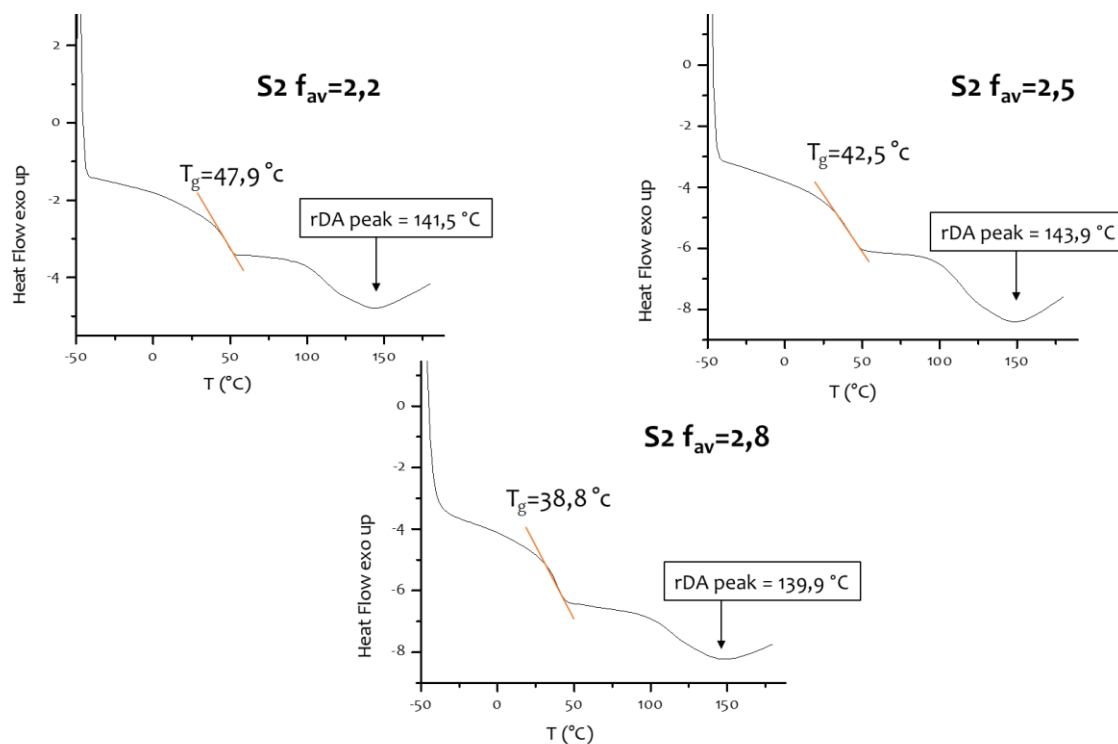


Figure 4.33 DSC of DA polymers 2

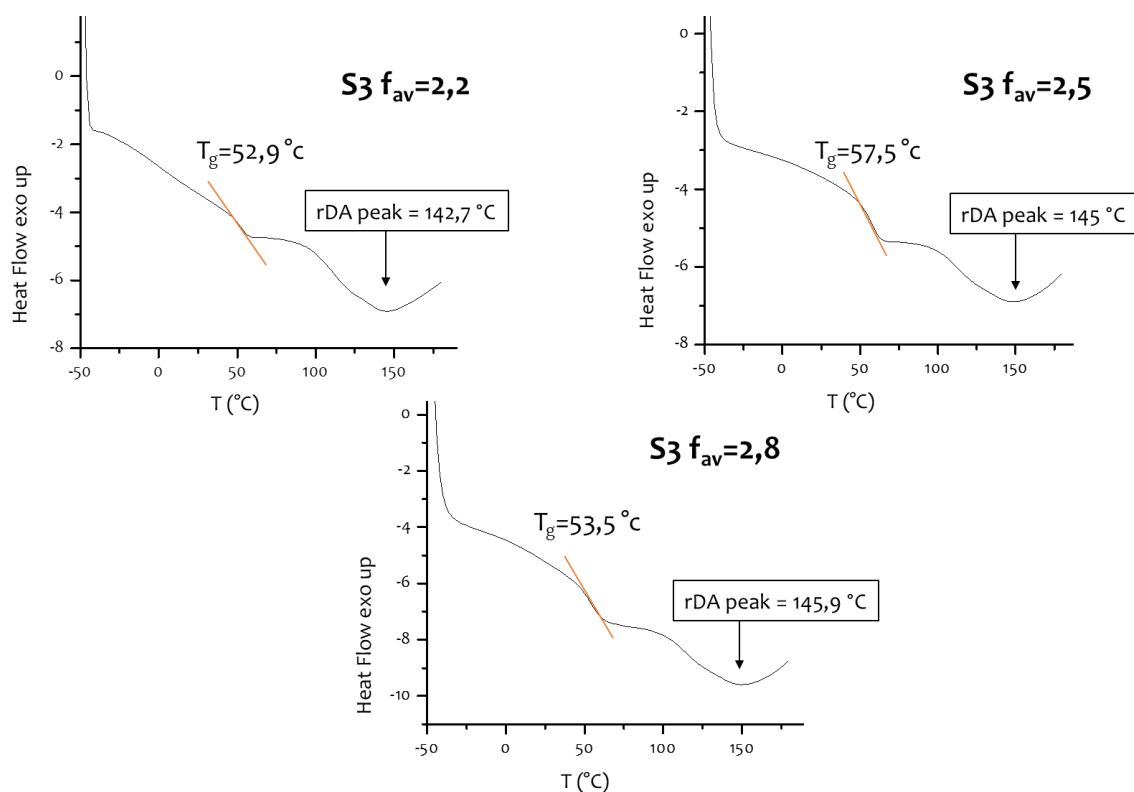


Figure 4.34 DSC of DA polymers 3

Table 4.8 summarized the  $T_g$  for all the DA polymers. It was possible to identify a trend, which depends on the aromatic weight fraction and on the degree of crosslinking: when these factors increased, the  $T_g$  increased too.

Overall, the average functionality increased with the increasing of 3F weight fraction, while it decreased when 2F weight fraction increased.

Moreover, the degree of crosslinking increased with the average functionality.

For S1, which contained aliphatic 2F, the weight fraction of aromatic molecules increased with the average functionality as well as the degree of crosslinking and so the polymer with the highest  $T_g$  was the one with  $f_{av}$  equal to 3, which contained only the aromatic 3F monomer.

As regard S2, an opposite trend of the values of  $T_g$  with respect to S1 could be observed. In fact, the polymer with an  $f_{av}$  equal to 2,2 was the one with the highest  $T_g$ , since in this case the aromatic weight fraction, which was given by aromatic 2F, decreased with the increasing of  $f_{av}$ . Therefore, in this case the aromaticity prevailed on the degree of crosslinking.

S3 contained both the aromatic furan compounds, so the aromatic weight fraction was given by the sum of the weight of the two furan components divided by the total mass of the system. This quantity was more or less constant for all the values of  $f_{av}$ , but the weight fraction of the two singular aromatic monomers changed with the same trend described above. The polymer with the highest  $T_g$  was the one with  $f_{av}$  equal to 2,5, because with this value of average functionality, the two influencing factors were counterbalanced. Indeed, it was important to notice that 2F contained two aromatic rings while 3F only one. Consequently, the increasing of  $f_{av}$  ( and so of the degree of crosslinking) lead to a decrease of the aromaticity and therefore of the  $T_g$ .

Table 4. 8  $T_g$  of DA polymers

Sample		$T_g$ [°C]
<b>S1</b>	$f_{av}=2,2$	22
	$f_{av}=2,5$	34
	$f_{av}=2,8$	41
	$f_{av}=3$	<b>57</b>
<b>S1</b>	$f_{av}=2,2$	<b>48</b>
	$f_{av}=2,5$	44
	$f_{av}=2,8$	43
<b>S3</b>	$f_{av}=2,2$	53
	$f_{av}=2,5$	<b>58</b>
	$f_{av}=2,8$	53

Polymers S1 with  $f_{av}=3$ ; S2 with  $f_{av}=2,2$  and S3 with  $f_{av}=2,5$  were selected for further analyses.

### 4.3.3 FT-IR

FTIR spectra of the DA polymers were compared with the one of bismaleimide in order to characterize the material and to calculate the conversion degree of crosslinking reaction, namely the percentage of formed DA adducts.

Two peaks were considered: the one at  $700\text{ cm}^{-1}$ , associated to the out-of-plane bending of C-H bonds attached the C=C in the maleimide ring (which is involved in the DA reaction) and the one at  $1712\text{ cm}^{-1}$ , which corresponded to the stretching of the maleimide carbonyl. The first peak was expected to decrease if the Diels-Alder reaction occurred, giving an indication of the DA adducts formation. The peak at  $1712\text{ cm}^{-1}$  was selected as the reference one since it was invariant during the reaction.

By comparing the intensity of these peaks, before and after the DA reaction, it was possible to evaluate the percentage of formed DA adducts with the following formula:

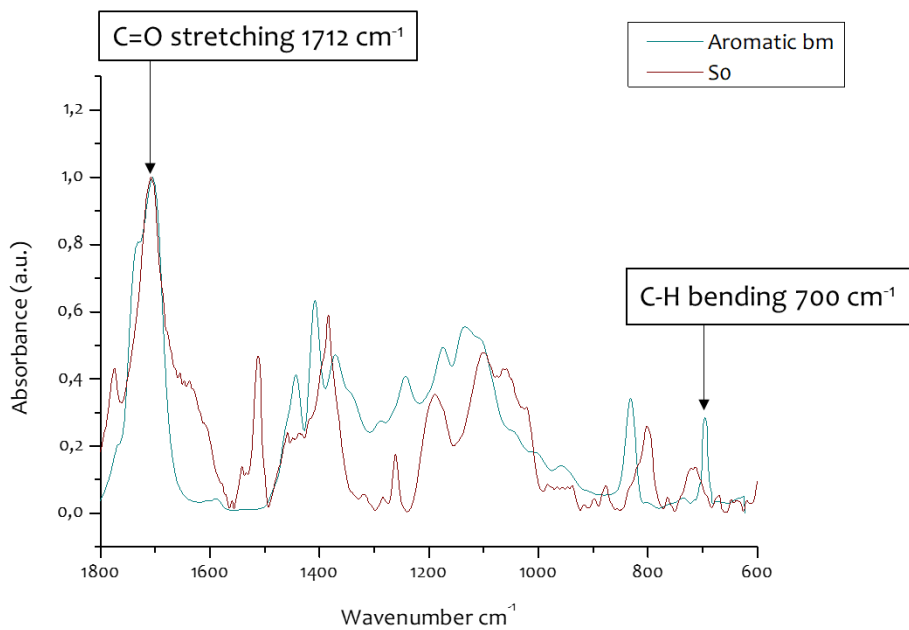
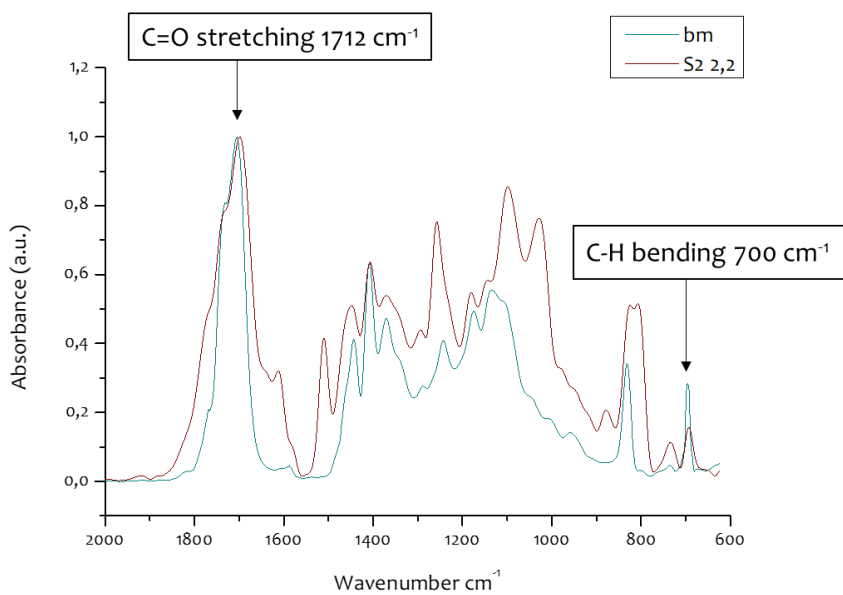
$$\%DA = \left( 1 - \frac{I_m^x / I_c^x}{I_m^{ref} / I_c^{ref}} \right) \times 100$$

where  $I_m^{ref}$  and  $I_c^{ref}$  are the reference intensities of the maleimide peak and the carbonyl peak, respectively, whereas  $I_m^x$  and  $I_c^x$  are the intensities of the above mentioned peaks in the spectrum of the characterized polymer.

The spectra of S0 and of the selected systems (S1 with  $f_{av}=3$ , S2 with  $f_{av}=2,2$  and S3 with  $f_{av} 2,5$ ) are reported in Figure 4. 35, Figure 4. 36 and in Figure 4. 37.

These spectra were compared with the utilized bismaleimide, and so the spectrum of S0 was compared with the one of the aromatic bismaleimide and the spectra of the above mentioned systems were compared with the spectra of the aliphatic bismaleimide.

From all the graphs a decrease of the absorption band at  $700\text{ cm}^{-1}$  could be noticed, as predicted, which means that the maleimide groups reacted forming DA adducts with furan functional groups.

Figure 4. 35 IR of So with  $f_{av}=2,2$ Figure 4. 36 FT-IR of DA polymers 2 with  $f_{av} 2,2$  and bismaleimide

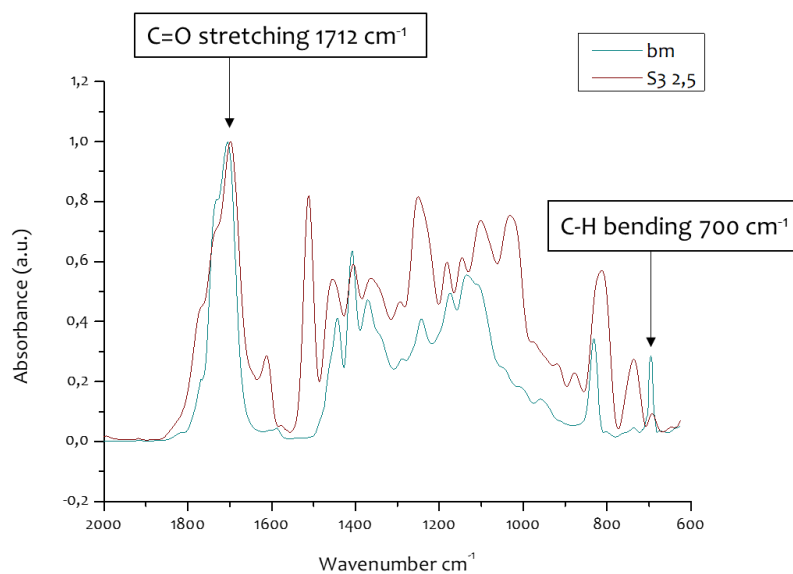


Figure 4. 37 FT-IR of DA polymers 3 with  $f_{av}$  2,5 and bismaleimide

The %DA are reported in Table 4. 9: **Errore. L'origine riferimento non è stata trovata.**

Table 4. 9 DA %

<b>Sample</b>	<b><math>f_{av}</math></b>	<b>% DA adducts</b>
<b>S0</b>	2,2	83%
<b>S1</b>	3	ND
<b>S2</b>	2,2	60%
<b>S3</b>	2,5	83%

The lower %DA value obtained in the case of S2 was probably due to the functionality of aliphatic 3F which was lower than 3, the predicted one.

#### 4.3.4 Gel content

Gel content tests provided another proof of the formation of a crosslinked network. The DA polymer was immersed in THF and kept under magnetic stirring for 24 hours. In this period, the crosslinked material swelled and part of it split in small pieces. Anyway, all the pieces were not soluble in the solvent so they could be taken into account for the calculation of the crosslinked fraction.

The solution was filtered and then all the extractable solid was dried.

The initial mass, the final mass of the polymer and the gel content %, which correspond to the % of crosslinked material are summarized in Table 4. 10.<sup>1</sup>

Table 4. 10 Gel content measurements

	<b>Initial weight [g]</b>	<b>Final Weight [g]</b>	<b>Crosslinked material [%]</b>
<b>S1 <math>f_{av}=3</math></b>	ND	ND	ND
<b>S2 <math>f_{av}=2,2</math></b>	ND	ND	ND
<b>S3 <math>f_{av}=2,5</math></b>	0,32	0,29	90%

This good value of gel content confirms the efficiency of the DA reaction in the formation of an insoluble polymer network, even if it was not possible to convert completely all the furan and maleimide functional groups present.

<sup>1</sup> Gel content measurements of polymer S1  $f_{av}=3$  and S3  $f_{av}=2,5$  were not determined because of the lockdown.

### 4.3.5 TGA

TGA analyses were performed in order to evaluate the thermal stability of the Diels-Alder polymers, which was needed in order to guarantee thermal-reversibility. The three polymers with the highest  $T_g$  were analysed from room temperature up to 800°C in air at 20°C/min, in order to consider the worst conditions for the material.

The graphs are reported in Figure 4. 38 and Figure 4. 39, which show mass variation and its derivative (both expressed in percentage) versus temperature.

The parameters kept into account to study the stability of the different crosslinked polymers were:

- The temperature at which 2% of the starting weight is lost ( $T_{2\%}$ )
- The temperature at which 5% of the starting weight is lost ( $T_{5\%}$ )
- The temperature which corresponds to the maximum degradation rate ( $T_{MAXDR}$ )
- The percentage of residual mass at 700°C. (% mass<sub>700°C</sub>)

These values are summarized in Table 4. 11 TGA data.

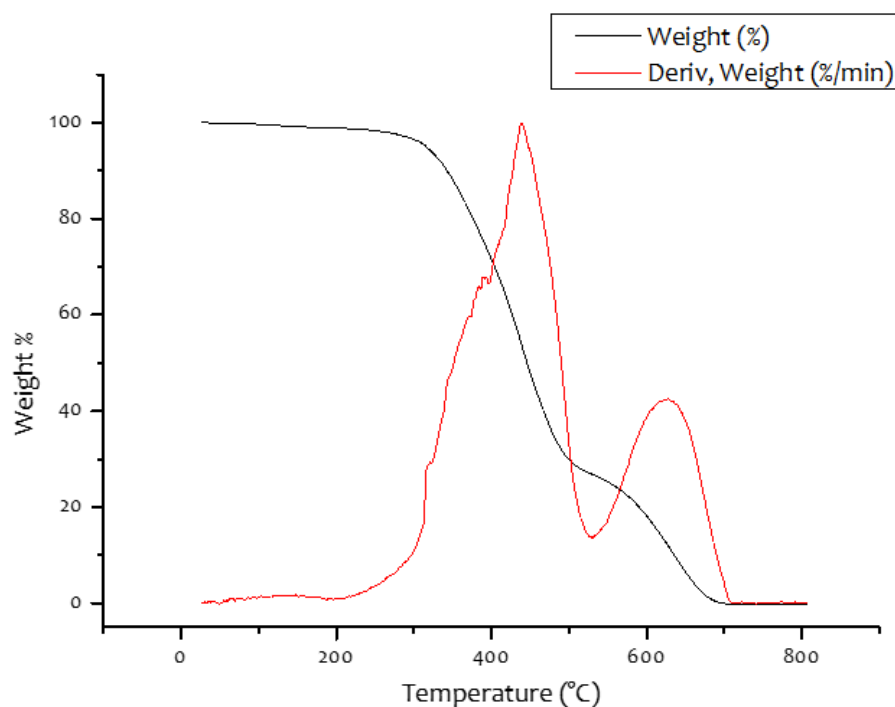


Figure 4. 38 TGA of S2 2,2



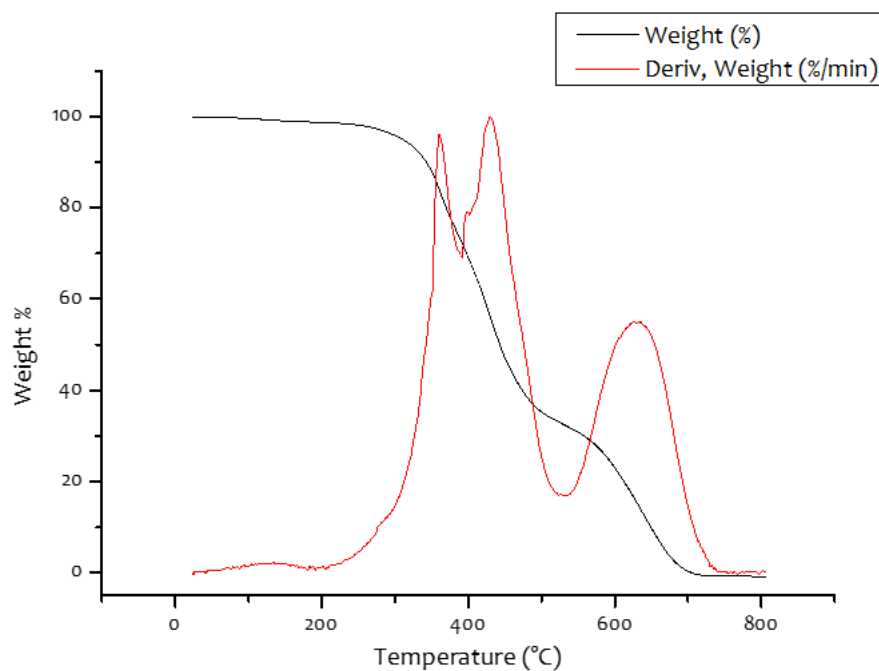


Figure 4. 39 TGA of S3 2,5

Table 4. 11 TGA data

	$T_{2\%}$ (°C)	$T_{5\%}$ (°C)	$T_{MAXDR}$ (°C)	$\%mass_{700^{\circ}C}$
<b>S1</b> $f_{av}=3$	ND	ND	ND	ND
<b>S2</b> $f_{av}=2,2$	250	305	440	0,5
<b>S3</b> $f_{av}=2,5$	250	310	450	1,5

All the three polymers exhibited good thermal stability: no significant loss in weight could be observed up to 300°C. Therefore, it could be concluded that at the retro-DA temperature the materials did not show degradation. In addition, it could be noticed that the polymers with the highest aromatic weight fraction (S3  $f_{av}=2,5$ ) displayed the highest thermal stability; demonstrating the better thermal properties of aromatic components compared to aliphatic ones.

## Conclusion

In this thesis work, a new procedure to obtain an aliphatic bismaleimide was investigated. IR and  $^1\text{H}$  NMR analyses demonstrated the success of the reaction when pyridine, the catalyst, was added to the mixing of toluene, MHA and 1,4BDE; showing a small amount of unreacted epoxy groups. After considering different ratios between the moles of epoxy groups and the moles of carboxylic acid, the ratio of 1:1 was selected as the best one according to  $^1\text{H}$  NMR analyses. Through DSC tests, the glass transition temperature was found, and it was demonstrated that a single product was obtained. The described procedure was easy, did not required complex purification steps and had a high reaction yield.

Moreover, two new aliphatic furan compounds were prepared according to an already known procedure (aliphatic 2F and aliphatic 3F). The decrease of the epoxy absorption band in the IR spectra of the products demonstrated the occurring of the reactions. Aromatic 2F and aromatic 3F were synthesized to be combined with aliphatic component such that to obtain suitable processing and thermomechanical properties.  $^1\text{H}$  NMR analyses allowed a quantification of functional furan groups revealing the effective functionalization of the molecules, which is slightly lower than the ones expected. From DSC graphs, it was possible to observe that the  $T_g$  of aromatic furan compound were higher than the  $T_g$  of aliphatic ones. Furthermore, the  $T_g$  of trifunctional furan monomers were higher with respect to the  $T_g$  of bifunctional ones, maybe because of the higher steric hindrance of 3F compounds.

By mixing, without solvent, a bifunctional furan compound, a trifunctional furan compound and the aliphatic bismaleimide, three new DA polymers were obtained with different average functionalities:

- ❖ Aliphatic 2F + aromatic 3F + aliphatic bismaleimide (S1)
- ❖ Aromatic 2F + aliphatic 3F + aliphatic bismaleimide (S2)
- ❖ Aromatic 2F + aromatic 3F + aliphatic bismaleimide (S3)

All the DA materials were characterized with solubility tests, which showed their thermal reversibility: all polymers were insoluble at low temperature and become soluble by heating at 110/115°C which corresponds to the temperature of retro-DA. DSC

analyses were performed on all the DA polymers: the  $T_g$  was found to depend on the degree of crosslinking and on the aromaticity. The three polymers with highest  $T_g$  were: S1 with  $f_{av} = 3$ ; S2 with  $f_{av} = 2,2$  and S3 with  $f_{av} = 2,5$ . The degree of crosslinking was calculated as the percentage of formed DA adducts through IR analyses, by comparing IR spectra of the polymers with the one of the aliphatic bismaleimide. The highest degree of crosslinking was found for polymer S3 with  $f_{av} = 2,5$ , while for polymer S2 with  $f_{av} = 2,2$  the degree of crosslinking was lower, probably due to the fact that the functionality of aliphatic 3F which was lower than the one predicted. The obtained matrices exhibited also a good thermal stability, as revealed by TGA analyses, since no significant loss of weight occurred up to 300°C. Finally, it was demonstrated that it was possible to obtain composite materials with one of these new DA matrices and both carbon and glass fibers.

In conclusion, in this project, a completely novel straightforward approach to synthesize aliphatic bifunctional maleimide is presented and successful results are demonstrated. The exploitation of this new compound within DA-based system was performed and the properties of the final material were demonstrated to be tunable according to the precursors molecular structure. By means of an in-depth analysis of the obtained material and a further investigation over the composite properties, these DA systems could open significant potential pathway toward next-generation recyclable composite materials.

## Further development

Despite the good reaction yield of the aliphatic bismaleimide synthesis, the quantity of the product obtained for each reaction was around 3 grams, so a scaling up of this reaction could be studied.

In addition, DA polymers synthesized in this work showed promising results for what concerns solvent resistance and thermal stability, but a further in-depth analysis is required in order to ensure the effective applicability in composite materials.

Gel content measurement of all the set of samples would demonstrate the actual crosslinking degree of each material while tensile testing would confirm the mechanical performance of the obtained matrix.

Since it was found out that at around 80°C the DA polymers were fluid and can be cast, the mechanical properties of the different matrices could be studied with dynamical mechanical analyses. Furthermore, measurement of self-healing efficiency, reprocessing and mechanical recycling would provide a further demonstration of the thermo-responsive nature of the covalent network and the recycled material could be investigated such that to compare its properties with the ones of virgin polymer. Moreover, studies on composite materials obtained with these new DA matrices could be carried out. In this work, an attempt to obtain a composite material was made with S3 polymer with an average functionality of 2,5 with both carbon and glass fibers. Aromatic 3F, aromatic 2F and aliphatic BM were mixed in a beaker at 80°C until a homogenous system was obtained. The fluid system was spread over a piece of Teflon, then a layer of carbon or glass fibers was added followed by another layer of the matrix. Then, another piece of Teflon was added, and the composite was put in oven at 120°C, under a load in order to press it, for 1 hour.

The result was that the fibers seemed well impregnated in the matrix in both cases with carbon and glass fibers, so it was found out that it was possible to obtain a composite material with this new matrix.



*Figure 4. 40 Examples of Composites: A with glass fibers, B with non-woven carbon fibers, C with woven carbon fibers*

In Figure 4. 40 some examples of composite are reported. Picture B represents a composite obtained with only one layer of matrix and non-woven carbon fibers. From that, it was possible to observe that the matrix could impregnate the fibers on both sides. Photos A and C illustrate a composite obtained with glass fibers and with woven carbon fibers, respectively.

A better processing procedure to obtain a defect-free composite material could be set, in order to guarantee a good impregnation of the fibers. Then, a characterization of the final compound from a mechanical point of view would be necessary to determine the actual application of this stimuli-responsive material. Finally, the dissolution of the matrix by means of high temperature solvent, recovering of neat fibers and reclamation of the polymeric material could be considered as a final demonstration of the composite recyclability.

## References

1. Mahajan G V, Aher VS. Composite material: A review over current development and automotive application. *Int J Sci Res Publ.* 2012;2(11):2250-3153. www.ijsrp.org
2. Altin Karataş M, Gökkaya H. A review on machinability of carbon fiber reinforced polymer (CFRP) and glass fiber reinforced polymer (GFRP) composite materials. *Def Technol.* 2018;14(4):318-326. doi:10.1016/j.dt.2018.02.001
3. Chung DDL. Composite Materials- Science and Applications. Published online 2010.
4. Rajak DK, Pagar DD, Kumar R, Pruncu CI. Recent progress of reinforcement materials: A comprehensive overview of composite materials. *J Mater Res Technol.* 2019;8(6):6354-6374. doi:10.1016/j.jmrt.2019.09.068
5. Thoppul SD, Finegan J, Gibson RF. Mechanics of mechanically fastened joints in polymer-matrix composite structures - A review. *Compos Sci Technol.* 2009;69(3-4):301-329. doi:10.1016/j.compscitech.2008.09.037
6. Callister WD, Rethwisch DG. *Scienza e Ingegneria Dei Materiali.* EdiSES; 2011.
7. Astrom BT. *Manufacturing of Polymer Composites.*; 2018.
8. Dey SK, Xanthos M. Glass Fibers. *Funct Fill Plast.* 2010;(December):141-162. doi:10.1002/9783527629848.ch7
9. Thomason JL. Glass fibre sizing: A review. *Compos Part A Appl Sci Manuf.* 2019;127(September). doi:10.1016/j.compositesa.2019.105619
10. Huang X. Fabrication and properties of carbon fibers. *Materials (Basel).* 2009;2(4):2369-2403. doi:10.3390/ma2042369
11. Park S-J. *Springer Series in Materials Science 210 Carbon Fibers.* Vol 210.; 2015. doi:10.1007/978-94-017-9478-7
12. Campbell FC. Fibers and Reinforcement: the String that Provides the Strength. *Manuf Process Adv Compos.* Published online 2004.
13. Ma S, Webster DC. Degradable thermosets based on labile bonds or linkages: A review. *Prog Polym Sci.* 2018;76:65-110. doi:10.1016/j.progpolymsci.2017.07.008
14. Zhang ZP, Rong MZ, Zhang MQ. Polymer engineering based on reversible covalent chemistry: A promising innovative pathway towards new materials and new functionalities. *Prog Polym Sci.* 2018;80:39-93. doi:10.1016/j.progpolymsci.2018.03.002
15. Morin C, Loppinet-Serani A, Cansell F, Aymonier C. Near- and supercritical solvolysis of carbon fibre reinforced polymers (CFRPs) for recycling carbon fibers as a valuable resource: State of the art. *J Supercrit Fluids.* 2012;66:232-240.

- doi:10.1016/j.supflu.2012.02.001
16. Witik RA, Teuscher R, Michaud V, Ludwig C, Månson JAE. Carbon fibre reinforced composite waste: An environmental assessment of recycling, energy recovery and landfilling. *Compos Part A Appl Sci Manuf.* 2013;49:89-99. doi:10.1016/j.compositesa.2013.02.009
  17. Pickering SJ. Recycling technologies for thermoset composite materials-current status. *Compos Part A Appl Sci Manuf.* 2006;37(8):1206-1215. doi:10.1016/j.compositesa.2005.05.030
  18. Nunes AO, Viana LR, Guineheuc PM, et al. Life cycle assessment of a steam thermolysis process to recover carbon fibers from carbon fiber-reinforced polymer waste. *Int J Life Cycle Assess.* 2018;23(9):1825-1838. doi:10.1007/s11367-017-1416-6
  19. Oliveux G, Dandy LO, Leeke GA. Current status of recycling of fibre reinforced polymers: Review of technologies, reuse and resulting properties. *Prog Mater Sci.* 2015;72:61-99. doi:10.1016/j.pmatsci.2015.01.004
  20. Yoon KH, DiBenedetto AT, Huang SJ. Recycling of unsaturated polyester resin using propylene glycol. *Polymer (Guildf).* 1997;38(9):2281-2285. doi:10.1016/S0032-3861(96)00951-2
  21. Fortunato G, Anghileri L, Griffini G, Turri S. Simultaneous recovery of matrix and fiber in carbon reinforced composites through a diels-alder solvolysis process. *Polymers (Basel).* 2019;11(6). doi:10.3390/polym11061007
  22. Jin Y, Lei Z, Taynton P, Huang S, Zhang W. Malleable and Recyclable Thermosets: The Next Generation of Plastics. *Matter.* 2019;1(6):1456-1493. doi:10.1016/j.matt.2019.09.004
  23. Capelot M, Unterlass MM, Tournilhac F, Leibler L. Catalytic control of the vitrimer glass transition. *ACS Macro Lett.* 2012;1(7):789-792. doi:10.1021/mz300239f
  24. Nicolaou KC, Snyder SA, Montagnon T, Vassilikogiannakis G. The Diels-Alder reaction in total synthesis. *Angew Chemie - Int Ed.* 2002;41(10):1668-1698. doi:10.1002/1521-3773(20020517)41:10<1668::AID-ANIE1668>3.0.CO;2-Z
  25. Gregoritza M, Brandl FP. The Diels-Alder reaction: A powerful tool for the design of drug delivery systems and biomaterials. *Eur J Pharm Biopharm.* 2015;97:438-453. doi:10.1016/j.ejpb.2015.06.007
  26. Leal RC, Pereira DH, Custodio R. An energetic analysis of the Diels-Alder endo:exo selectivity reaction by using composite methods. *Comput Theor Chem.* 2018;1123:161-168. doi:10.1016/j.comptc.2017.12.002

27. Kolb HC, Finn MG, Sharpless KB. Click Chemistry: Diverse Chemical Function from a Few Good Reactions. *Angew Chemie - Int Ed.* 2001;40(11):2004-2021. doi:10.1002/1521-3773(20010601)40:11<2004::AID-ANIE2004>3.0.CO;2-5
28. Barner-Kowollik C, Du Prez FE, Espeel P, et al. "Clicking" polymers or just efficient linking: What is the difference? *Angew Chemie - Int Ed.* 2011;50(1):60-62. doi:10.1002/anie.201003707
29. Gandini A. The furan/maleimide Diels-Alder reaction: A versatile click-unclick tool in macromolecular synthesis. *Prog Polym Sci.* 2013;38(1):1-29. doi:10.1016/j.progpolymsci.2012.04.002
30. Canadell J, Fischer H, De With G, Van Benthem RATM. Stereoisomeric effects in thermo-remendable polymer networks based on diels-alder crosslink reactions. *J Polym Sci Part A Polym Chem.* 2010;48(15):3456-3467. doi:10.1002/pola.24134
31. He X, Sastri V, Tesoro G. 1,4-Bis(5-methylfurfuryl)benzene: Polymerization with siloxane containing dimaleimides. *Die Makromol Chemie, Rapid Commun.* 1988;9(3):191-194. doi:10.1002/marc.1988.030090313
32. Goussé C, Gandini A. Synthesis of 2-furfurylmaaleimide and preliminary study of its Diels-Alder polycondensation. *Polym Bull.* 1998;40(4-5):389-394. doi:10.1007/s002890050267
33. Gandini A, Coelho D, Silvestre AJD. Reversible click chemistry at the service of macromolecular materials. Part 1: Kinetics of the Diels-Alder reaction applied to furan-maleimide model compounds and linear polymerizations. *Eur Polym J.* 2008;44(12):4029-4036. doi:10.1016/j.eurpolymj.2008.09.026
34. Liu YL, Hsieh CY. Crosslinked epoxy materials exhibiting thermal remendablility and removability from multifunctional maleimide and furan compounds. *J Polym Sci Part A Polym Chem.* 2006;44(2):905-913. doi:10.1002/pola.21184
35. Gotsmann B, Duerig U, Frommer J, Hawker CJ. Exploiting chemical switching in a diels-alder polymer for nanoscale probe lithography and data storage. *Adv Funct Mater.* 2006;16(11):1499-1505. doi:10.1002/adfm.200500724
36. Yamashiro M, Inoue K, Iji M. Recyclable shape-memory and mechanical strength of poly(lactic acid) compounds cross-linked by thermo-reversible diels-alder reaction. *Polym J.* 2008;40(7):657-662. doi:10.1295/polymj.PJ2008042
37. Chujo Y, Sada K, Saegusa T. Reversible Gelation of Polyoxazoline by Means of Diels-Alder Reaction. *Macromolecules.* 1990;23(10):2636-2641. doi:10.1021/ma00212a007
38. McElhanon JR, Zifer T, Kline SR, et al. Thermally cleavable surfactants based on furan-



- maleimide diels-alder adducts. *Langmuir*. 2005;21(8):3259-3266. doi:10.1021/la047074z
39. Noguchi H, Michinobu T, Fujii N, Funahashi M. Side Chain Liquid Crystal Poly ( fumarate ) s Bearing Tolane-Based Mesogens. *J Polym Sci Part A Polym Chem*. 2008;46(March):5101-5114. doi:10.1002/pola
40. Patel DG, Graham KR, Reynolds JR. A Diels-Alder crosslinkable host polymer for improved PLED performance: The impact on solution processed doped device and multilayer device performance. *J Mater Chem*. 2012;22(7):3004-3014. doi:10.1039/c2jm14591j
41. Weizman H, Nielsen C, Weizman OS, Nemat-Nasser S. Synthesis of a self-healing polymer based on reversible Diels-Alder reaction: An advanced undergraduate laboratory at the interface of organic chemistry and materials science. *J Chem Educ*. 2011;88(8):1137-1140. doi:10.1021/ed101109f
42. Postiglione G, Turri S, Levi M. Effect of the plasticizer on the self-healing properties of a polymer coating based on the thermoreversible Diels-Alder reaction. *Prog Org Coatings*. 2015;78:526-531. doi:10.1016/j.porgcoat.2014.05.022
43. Diaz MM, Van Assche G, Maurer FHJ, Van Mele B. Thermophysical characterization of a reversible dynamic polymer network based on kinetics and equilibrium of an amorphous furan-maleimide Diels-Alder cycloaddition. *Polymer (Guildf)*. 2017;120:176-188. doi:10.1016/j.polymer.2017.05.058
44. Pramanik NB, Nando GB, Singha NK. Self-healing polymeric gel via RAFT polymerization and Diels-Alder click chemistry. *Polymer (Guildf)*. 2015;69:349-356. doi:10.1016/j.polymer.2015.01.023
45. Teramoto N, Arai Y, Shibata M. Thermo-reversible Diels-Alder polymerization of difurfurylidene trehalose and bismaleimides. *Carbohydr Polym*. 2006;64(1):78-84. doi:10.1016/j.carbpol.2005.10.029
46. Magana S, Zerroukhi A, Jegat C, Mignard N. Thermally reversible crosslinked polyethylene using Diels-Alder reaction in molten state. *React Funct Polym*. 2010;70(7):442-448. doi:10.1016/j.reactfunctpolym.2010.04.007
47. Fortunato G, Tatsi E, Rigatelli B, Turri S, Griffini G. Highly Transparent and Colorless Self-Healing Polyacrylate Coatings Based on Diels–Alder Chemistry. *Macromol Mater Eng*. 2020;305(2):1-6. doi:10.1002/mame.201900652
48. Iredale RJ, Ward C, Hamerton I. Modern advances in bismaleimide resin technology: A 21st century perspective on the chemistry of addition polyimides. *Prog Polym Sci*. 2017;69:1-21. doi:10.1016/j.progpolymsci.2016.12.002

49. Kossmehl G, Nagel H -I, Pahl A. Cross-linking reactions on polyamides by bis- and tris(maleimide)s. *Die Angew Makromol Chemie.* 1995;227(1):139-157. doi:10.1002/apmc.1995.052270114
50. Stark YJ, Bend N, Data PP, Interaction C. ( 12 ) United States Patent. 2012;2(12).
51. Heo Y, Sodano HA. Thermally responsive self-healing composites with continuous carbon fiber reinforcement. *Compos Sci Technol.* 2015;118:244-250. doi:10.1016/j.compscitech.2015.08.015
52. Cai C, Zhang Y, Zou X, et al. Rapid self-healing and recycling of multiple-responsive mechanically enhanced epoxy resin/graphene nanocomposites. *RSC Adv.* 2017;7(73):46336-46343. doi:10.1039/c7ra09258j
53. Cai C, Zhang Y, Li M, et al. Multiple-responsive shape memory polyacrylonitrile/graphene nanocomposites with rapid self-healing and recycling properties. *RSC Adv.* 2018;8(3):1225-1231. doi:10.1039/c7ra11484b
54. Chen J, Luo K, Zhu J, Yu J, Wang Y, Hu Z. Reversibly cross-linked fullerene/polyamide composites based on Diels-Alder reaction. *Compos Sci Technol.* 2019;176(November 2018):9-16. doi:10.1016/j.compscitech.2019.03.021
55. Peterson AM, Jensen RE, Palmese GR. Thermoreversible and remendable glass-polymer interface for fiber-reinforced composites. *Compos Sci Technol.* 2011;71(5):586-592. doi:10.1016/j.compscitech.2010.11.022
56. Thanuja J, Srinivasan M. Synthesis and characterization of some polyazo(amide-imide)s. *Eur Polym J.* 1992;28(5):547-551. doi:10.1016/0014-3057(92)90131-K
57. Brown, Foote, Iverson, Anslyn. *Chimica Organica.* EdiSES; 2010.
58. Mclaughlin SR, Brook B. ( 12 ) United States Patent. 2001;1(12).
59. Vicini S, Princi E. *Tecniche Di Caratterizzazione Dei Polimeri.* Nuova Cultura; 2013.
60. Blank WJ, He ZA, Picci M. Catalysis of the epoxy-carboxyl reaction. *J Coatings Technol.* 2002;74(926):33-41. doi:10.1007/bf02720158
61. Socrates G. *Infrared and Raman Characteristic Group Frequencies. Tables and Charts.* John Wiley & Sons; 2001. doi:10.1002/jrs.1238
62. Cai T, Chen Y, Wang Y, et al. Functional 2-methylene-1,3-dioxepane terpolymer: A versatile platform to construct biodegradable polymeric prodrugs for intracellular drug delivery. *Polym Chem.* 2014;5(13):4061-4068. doi:10.1039/c4py00259h
63. [https://www.chemicalbook.com/SpectrumEN\\_2425-79-8\\_1HNMR.htm](https://www.chemicalbook.com/SpectrumEN_2425-79-8_1HNMR.htm).
64. Ishihara K, Nakayama M, Ohara S, Yamamoto H. Direct ester condensation from a 1:1

- mixture of carboxylic acids and alcohols catalyzed by hafnium(IV) or zirconium(IV) salts. *Tetrahedron*. 2002;58(41):8179-8188. doi:10.1016/S0040-4020(02)00966-3
65. Dworakowska S, Cornille A, Bogdał D, Boutevin B, Caillo S. Formulation of bio-based epoxy foams from epoxidized cardanol and vegetable oil amine. *Eur J Lipid Sci Technol*. Published online 2015.
66. Duarah R, Karak N. A starch based sustainable tough hyperbranched epoxy thermoset. *RSC Adv*. 2015;5(79):64456-64465. doi:10.1039/c5ra09955b

